Computation of the Probability Density Function and the Cumulative Distribution Function of the Generalized Gamma Variance Model

by

Xiaofang Ma

A thesis submitted in conformity with the requirements
for the degree of Master of Science
Graduate Department of Computer Science
University of Toronto

Abstract

Computation of the Probability Density Function and the Cumulative Distribution Function of the Generalized Gamma Variance Model

Xiaofang Ma

Master of Science

Graduate Department of Computer Science

University of Toronto

2002

Numerical methods for computing the probability density function (pdf) (satisfying a relative accuracy requirement) and the cumulative distribution function (cdf) (satisfying an absolute accuracy requirement) of the generalized Gamma variance model are investigated.

A hybrid method is developed to calculate the pdf. This hybrid method chooses between several basic methods to evaluate the pdf depending on the value of the risk factor and the values of the shape parameters. Extensive numerical experiments are performed to verify the robustness of the proposed hybrid method. Comparison with some existing methods for special cases suggests that this hybrid method is accurate. To improve the performance of the hybrid method, a strategy suggested by Alex Levin is adopted in the present program.

A method for computing the cdf is also developed. Numerical comparisons for several special cases are carried out to verify the correctness and the accuracy of the proposed method.

Acknowledgements

I would like to express my special thanks to my supervisors Professor Ken Jackson and Professor Tom Fairgrieve for their encouragement, support, and patient guidance during my MSc program. I would also like to express my thanks to Dr. Alex Levin at the Bank of Montreal for providing me with a summer job, introducing me to this topic, teaching me the necessary background material for the thesis, and valuable discussions and suggestions. Finally, I thank the Department of Computer Science for its financial support and providing a stimulating environment in which to work.

Contents

List of Tables

List of Figures

Chapter 1

Introduction

Value at risk (VaR) is a single, summary, statistical measure of possible portfolio losses. As a tool for market risk management, VaR has been widely used by major derivative dealers to measure and manage market risk, and used even by non-financial corporations and institutional investors [6, Chapter 15] [13]. VaR aggregates all of the risk factors (RF) in a portfolio into an easy to understand number. In the market risk management literature, a market risk factor X is usually defined as a random variable with some known (or estimated) probability density function (pdf) and its value is usually defined either in terms of daily log-returns

$$x_i = \ln \frac{S_i}{S_{i-1}},\ \ i = 1, 2, \ldots,$$

relative changes

$$x_i = \frac{S_i - S_{i-1}}{S_{i-1}},\ \ i = 1, 2, \ldots,$$

or absolute changes

$$x_i = S_i - S_{i-1},\ \ i = 1, 2, \ldots,$$

of the financial data $S_0, S_1, S_2, S_3, \ldots,$ under consideration. The data are often provided in the form of a discrete time series, where S_i denotes the price of a certain security (for example, the S&P 500 Stock Index, a unit of IBM Stock, or the CAD/USD FX Rate) at time point i.

In classical models, the normal distribution is usually used as the pdf for a market risk factor. Despite the success of such models, there exist extensive empirical evidence that the RF distributions for many underlyings have high peaks, less flanks, heavy tails, and sometimes even skewness. This means that both tiny and large price movements occur with higher frequency, while middle sized price movements occur with lower frequency, than would be expected if the RFs were normally distributed [4, 12]. As an example, the observed distribution of the S&P 500 Stock Index daily log-returns (normalized to have standard deviation 1) between October 28, 1988 and September 18, 1998 is shown in Figure 1.1 together with a normal distribution (with mean 0 and standard deviation 1) for comparison. We can see that the observed distribution has the characteristics of a high peak, less flanks, heavy tails, and a little skewness. We also notice from Figure 1.1 that the normal distribution is not a good approximation to the observed distribution in this case.

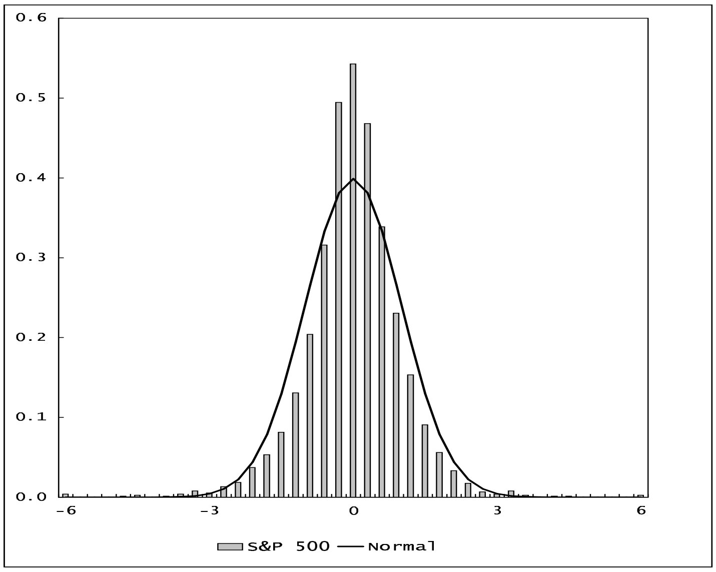

Figure 1.1: Empirical distribution of the S&P 500 log-returns

It is well-known that some RFs exhibit jumps as large as 5-10 daily standard deviations [4, 12]. Such events have a very low probability to occur in a normal model.

As a result, normal distribution models often significantly underestimate VaR. To properly evaluate the VaRs for different underlyings, some effort has been made to develop practical pdfs that capture all or some of these statistical properties [3, 4, 12, 19]. Extremely large jumps in the RFs have often been described by distributions with heavy tails, specifically by stable Paretian distributions [19]. However, as pointed out by Levin and Tchernitser [12], stable Paretian distributions do not have finite variance (volatility), which contradicts the majority of empirical observations. Also, volatility is a main tool in financial risk management and pricing. Therefore, heavy tailed distributions with finite variance are of considerable interest for finance applications. The family of generalized Gamma variance pdfs introduced by Levin and Tchernitser in [12] is an attempt to obtain a better match between a theoretical pdf and the observed distributions.

Instead of assuming the RF X to be normally distributed with mean μ and variance σ^2 with the pdf $p_X(x)$ in the form

$$p_X(x) = \frac{1}{\sigma\sqrt{2\pi}} e^{-\frac{(x-\mu)^2}{2\sigma^2}},$$

they assume the RF X to be normally conditioned upon the stochastic variance V. That is, the pdf is expressed as

$$p_X(x) = \int_0^\infty \frac{1}{\sqrt{2\pi v}} e^{-\frac{(x-\mu)^2}{2v}} p_V(v)dv,$$

with the stochastic variance V having pdf $p_V(v)$. To properly determine the pdf of the stochastic variance V, they employ a maximum entropy principal. The pdf is obtained by solving the entropy maximization problem $\max H(p_V)$, where

$$H(p_V) = -\int_0^\infty p_V(v) \ln p_V(v) dv$$

with constraints

$$p_V(v) \geq 0 \quad \text{for all} \quad v \geq 0,$$
$$\int_0^\infty \ln(v) p_V(v) dv = E\left\{\ln(V)\right\},$$

$$\int_0^\infty v^{1/\nu} p_V(v)dv = E\left\{V^{1/\nu}\right\},$$
$$\int_0^\infty p_V(v)dv = 1.$$

It is assumed here that both $E\{\ln(V)\}$ and $E\left\{V^{1/\nu}\right\}$ are known. A solution to the constrained entropy maximization problem is a generalized Gamma density for the stochastic variance V:

$$p_V(v) = \frac{v^{\frac{\alpha}{\nu}-1}}{|\nu|\Gamma(\alpha)\beta^\alpha} e^{-\frac{v^{1/\nu}}{\beta}},$$

where $\alpha > 0$ and ν are two shape parameters, $\beta > 0$ is a scaling factor, α and β are determined by $E\{\ln(V)\}$ and $E\left\{V^{1/\nu}\right\}$ and $\Gamma(\alpha) = \int_0^\infty t^{\alpha-1}e^{-t}dt$, $\alpha > 0$, is the Gamma function (see [1, Chapter 6] for more information). Thus the pdf of the RF X can be written as

$$p_X(x) = \int_0^\infty \frac{1}{\sqrt{2\pi v}} e^{-\frac{(x-\mu)^2}{2v}} \frac{v^{\frac{\alpha}{\nu}-1}}{|\nu|\Gamma(\alpha)\beta^\alpha} e^{-\frac{v^{1/\nu}}{\beta}} dv.$$

Note that $p_X(x)$ not only depends on x but also depends on the shape parameters α and ν, the scaling factor β, and the mean μ. However, without loss of generality, we can take $\mu = 0$, so we will from now on write $p_X(x)$ as

$$p(x;\alpha,\nu,\beta) = \int_0^\infty \frac{1}{\sqrt{2\pi v}} e^{-\frac{x^2}{2v}} \frac{1}{|\nu|\Gamma(\alpha)\beta^\alpha} v^{\frac{\alpha}{\nu}-1} e^{-\frac{v^{1/\nu}}{\beta}} dv. \tag{1.1}$$

If $\nu = 1$, then this pdf reduces to the Gamma variance density which was applied to finance by Madan and Seneta [15]. Therefore, we call this pdf $p(x;\alpha,\nu,\beta)$ the generalized Gamma variance (GGV) pdf.

From (1.1) and the definition of the variance, we have that RF X's variance

$$\begin{aligned}
\sigma_X^2 &= E\{X^2\} = \int_{-\infty}^{+\infty} x^2 p(x;\alpha,\nu,\beta)dx \\
&= \int_{-\infty}^{+\infty} x^2 \left[\int_0^\infty \frac{1}{\sqrt{2\pi v}} e^{-\frac{x^2}{2v}} \frac{1}{|\nu|\Gamma(\alpha)\beta^\alpha} v^{\frac{\alpha}{\nu}-1} e^{-\frac{v^{1/\nu}}{\beta}} dv\right] dx. \qquad (1.2)
\end{aligned}$$

Before continuing to evaluate (1.2), we consider the related integral

$$\int_0^\infty \frac{1}{\sqrt{2\pi v}} \frac{1}{|\nu|\Gamma(\alpha)\beta^\alpha} v^{\frac{\alpha}{\nu}-1} e^{-\frac{v^{1/\nu}}{\beta}} \left[\int_{-\infty}^{+\infty} x^2 e^{-\frac{x^2}{2v}} dx\right] dv \tag{1.3}$$

$$
\begin{aligned}
&= \int_0^\infty \frac{1}{|\nu|\Gamma(\alpha)\beta^\alpha} v^{\frac{\alpha}{\nu}} e^{-\frac{v^{1/\nu}}{\beta}} dv \qquad \text{(noting that } \textstyle\int_{-\infty}^{+\infty} x^2 e^{-\frac{x^2}{2v}} dx = \sqrt{2\pi} v^{\frac{3}{2}}\text{)} \\
&= \int_0^\infty \frac{\beta^\nu}{\Gamma(\alpha)} z^{\alpha+\nu-1} e^{-z} dz \qquad \text{(by letting } z = (v^{1/\nu})/\beta\text{)} \\
&= \frac{\Gamma(\alpha+\nu)}{\Gamma(\alpha)} \beta^\nu.
\end{aligned} \tag{1.4}
$$

Since (1.3) exists, by the Fubini-Tonelli Theorem [21, page 18] it equals (1.2). Thus we have

$$\sigma_X^2 = \frac{\Gamma(\alpha+\nu)}{\Gamma(\alpha)} \beta^\nu.$$

Since only finite variance is of interest, in addition to $\alpha > 0$, we assume throughout this thesis that $\alpha + \nu > 0$.

The related cumulative distribution function (cdf) $F(\xi; \alpha, \nu, \beta) = Pr\{X \leq \xi\}$ satisfies

$$F(\xi; \alpha, \nu, \beta) = \int_{-\infty}^{\xi} p(x; \alpha, \nu, \beta) dx, \tag{1.5}$$

where $\xi \in (-\infty, +\infty)$ is the upper bound on RF X.

Note that $p(x; \alpha, \nu, \beta)$ defined by (1.1) depends on the RF value x and the other three parameters, α, ν and β (or alternatively σ_X). If X is normalized, so that the standard deviation is set to 1, then it is expected that the integral that defines the pdf will be independent of β (or alternatively σ_X). Furthermore this standardization makes the integration less complicated.

To be more specific, we first introduce a new RF Y by letting $y = x/\sigma_X$. Thus

$$
\begin{aligned}
p(x; \alpha, \nu, \beta) &= \int_0^\infty \frac{1}{\sqrt{2\pi v}} e^{-\frac{x^2}{2v}} \frac{1}{|\nu|\Gamma(\alpha)\beta^\alpha} v^{\frac{\alpha}{\nu}-1} e^{-\frac{v^{1/\nu}}{\beta}} dv \\
&= \int_0^\infty \frac{1}{\sqrt{2\pi v}} e^{-\frac{y^2}{2v}\frac{\Gamma(\alpha+\nu)}{\Gamma(\alpha)}\beta^\nu} \frac{1}{|\nu|\Gamma(\alpha)\beta^\alpha} v^{\frac{\alpha}{\nu}-1} e^{-\frac{v^{1/\nu}}{\beta}} dv.
\end{aligned}
$$

Next let $\frac{v^{1/\nu}}{\beta} = t$, or equivalently $v = (\beta t)^\nu$, then $dv = \nu\beta^\nu t^{\nu-1} dt$ and

$$
\begin{aligned}
\hat{p}(y; \alpha, \nu, \beta) &\triangleq \int_0^\infty \frac{1}{\sqrt{2\pi v}} e^{-\frac{y^2}{2v}\frac{\Gamma(\alpha+\nu)}{\Gamma(\alpha)}\beta^\nu} \frac{1}{|\nu|\Gamma(\alpha)\beta^\alpha} v^{\frac{\alpha}{\nu}-1} e^{-\frac{v^{1/\nu}}{\beta}} dv \\
&= \int_0^\infty \frac{1}{\sqrt{2\pi(\beta t)^\nu}} e^{-\frac{y^2}{2}\frac{\Gamma(\alpha+\nu)}{\Gamma(\alpha)}\frac{1}{t^\nu}} \frac{1}{|\nu|\Gamma(\alpha)\beta^\alpha} \beta^{\alpha-\nu} t^{\alpha-\nu} e^{-t} |\nu| \beta^\nu t^{\nu-1} dt \\
&= \frac{1}{\Gamma(\alpha)\beta^{\frac{\nu}{2}}} \frac{1}{\sqrt{2\pi}} \int_0^\infty e^{-\frac{y^2}{2}\frac{\Gamma(\alpha+\nu)}{\Gamma(\alpha)}\frac{1}{t^\nu}} t^{\alpha-\frac{\nu}{2}-1} e^{-t} dt,
\end{aligned}
$$

where the symbol " $\triangleq$ " stands for "is defined as". Noting $\sigma_X(\beta) = \sqrt{\frac{\Gamma(\alpha+\nu)}{\Gamma(\alpha)}\beta^{\nu}}$, we have

$$\hat{p}(y;\alpha,\nu,\beta) = \frac{1}{\sigma_X(\beta)}\frac{1}{\Gamma(\alpha)}\sqrt{\frac{\Gamma(\alpha+\nu)}{2\pi\Gamma(\alpha)}}\int_0^{\infty} e^{-\frac{y^2}{2}\frac{\Gamma(\alpha+\nu)}{\Gamma(\alpha)}\frac{1}{t^{\nu}}} t^{\alpha-\frac{\nu}{2}-1}e^{-t}dt.$$

Letting $p(y;\alpha,\nu)$ denote the pdf of the standardized RF Y with $\sigma_X(\beta) = 1$, we see

$$p(y;\alpha,\nu) = \frac{1}{\Gamma(\alpha)}\sqrt{\frac{\Gamma(\alpha+\nu)}{2\pi\Gamma(\alpha)}}\int_0^{\infty} e^{-\frac{y^2}{2}\frac{\Gamma(\alpha+\nu)}{\Gamma(\alpha)}\frac{1}{t^{\nu}}} t^{\alpha-\frac{\nu}{2}-1}e^{-t}dt. \tag{1.6}$$

Furthermore, for $\sigma_X \neq 1$, the relationship between $p(x;\alpha,\nu,\beta)$ and $p(y;\alpha,\nu)$ can be expressed as

$$p(x;\alpha,\nu,\beta) = \frac{1}{\sigma_X(\beta)}p(y;\alpha,\nu), \tag{1.7}$$

where $y = x/\sigma_X$. It can be verified that $p(y;\alpha,\nu)$ is a pdf because (1) $p(y;\alpha,\nu) \geq 0$ (maybe $+\infty$ when $y = 0$) for any $y \in (-\infty,+\infty)$ and any shape parameters $\alpha > 0$ and $\nu \in (-\alpha,+\infty)$, and (2) $\int_{-\infty}^{+\infty} p_Y(\alpha,\nu)dy = 1$ since from the Fubini-Tonelli theorem the iterated integral

$$\int_{-\infty}^{+\infty} p(y;\alpha,\nu)dy = \int_{-\infty}^{+\infty}\frac{1}{\Gamma(\alpha)}\sqrt{\frac{\Gamma(\alpha+\nu)}{2\pi\Gamma(\alpha)}}\int_0^{\infty} e^{-\frac{y^2}{2}\frac{\Gamma(\alpha+\nu)}{\Gamma(\alpha)}\frac{1}{t^{\nu}}} t^{\alpha-\frac{\nu}{2}-1}e^{-t}dtdy,$$

exists and equals the iterated integral

$$\begin{aligned}
&\frac{1}{\Gamma(\alpha)}\sqrt{\frac{\Gamma(\alpha+\nu)}{2\pi\Gamma(\alpha)}}\int_0^{\infty} t^{\alpha-\frac{\nu}{2}-1}e^{-t}\left[\int_{-\infty}^{+\infty} e^{-\frac{y^2}{2}\frac{\Gamma(\alpha+\nu)}{\Gamma(\alpha)}\frac{1}{t^{\nu}}}dy\right]dt \\
&= \frac{1}{\Gamma(\alpha)}\sqrt{\frac{\Gamma(\alpha+\nu)}{2\pi\Gamma(\alpha)}}\int_0^{\infty} t^{\alpha-\frac{\nu}{2}-1}e^{-t}\left[\sqrt{\frac{2\pi\Gamma(\alpha)t^{\nu}}{\Gamma(\alpha+\nu)}}\frac{1}{\sqrt{2\pi}}\int_{-\infty}^{+\infty} e^{-\frac{\tau^2}{2}}d\tau\right]dt \\
&= \frac{1}{\Gamma(\alpha)}\sqrt{\frac{\Gamma(\alpha+\nu)}{2\pi\Gamma(\alpha)}}\int_0^{\infty} t^{\alpha-\frac{\nu}{2}-1}e^{-t}\left[\sqrt{\frac{2\pi\Gamma(\alpha)t^{\nu}}{\Gamma(\alpha+\nu)}}\right]dt \\
&= \frac{1}{\Gamma(\alpha)}\int_0^{\infty} t^{\alpha-1}e^{-t}\cdot 1\,dt \\
&= 1.
\end{aligned}$$

Thus the cdf $F(\xi;\alpha,\nu,\beta)$ defined by (1.5) can be written as

$$F(\xi;\alpha,\nu,\sigma_X) = \int_{-\infty}^{\xi/\sigma_X}\frac{1}{\sigma_X}p(y;\alpha,\nu)d(\sigma_X y) = \int_{-\infty}^{\xi/\sigma_X} p(y;\alpha,\nu)dy$$

$$= \int_{-\infty}^{\xi/\sigma_X} \frac{1}{\Gamma(\alpha)} \sqrt{\frac{\Gamma(\alpha+\nu)}{2\pi\Gamma(\alpha)}} \int_0^\infty e^{-\frac{y^2}{2}\frac{\Gamma(\alpha+\nu)}{\Gamma(\alpha)}\frac{1}{t^\nu}} t^{\alpha-\frac{\nu}{2}-1} e^{-t} dt dy$$

$$= \frac{1}{\Gamma(\alpha)} \sqrt{\frac{\Gamma(\alpha+\nu)}{2\pi\Gamma(\alpha)}} \int_{-\infty}^{\xi/\sigma_X} \int_0^\infty e^{-\frac{y^2}{2}\frac{\Gamma(\alpha+\nu)}{\Gamma(\alpha)}\frac{1}{t^\nu}} t^{\alpha-\frac{\nu}{2}-1} e^{-t} dt dy. \quad (1.8)$$

This thesis investigates effective numerical methods for computing the pdf $p(y;\alpha,\nu)$ with RF Y and the shape parameters α and ν in the reasonable ranges $y \in [-10, 10]$, $0.5 \le \alpha \le 90$, $-10 \le \nu \le -0.5$, and $0.5 \le \nu \le 10$, and the related cdf $F(\xi;\alpha,\nu,\sigma_X)$. In what follows, we focus on the standardized pdf (1.6) and the standardized cdf (1.8). The pdf (1.6) is used as a building block in the calibration of a multi-factor generalized stochastic variance model for comprehensive VaR, as described in more detail in [11, 12]. In this context, the pdf $p(y;\alpha,\nu)$ is calculated hundreds, or even thousands, of times. In an example considered in Chapter 4, this function is calculated 2500 times for a pair of fixed shape parameters. There is no known closed-form analytical expression for $p(y;\alpha,\nu)$ in general although some special cases with closed-form expressions are given in Chapter 4 for comparison purposes. Moreover, there is no existing numerical software available to compute this pdf for general shape parameters. Therefore, it is necessary to develop an effective numerical method for this purpose. The cdf (1.8) is also useful when the Pearson χ^2 test is performed with a fixed pair of shape parameters. There is no known closed-form analytical expression for $F(\xi;\alpha,\nu,\sigma_X)$ and there is no existing numerical software available to compute this cdf for general shape parameters. Therefore, it is also necessary to develop an effective numerical method for computing this cdf.

This thesis is organized as follows. Chapter 2 presents the asymptotic properties of the pdf (1.6), the properties of the integrand function relevant to it, and the upper bounds on $p(y;\alpha,\nu)$. Some examples are given to show the evolution processes of the integrand function. In the first part of Chapter 3, a high-level algorithm for computing the pdf is given. In Section 3.2 and Section 3.3, methods for computing the pdf depending on whether $\nu > 0$ or $\nu < 0$, respectively, are proposed. An improved method suggested by Levin for $\nu < 0$ is discussed in Section 3.4. A C program based on this hybrid method was produced. Extensive numerical experiments for testing the proposed method are reported in Chapter 4. A numerical method for calculating the cdf is proposed and tested in Chapter 5. A Windows application program based on this method is also described in the same chapter. Finally, some possible improvements to the hybrid method for the pdf are discussed and conclusions about the methods for computing the pdf and the cdf are drawn in Chapter 6. The source code for our programs is available at http://www.cs.toronto.edu /NA/reports.html.

Chapter 2

Properties of the Probability Density Function

2.1 Asymptotic Properties of the pdf

Limiting behavior of the pdf as the RF value y approaches ∞ is studied by means of Laplace's method [20], a classical asymptotic method. This limiting behavior manifests the tail's trend of a distribution. The analysis is carried out in three parts depending on whether $\nu = 0$, $\nu < 0$, or $\nu > 0$.

First, when $\nu = 0$, for any y, we have

$$\begin{aligned} p(y; \alpha, 0) &= \frac{1}{\Gamma(\alpha)} \frac{1}{\sqrt{2\pi}} \int_0^\infty e^{-\frac{y^2}{2}} t^{\alpha-1} e^{-t} dt \\ &= \frac{1}{\sqrt{2\pi}} e^{-\frac{y^2}{2}} \frac{1}{\Gamma(\alpha)} \int_0^\infty t^{\alpha-1} e^{-t} dt \\ &= \frac{1}{\sqrt{2\pi}} e^{-\frac{y^2}{2}}. \end{aligned} \tag{2.1}$$

From (2.1), we see that, if $\nu = 0$, then the pdf $p(y; \alpha, 0)$ reduces to the normal distribution [1, Chapter 26]. Thus, the distribution $p(y; \alpha, 0)$ has exponential tails.

To perform the asymptotic analysis for the other two cases, $\nu < 0$ and $\nu > 0$, Laplace's method will be used. This technique applies to an integral of the form

$$I(\kappa) = \int_a^b \varphi(t) e^{-\kappa h(t)} dt, \tag{2.2}$$

where κ is a large positive parameter, $h(t)$ has only one minimum in $[a, b]$ which occurs at a, $h(t)$ satisfies

$$h(t) \sim h(a) + \sum_{i=0}^{\infty} a_i (t-a)^{i+\mu}, \tag{2.3}$$

as $t \to a^+$, the expansion (2.3) can be termwise differentiated, that is

$$h'(t) \sim \sum_{i=0}^{\infty} a_i (i+\mu)(t-a)^{i+\mu-1} \tag{2.4}$$

as $t \to a^+$, and $\varphi(t)$ satisfies

$$\varphi(t) \sim \sum_{i=0}^{\infty} b_i (t-a)^{i+\theta-1} \tag{2.5}$$

as $t \to a^+$. By $f(t) \sim g(t)$ we mean either $\lim_{t\to\infty} f(t)/g(t) = 1$ or $\lim_{t\to t_0} f(t)/g(t) = 1$ for some finite t_0, where the limiting value for t will be clear from the context. Here μ and θ are two positive constants. Without loss of generality, it is assumed that $a_0 \neq 0$ and $b_0 \neq 0$. The asymptotic behavior of the integral $I(\kappa)$ as $\kappa \to +\infty$ is characterized in the following lemma.

LEMMA 1 [20, Theorem 1, page 58] *For the integral $I(\kappa)$ defined by (2.2), if* (i) *$h(t) > h(a)$ for all $t \in (a, b)$, and for every $\delta > 0$ the infimum of $h(t) - h(a)$ in $[a+\delta, b)$ is positive;* (ii) *$h'(t)$ and $\varphi(t)$ are continuous in a neighbourhood of $t = a$, except possibly at a;* (iii) *the expansions (2.3), (2.4) and (2.5) hold; and* (iv) *the integral $I(\kappa)$ converges absolutely for all sufficiently large κ, then*

$$I(\kappa) \sim e^{-\kappa h(a)} \sum_{i=0}^{\infty} \Gamma\left(\frac{i+\theta}{\mu}\right) \frac{c_i}{\kappa^{(i+\theta)/\mu}}, \tag{2.6}$$

as $\kappa \to +\infty$, where the coefficients c_i are expressible in terms of $\{a_i\}$ and $\{b_i\}$. In particular, the first two coefficients c_0 and c_1 are

$$c_0 = \frac{b_0}{\mu a_0^{\theta/\mu}} \quad \textit{and} \quad c_1 = \left\{\frac{b_1}{\mu} - \frac{(\theta+1)a_1 b_0}{\mu^2 a_0}\right\} \frac{1}{a_0^{(\theta+1)/\mu}}.$$

For convenience, we introduce two symbols $K(\alpha,\nu)$ and λ defined by

$$K(\alpha,\nu)=\frac{1}{\Gamma(\alpha)}\sqrt{\frac{\Gamma(\alpha+\nu)}{2\pi\Gamma(\alpha)}} \quad \text{and} \quad \lambda=\frac{y^2}{2}\frac{\Gamma(\alpha+\nu)}{\Gamma(\alpha)}. \tag{2.7}$$

To apply LEMMA 1 to the case $\nu<0$, $p(y;\alpha,\nu)$ is rewritten as

$$\begin{aligned} p(y;\alpha,\nu) &= K(\alpha,\nu)\int_0^\infty e^{-\frac{\lambda}{t^\nu}}t^{\alpha-\frac{\nu}{2}-1}e^{-t}dt \\ &= K(\alpha,\nu)\int_0^\infty e^{-\lambda t^{|\nu|}}t^{\alpha-\frac{\nu}{2}-1}e^{-t}dt \\ &= K(\alpha,\nu)\int_0^\infty e^{-\lambda h(t)}\varphi(t)dt, \end{aligned}$$

where $h(t)=t^{|\nu|}$ and $\varphi(t)=t^{\alpha-\frac{\nu}{2}-1}e^{-t}$. Note that $h(t)$ attains its minimum at $t=0$. Moreover, $\varphi(t)$'s expansion at 0 is

$$\begin{aligned} \varphi(t) &= t^{\alpha-\frac{\nu}{2}-1}e^{-t} \\ &\sim t^{\alpha-\frac{\nu}{2}-1}\left(1-t+\frac{1}{2!}t^2-\frac{1}{3!}t^3+\cdots\right) \\ &\sim \sum_{i=0}^{\infty}\frac{(-1)^i}{i!}t^{i+\alpha-\frac{\nu}{2}-1}. \end{aligned}$$

It is easy to check that all four conditions of LEMMA 1 are satisfied. By applying LEMMA 1 with $a=0$ and $b=+\infty$, and with coefficients $\kappa=\lambda$, $a_0=1$, $b_0=1$, $\mu=|\nu|$ and $\theta=\alpha-\frac{\nu}{2}$, we find that $c_0=1/|\nu|$, and so, when $\lambda\to\infty$, the first term of (2.6) for the asymptotic expansion of $p(y;\alpha,\nu)$ is given by

$$K(\alpha,\nu)\Gamma\left(\frac{\theta}{\mu}\right)\frac{c_0}{\lambda^{\theta/\mu}}=K(\alpha,\nu)\Gamma\left(\frac{\alpha-\frac{\nu}{2}}{|\nu|}\right)\frac{1}{|\nu|\lambda^{\frac{\alpha-\frac{\nu}{2}}{|\nu|}}}.$$

Substituting the definition of λ into this formula we have

$$p(y;\alpha,\nu)\sim K(\alpha,\nu)\Gamma\left(\frac{\alpha-\frac{\nu}{2}}{|\nu|}\right)\frac{1}{|\nu|\left(\frac{\Gamma(\alpha+\nu)}{2\Gamma(\alpha)}\right)^{\frac{\alpha-\frac{\nu}{2}}{|\nu|}}}y^{-\frac{2\alpha-\nu}{|\nu|}} \tag{2.8}$$

as $|y|\to\infty$. Thus, the tails behavior of the pdf for negative ν is polynomial since $\frac{2\alpha-\nu}{|\nu|}=2\alpha/|\nu|+1>3$ since $\alpha>-\nu>0$.

Although for $\nu>0$ Laplace's method is not directly applicable to $p(y;\alpha,\nu)$, this pdf can be transformed by variable changes into a form for which Laplace's method is applicable. In this case, some details similar to those given in the previous part on how to apply LEMMA 1 step by step are omitted.

To analyze $p(y;\alpha,\nu)$, we first let $\tau = 1/t^\nu$, or equivalently, $t = \tau^{-1/\nu}$. Hence $dt = -\frac{1}{\nu}\tau^{-1/\nu-1}d\tau$ and

$$p(y;\alpha,\nu) = \frac{K(\alpha,\nu)}{\nu}\int_0^\infty \tau^{-\frac{\alpha}{\nu}+\frac{1}{2}-1}e^{-\lambda\tau-\tau^{-\frac{1}{\nu}}}d\tau.$$

Next let

$$\tau = \left(\frac{1}{\lambda\nu}\right)^{\frac{\nu}{\nu+1}} z,$$

whence we have

$$p(y;\alpha,\nu) = \frac{K(\alpha,\nu)}{\nu}\left(\frac{1}{\lambda\nu}\right)^{\frac{\nu}{\nu+1}\left(-\frac{\alpha}{\nu}+\frac{1}{2}\right)}\int_0^\infty z^{-\frac{\alpha}{\nu}+\frac{1}{2}-1}e^{-\rho\left(z+\nu z^{-\frac{1}{\nu}}\right)}dz,$$

where $\rho = \left(\frac{\lambda^{\frac{1}{\nu}}}{\nu}\right)^{\frac{\nu}{\nu+1}}$. Note the minimum value of $z+\nu z^{-1/\nu}$ in $(0,\infty)$ is $1+\nu$ and occurs at $z=1$. To apply LEMMA 1, we split the integral at $z=1$ and rewrite it as

$$p(y;\alpha,\nu) = \frac{K(\alpha,\nu)}{\nu}\left(\frac{1}{\lambda\nu}\right)^{\frac{\nu}{\nu+1}\left(-\frac{\alpha}{\nu}+\frac{1}{2}\right)}[I_1(\rho)+I_2(\rho)], \tag{2.9}$$

where

$$\begin{aligned} I_1(\rho) &= \int_0^1 z^{-\frac{\alpha}{\nu}+\frac{1}{2}-1}e^{-\rho\left(z+\nu z^{-\frac{1}{\nu}}\right)}dz, \\ I_2(\rho) &= \int_1^\infty z^{-\frac{\alpha}{\nu}+\frac{1}{2}-1}e^{-\rho\left(z+\nu z^{-\frac{1}{\nu}}\right)}dz. \end{aligned}$$

For the integral $I_2(\rho)$, $a_2 = 1$, $b_2 = \infty$, $\varphi_2(z) = z^{-\frac{\alpha}{\nu}+\frac{1}{2}-1}$, and $h_2(z) = z+\nu z^{-1/\nu}$, so we have the expansions

$$h_2(z) \sim h_2(1) + a_{2,0}(z-1)^{\mu_2} + a_{2,1}(z-1)^{1+\mu_2} + \cdots$$

with

$$\begin{aligned} &h_2(1) = 1+\nu, \qquad \mu_2 = 2, \\ &a_{2,0} = \frac{1}{2!}\left(\frac{1}{\nu}+1\right), \\ &a_{2,1} = -\frac{1}{3!}\left(\frac{1}{\nu}+1\right)\left(\frac{1}{\nu}+2\right), \end{aligned}$$

and

$$\varphi_2(z) \sim b_{2,0}(z-1)^{\theta_2-1} + b_{2,1}(z-1)^{1+\theta_2-1} + \frac{1}{2!}b_{2,2}(z-1)^{2+\theta_2-1} + \cdots,$$

where $\theta_2 = 1$, $b_{2,0} = 1$ and $b_{2,1} = \left(-\frac{\alpha}{\nu} + \frac{1}{2} - 1\right)$. Thus by LEMMA 1 we have

$$I_2(\rho) \sim e^{-\rho(1+\nu)} \sum_{i=0}^{\infty} \Gamma\left(\frac{i+1}{2}\right) \frac{c_{2,i}}{\rho^{(i+1)/2}}, \tag{2.10}$$

where the coefficients $c_{2,i}$ are determined by the expansions of $\varphi_2(z)$ and $h_2(z)$ at 1, specifically

$$\begin{aligned}
c_{2,0} &= \frac{1}{2\left[\frac{1}{2!}\left(\frac{1}{\nu}+1\right)\right]^{1/2}} = \sqrt{\frac{\nu}{2(\nu+1)}}, \\
c_{2,1} &= \left\{ \frac{\left(-\frac{\alpha}{\nu}+\frac{1}{2}-1\right)}{2} - \frac{2\left[-\frac{1}{6}\left(\frac{1}{\nu}+1\right)\left(\frac{1}{\nu}+2\right)\right]\cdot 1}{2^2\frac{1}{2}\left(\frac{1}{\nu}+1\right)} \right\} \frac{2\nu}{\nu+1} \\
&= \left[-\frac{\alpha}{2\nu} - \frac{1}{4} + \frac{1}{6}\left(\frac{1}{\nu}+2\right)\right] \frac{2\nu}{\nu+1} \\
&= \frac{-\alpha + \frac{1}{6}\nu + \frac{1}{3}}{\nu+1}.
\end{aligned}$$

To apply LEMMA 1 to $I_1(\rho)$, we first perform the changes of variable $z = -\hat{z}$ to get

$$I_1(\rho) = \int_{-1}^{0} (-\hat{z})^{-\frac{\alpha}{\nu}+\frac{1}{2}-1} e^{-\rho\left[-\hat{z}+\nu(-\hat{z})^{-\frac{1}{\nu}}\right]} d\hat{z}.$$

Now the minimum of $h_1(\hat{z}) = -\hat{z} + \nu(-\hat{z})^{-1/\nu}$ occurs at the left end point $a_1 = -1$ of the interval of integration $[-1, 0]$. Consequently, we can apply LEMMA 1 with $a_1 = -1$, $b_1 = 0$, $\varphi_1(\hat{z}) = (-\hat{z})^{-\frac{\alpha}{\nu}+\frac{1}{2}-1}$ and $h_1(\hat{z}) = -\hat{z} + \nu(-\hat{z})^{-\frac{1}{\nu}}$. We have the expansion

$$h_1(\hat{z}) \sim h_1(-1) + a_{1,0}(\hat{z}+1)^{\mu_1} + a_{1,1}(\hat{z}+1)^{1+\mu_1} + \cdots$$

with

$$\begin{aligned}
h_1(-1) &= 1+\nu, \qquad \mu_1 = 2, \\
a_{1,0} &= \frac{1}{2!}\left(\frac{1}{\nu}+1\right), \\
a_{1,1} &= \frac{1}{3!}\left(\frac{1}{\nu}+1\right)\left(\frac{1}{\nu}+2\right),
\end{aligned}$$

and

$$\varphi_1(z) \sim b_{1,0}(z+1)^{\theta_1-1} + b_{1,1}(z+1)^{1+\theta_1-1} + \frac{1}{2!}b_{1,2}(z+1)^{2+\theta_1-1} + \cdots,$$

with $\theta_1 = 1$, $b_{1,0} = 1$ and $b_{1,1} = -\left(-\frac{\alpha}{\nu} + \frac{1}{2} - 1\right)$. Thus LEMMA 1 gives

$$I_1(\rho) \sim e^{-\rho(1+\nu)} \sum_{i=0}^{\infty} \Gamma\left(\frac{i+1}{2}\right) \frac{c_{1,i}}{\rho^{(i+1)/2}}, \tag{2.11}$$

where the coefficients $c_{1,i}$ are determined by the expansions of the corresponding $\varphi_1(z)$ and $h_1(z)$ at -1; specifically

$$c_{1,0} = \sqrt{\frac{\nu}{2(\nu+1)}} = c_{2,0}, \quad c_{1,1} = -\frac{-\alpha + \frac{1}{6}\nu + \frac{1}{3}}{\nu+1} = -c_{2,1}.$$

Then the first term of $I_1(\rho) + I_2(\rho)$ is

$$e^{-\rho(1+\nu)}\Gamma\left(\frac{1}{2}\right)\sqrt{\frac{2\nu}{\nu+1}}\rho^{-\frac{1}{2}} = e^{-\rho(1+\nu)}\sqrt{\frac{2\pi\nu}{\nu+1}}\rho^{-\frac{1}{2}},$$

where we used $\Gamma\left(\frac{1}{2}\right) = \sqrt{\pi}$. Furthermore, from (2.9), we have

$$p(y;\alpha,\nu) \sim \frac{K(\alpha,\nu)}{\nu}\left(\frac{1}{\lambda\nu}\right)^{\frac{\nu}{\nu+1}\left(-\frac{\alpha}{\nu}+\frac{1}{2}\right)} e^{-\rho(1+\nu)}\sqrt{\frac{2\pi\nu}{\nu+1}}\rho^{-\frac{1}{2}} \tag{2.12}$$

as $|y|$ tends to ∞. Substituting the expression for λ and ρ into (2.12) we have

$$p(y;\alpha,\nu) \sim A_1 e^{-A_2 y^{\frac{2}{\nu+1}}} y^{\frac{2\alpha}{\nu+1}-1}, \tag{2.13}$$

where

$$\begin{aligned} A_1 &= \frac{K(\alpha,\nu)}{\nu}\nu^{\frac{\alpha}{\nu+1}}\sqrt{\frac{2\pi\nu}{\nu+1}}\left(\frac{\Gamma(\alpha+\nu)}{2\Gamma(\alpha)}\right)^{\frac{\alpha}{\nu+1}-\frac{1}{2}}, \\ A_2 &= \left(\frac{\Gamma(\alpha+\nu)}{2\Gamma(\alpha)}\right)^{\frac{1}{\nu+1}}\frac{\nu+1}{\nu^{\frac{\nu}{\nu+1}}}. \end{aligned}$$

Thus the tails behavior of the pdf for positive ν is exponential. Hence, the tails of the pdf for positive ν are lighter than the polynomial tails of the pdf for negative ν, but heavier than the pure exponential tails of the normal distribution.

Summarizing these asymptotic formulae together we have

THEOREM 1 *Suppose that the two shape parameters α and ν are valid. Then the following asymptotic results hold:*

1. $p(y;\alpha,0) = \frac{1}{\sqrt{2\pi}} e^{-\frac{y^2}{2}}$ *for any* $y \in (-\infty, +\infty)$;

2. $p(y;\alpha,\nu) \sim A_1 y^{-\frac{2\alpha-\nu}{|\nu|}}$ *for any* $\nu < 0$ *as* $|y| \to \infty$, *where*

$$A_1 = K(\alpha,\nu)\Gamma\left(\frac{\alpha - \frac{\nu}{2}}{|\nu|}\right) \frac{1}{|\nu| \left(\frac{\Gamma(\alpha+\nu)}{2\Gamma(\alpha)}\right)^{\frac{\alpha-\frac{\nu}{2}}{|\nu|}}};$$

3. $p(y;\alpha,\nu) \sim A_1 e^{-A_2 y^{\frac{2}{\nu+1}}} y^{\frac{2\alpha}{\nu+1}-1}$ *for any* $\nu > 0$ *as* $|y| \to \infty$, *where*

$$\begin{aligned} A_1 &= \frac{K(\alpha,\nu)}{\nu} \nu^{\frac{\alpha}{\nu+1}} \sqrt{\frac{2\pi\nu}{\nu+1}} \left(\frac{\Gamma(\alpha+\nu)}{2\Gamma(\alpha)}\right)^{\frac{\alpha}{\nu+1}-\frac{1}{2}}, \\ A_2 &= \left(\frac{\Gamma(\alpha+\nu)}{2\Gamma(\alpha)}\right)^{\frac{1}{\nu+1}} \frac{\nu+1}{\nu^{\frac{\nu}{\nu+1}}}. \end{aligned}$$

We illustrate the polynomial tails in case 2 and the exponential tails in cases 1 and 3 in Figure 2.1. From the left plot, we can see that the pdfs corresponding to case 2 with $\alpha = 7, \nu = -2$ and case 3 with $\alpha = 4, \nu = 2$ have higher peaks than the normal distribution. From the right plot, we can observe that the pdf corresponding to case 2 has the heaviest tails among these three distributions, while the normal distribution has the lightest tails.

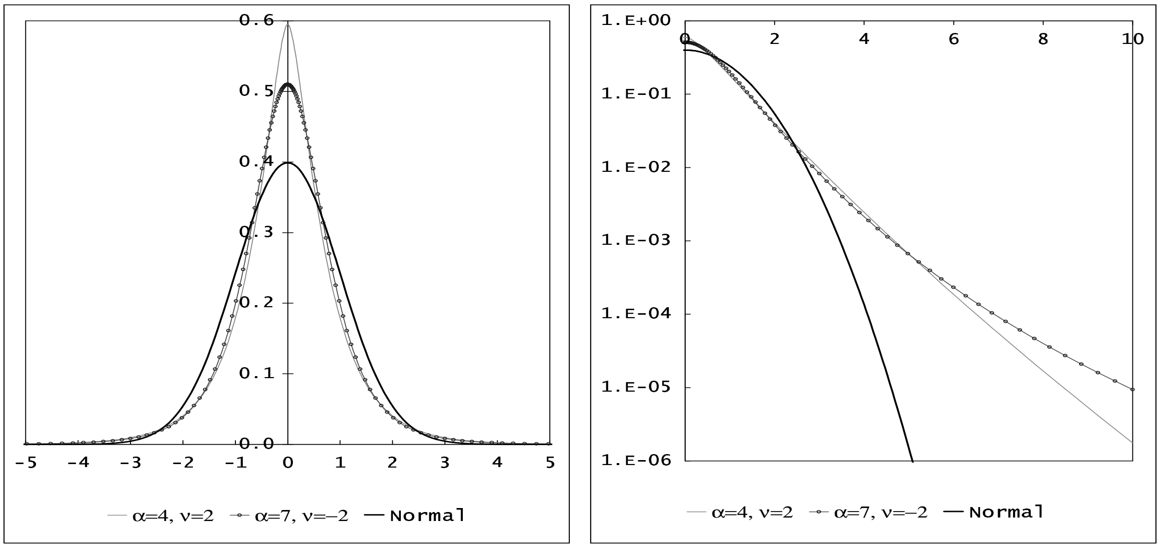

Figure 2.1: Illustration of tails behavior

2.2 Maximum of the Integrand Function

To compute the integral that defines the pdf, it is quite important to locate the maximum of the associated integrand function, because the major contribution to the integral comes from a neighbourhood of the maximum of the integrand. Because at $y = 0$ the pdf (1.6) has a closed form, we consider $y \neq 0$ from now on. Thus from the definition of λ (2.7) it follows immediately that $\lambda > 0$. Let

$$f(t) = e^{-\frac{\lambda}{t^\nu}} t^{\alpha - \frac{\nu}{2} - 1} e^{-t}. \tag{2.14}$$

THEOREM 2 *If $y \neq 0$ and $\nu > 0$, then the integrand function $f(t)$ has a unique maximizer $t_{\max} \in (0, \infty)$ which satisfies*

$$\begin{aligned}
t_{\max} &\in \left(0, (\lambda\nu)^{\frac{1}{\nu+1}}\right), \quad if \quad \alpha - \frac{\nu}{2} - 1 < 0; && (2.15)\\
t_{\max} &= (\lambda\nu)^{\frac{1}{\nu+1}}, \quad if \quad \alpha - \frac{\nu}{2} - 1 = 0; && (2.16)\\
t_{\max} &\in \left(\max\left\{(\lambda\nu)^{\frac{1}{\nu+1}}, \alpha - \frac{\nu}{2} - 1\right\}, (\lambda\nu + 1)\left(\alpha - \frac{\nu}{2}\right)\right), && (2.17)\\
&\qquad if \ \alpha - \frac{\nu}{2} - 1 > 0.
\end{aligned}$$

PROOF Note that $f(t) \to 0$ as $t \to 0$ or $t \to +\infty$ and $f(t) > 0$ for $t \in (0, \infty)$. Therefore, any maximizer must occur in $(0, \infty)$. To show that $f(t)$ has a unique maximizer in $(0, \infty)$ for any $\nu > 0$, we show that $f'(t) = 0$ has single solution in $(0, \infty)$. Note that

$$\begin{aligned}
f'(t) &= \frac{\lambda\nu}{t^{\nu+1}} e^{-\frac{\lambda}{t^\nu}} t^{\alpha - \frac{\nu}{2} - 1} e^{-t}\\
&\quad + \left(\alpha - \frac{\nu}{2} - 1\right) e^{-\frac{\lambda}{t^\nu}} t^{\alpha - \frac{\nu}{2} - 2} e^{-t}\\
&\quad - e^{-\frac{\lambda}{t^\nu}} t^{\alpha - \frac{\nu}{2} - 1} e^{-t}\\
&= \left(\frac{\lambda\nu}{t^{\nu+1}} + \frac{\alpha - \nu/2 - 1}{t} - 1\right) e^{-\frac{\lambda}{t^\nu}} t^{\alpha - \frac{\nu}{2} - 1} e^{-t},
\end{aligned}$$

and $e^{-\frac{\lambda}{t^\nu}} t^{\alpha - \frac{\nu}{2} - 1} e^{-t} > 0$ for any $t > 0$, so, if $f'(t) = 0$, we must have

$$\frac{\lambda\nu}{t^{\nu+1}} + \frac{\alpha - \nu/2 - 1}{t} - 1 = 0,$$

or equivalently

$$g(t) \triangleq \frac{\lambda\nu}{t^{\nu}} + \alpha - \frac{\nu}{2} - 1 - t = 0. \tag{2.18}$$

Note that $g(t)$ is a continuous function for $t \in (0, \infty)$ and that $\lambda > 0$, so the following two relations

$$g(t) \to +\infty \quad \text{when} \quad t \to 0^+,$$

and

$$g(t) \to -\infty \quad \text{when} \quad t \to +\infty.$$

hold. These two relations together with the continuity of $g(t)$ imply that there exists at least one positive solution to $g(t) = 0$. On the other hand, note that

$$g'(t) = -\frac{\lambda\nu^2}{t^{\nu+1}} - 1 < 0$$

for all $t \in (0, \infty)$, so $g(t)$ is strictly decreasing, thus it can have at most one root. These two facts together show that $g(t) = 0$ has a unique positive solution. Furthermore, we can show that this unique solution $t_{\max}$ is a maximizer of $f(t)$ by proving $f''(t_{\max}) < 0$. To this end, note that

$$f'(t) = \frac{g(t)}{t} f(t).$$

Therefore,

$$f''(t) = -\frac{g(t)}{t^2} f(t) + \frac{g'(t)}{t} f(t) + \frac{g(t)}{t} f'(t).$$

However, $t_{\max}$ was chosen to satisfy $f'(t_{\max}) = 0$ and $g(t_{\max}) = 0$. Therefore

$$f''(t_{\max}) = \frac{g'(t_{\max})}{t_{\max}} f(t_{\max}).$$

However, as noted above, $g'(t) < 0$ for all $t \in (0, \infty)$ and $f(t) > 0$ for all $t \in (0, \infty)$. Therefore

$$f''(t_{\max}) < 0.$$

So the integrand function $f(t)$ has a unique maximizer $t_{\max} \in (0, \infty)$.

To determine the maximizer $t_{\max}$ for given α and ν, equation (2.18), $g(t) = 0$, is rewritten in an equivalent form

$$\psi(t) = \lambda\nu + \left(\alpha - \frac{\nu}{2} - 1\right) t^{\nu} - t^{\nu+1} = 0. \tag{2.19}$$

For the first case, $\alpha - \nu/2 - 1 < 0$, we have

$$\begin{aligned} \psi\left((\lambda\nu)^{\frac{1}{\nu+1}}\right) &= \lambda\nu + \left(\alpha - \frac{\nu}{2} - 1\right)(\lambda\nu)^{\frac{\nu}{\nu+1}} - \lambda\nu \\ &= \left(\alpha - \frac{\nu}{2} - 1\right)(\lambda\nu)^{\frac{\nu}{\nu+1}} < 0. \end{aligned}$$

Note that

$$\psi(0) = \lambda\nu > 0.$$

Hence these two inequalities imply that $t_{\max} \in (0, (\lambda\nu)^{\frac{1}{\nu+1}})$.

For the second case, $\alpha - \nu/2 - 1 = 0$, it follows immediately from (2.19) that $t_{\max} = (\lambda\nu)^{\frac{1}{\nu+1}}$.

For the third case, $\alpha - \nu/2 - 1 > 0$, it can be shown that

$$\begin{aligned} \psi\left((\lambda\nu+1)\left(\alpha - \frac{\nu}{2}\right)\right) &= \lambda\nu + \left(\alpha - \frac{\nu}{2} - 1\right)\left[(\lambda\nu+1)\left(\alpha - \frac{\nu}{2}\right)\right]^{\nu} - \left[(\lambda\nu+1)\left(\alpha - \frac{\nu}{2}\right)\right]^{\nu+1} \\ &= \lambda\nu + (\lambda\nu+1)^{\nu}\left(\alpha - \frac{\nu}{2}\right)^{\nu}\left[\alpha - \frac{\nu}{2} - 1 - (\lambda\nu+1)\left(\alpha - \frac{\nu}{2}\right)\right] \\ &= \lambda\nu + (\lambda\nu+1)^{\nu}\left(\alpha - \frac{\nu}{2}\right)^{\nu}\left[-1 - \lambda\nu\left(\alpha - \frac{\nu}{2}\right)\right] \\ &< \lambda\nu - (\lambda\nu+1)^{\nu}\left(\alpha - \frac{\nu}{2}\right)^{\nu+1}\lambda\nu. \end{aligned}$$

Since $\alpha - \nu/2 - 1 > 0$, $\alpha - \nu/2 > 1$. Combining this inequality with $\lambda\nu + 1 > 1$, we have

$$(\lambda\nu+1)^{\nu}\left(\alpha - \frac{\nu}{2}\right)^{\nu+1}\lambda\nu > \lambda\nu.$$

Thus we have

$$\psi\left((\lambda\nu+1)\left(\alpha - \frac{\nu}{2}\right)\right) < 0. \tag{2.20}$$

Note that it follows immediately from (2.19) that

$$\psi\left((\lambda\nu)^{\frac{1}{\nu+1}}\right) = \left(\alpha - \frac{\nu}{2} - 1\right)^{\frac{\nu}{\nu+1}}(\lambda\nu)^{\frac{\nu}{\nu+1}} > 0, \tag{2.21}$$

and

$$\psi\left(\alpha - \frac{\nu}{2} - 1\right) = \lambda\nu > 0. \tag{2.22}$$

Therefore, (2.20), (2.21), and (2.22) together imply (2.17).

THEOREM 3 *If $y \neq 0$ and $\nu < 0$, then the integrand function $f(t)$ has a unique maximizer $t_{\max} \in [0, \infty)$ which satisfies*

$$t_{\max} = 0, \quad \textit{if} \quad \alpha - \frac{\nu}{2} - 1 \leq 0; \tag{2.23}$$

$$t_{\max} \in \left(0, \alpha - \frac{\nu}{2} - 1\right), \ \textit{if} \ \alpha - \frac{\nu}{2} - 1 > 0. \tag{2.24}$$

PROOF For $\nu < 0$, the integrand function can be written as

$$f(t) = e^{-\lambda t^{|\nu|}} t^{\alpha - \frac{\nu}{2} - 1} e^{-t}.$$

Again note that $f(t) \to 0$ as $t \to +\infty$ and $f(t) > 0$ for $t \in (0, \infty)$. Therefore, any maximizer must be in $[0, \infty)$.

If $\alpha - \frac{\nu}{2} - 1 = 0$, then $f(t) = e^{-\lambda t^{|\nu|}} e^{-t}$. Since $\lambda > 0$, $f(t)$ is a decreasing function of t for t in $[0, \infty)$, so it attains its maximum value at $t_{\max} = 0$.

For $\alpha - \frac{\nu}{2} - 1 \neq 0$, we have

$$\begin{aligned} f'(t) &= -\lambda|\nu| t^{|\nu|-1} e^{-\lambda t^{|\nu|}} t^{\alpha - \frac{\nu}{2} - 1} e^{-t} \\ &\quad + \left(\alpha - \frac{\nu}{2} - 1\right) e^{-\lambda t^{|\nu|}} t^{\alpha - \frac{\nu}{2} - 2} e^{-t} \\ &\quad - e^{-\lambda t^{|\nu|}} t^{\alpha - \frac{\nu}{2} - 1} e^{-t} \\ &= \left[-\lambda|\nu| t^{|\nu|-1} + \left(\alpha - \frac{\nu}{2} - 1\right)\frac{1}{t} - 1\right] e^{-\lambda t^{|\nu|}} t^{\alpha - \frac{\nu}{2} - 1} e^{-t} \\ &= \left[-\lambda|\nu| t^{|\nu|-1} + \left(\alpha - \frac{\nu}{2} - 1\right)\frac{1}{t} - 1\right] f(t) \end{aligned}$$

Therefore, if $\alpha - \frac{\nu}{2} - 1 < 0$, $f'(t) < 0$ for all $t \in (0, \infty)$. Hence $f(t)$ attains its maximum at $t_{\max} = 0$.

Finally, consider the case $\alpha - \frac{\nu}{2} - 1 > 0$. If $f'(t) = 0$, we must have either

$$f(t) = e^{-\lambda t^{|\nu|}} t^{\alpha - \frac{\nu}{2} - 1} e^{-t} = 0$$

which implies $t = 0$, or

$$-\lambda|\nu|t^{|\nu|-1} + \left(\alpha - \frac{\nu}{2} - 1\right)\frac{1}{t} - 1 = 0. \tag{2.25}$$

However, $f(t) > 0$ for $t \in (0, \infty)$, so the maximum does not occur at $t = 0$. Therefore, the maximum must occur at a root of (2.25). Rewrite (2.25) in the form

$$g(t) \triangleq -\lambda|\nu|t^{|\nu|} + \left(\alpha - \frac{\nu}{2} - 1\right) - t = 0. \tag{2.26}$$

Note that $g'(t) = -\lambda|\nu|^2 t^{|\nu|-1} - 1 < 0$ for all $t \in [0, \infty)$, so $g(t)$ is strictly decreasing, thus it has at most one root. On the other hand, noting that $\alpha - \frac{\nu}{2} - 1 > 0$, we have

$$\begin{aligned} g(0) &= \alpha - \frac{\nu}{2} - 1 > 0, \\ g\left(\alpha - \frac{\nu}{2} - 1\right) &= -\lambda|\nu|\left(\alpha - \frac{\nu}{2} - 1\right)^{|\nu|} < 0, \end{aligned}$$

which implies that $g(t)$ has at least one root. These two facts together show that $g(t) = 0$ has a unique solution $t_{\max} \in (0, \alpha - \frac{\nu}{2} - 1)$. Furthermore, we can show that this unique root $t_{\max}$ is a maximizer of $f(t)$ by proving $f''(t_{\max}) < 0$. To this end, note that

$$f'(t) = \frac{g(t)}{t} f(t).$$

Therefore,

$$f''(t) = -\frac{g(t)f(t)}{t^2} + \frac{g'(t)}{t} f(t) + \frac{g(t)}{t} f'(t).$$

However, $t_{\max}$ was chosen to satisfy $f'(t_{\max}) = 0$ and $g(t_{\max}) = 0$. Therefore

$$f''(t_{\max}) = \frac{g'(t_{\max})}{t_{\max}} f(t_{\max}).$$

However, as noted above, $g'(t) < 0$ for all $t \in (0, \infty)$ and $f(t) > 0$ for all $t \in (0, \infty)$. Therefore

$$f''(t_{\max}) < 0.$$

So the unique solution $t_{\max} \in (0, \alpha - \frac{\nu}{2} - 1)$ is a maximizer of $f(t)$.

2.3 Upper Bounds on the pdf

In this section we discuss the evaluation of the pdf $p(y;\alpha,\nu)$. Suppose that $y \neq 0$ and the integrand function's unique maximizer $t_{\max}$ is available by some numerical method based on THEOREM 2 and THEOREM 3. As noted before the major contribution to the integral comes from the neighbourhood of the unique maximizer of the integrand function. So our estimation will capture the maximizer $t_{\max}$.

Note for $\nu > 0$ we always have $t_{\max} > 0$. The integrand function $f(t)$ can be considered as the multiplication of two functions of the form

$$f(t) = \left(e^{-\frac{\lambda}{t^\nu}} t^{-\zeta_+}\right) \cdot \left(t^{\alpha-\frac{\nu}{2}+\zeta_+-1} e^{-t}\right)$$

for some $\zeta_+ > 0$. By choosing ζ_+ appropriately, we can ensure that these two functions $e^{-\frac{\lambda}{t^\nu}} t^{-\zeta_+}$ and $t^{\alpha-\frac{\nu}{2}+\zeta_+-1} e^{-t}$ also attain their maximum values at $t_{\max}$. To this end, note that the maximum of $e^{-\frac{\lambda}{t^\nu}} t^{-\zeta_+}$ occurs at a value of t that satisfies

$$\left(e^{-\frac{\lambda}{t^\nu}} t^{-\zeta_+}\right)' = \left(\frac{\lambda\nu}{t^{\nu+1}} - \frac{\zeta_+}{t}\right) e^{-\frac{\lambda}{t^\nu}} t^{-\zeta_+} = 0.$$

Thus, the maximizer satisfies either

$$e^{-\frac{\lambda}{t^\nu}} t^{-\zeta_+} = 0,$$

which implies $t = 0$, or

$$\frac{\lambda\nu}{t^{\nu+1}} - \frac{\zeta_+}{t} = 0,$$

which implies $\zeta_+ = \frac{\lambda\nu}{t^\nu}$. It is obvious that $t = 0$ is not a maximizer of $e^{-\frac{\lambda}{t^\nu}} t^{-\zeta_+}$. So we let $\zeta_+ = \frac{\lambda\nu}{t_{\max}^\nu}$, which makes $t_{\max}$ the unique maximizer of $e^{-\frac{\lambda}{t^\nu}} t^{-\zeta_+}$. Now note that

$$\alpha - \frac{\nu}{2} + \zeta_+ - 1 = \alpha - \frac{\nu}{2} + \frac{\lambda\nu}{t_{\max}^\nu} - 1 = t_{\max} > 0 \tag{2.27}$$

since $t_{\max}$ is a root of (2.18).

Similarly, $m(t) = t^{\alpha-\frac{\nu}{2}+\zeta_+-1} e^{-t}$ attains its maximum at some point $\hat{t} \in (0,\infty)$ that satisfies $m'(\hat{t}) = 0$. However,

$$m'(t) = \left(\frac{\alpha - \frac{\nu}{2} + \zeta_+ - 1}{t} - 1\right) t^{\alpha-\frac{\nu}{2}+\zeta_+-1} e^{-t},$$

which implies that

$$\hat{t} = \alpha - \frac{\nu}{2} + \zeta_+ - 1 = t_{\max}$$

by (2.27). Therefore $t_{\max}$ is also the unique maximizer of $t^{\alpha-\frac{\nu}{2}+\zeta_+-1}e^{-t} = t^{t_{\max}}e^{-t}$.

Thus from the partition of $f(t)$ we can give an estimate

$$\begin{aligned}
p(y;\alpha,\nu) &= K(\alpha,\nu)\int_0^\infty e^{-\frac{\lambda}{t^\nu}}t^{\alpha-\frac{\nu}{2}-1}e^{-t}dt \\
&= K(\alpha,\nu)\int_0^\infty \left(e^{-\frac{\lambda}{t^\nu}}t^{-\zeta_+}\right)\left(t^{t_{\max}}e^{-t}\right)dt \\
&\le K(\alpha,\nu)e^{-\frac{\lambda}{t_{\max}^\nu}}t_{\max}^{-\zeta_+}\int_0^\infty t^{t_{\max}}e^{-t}dt \\
&= K(\alpha,\nu)e^{-\frac{\lambda}{t_{\max}^\nu}}t_{\max}^{-\zeta_+}\Gamma(t_{\max}+1) \\
&= K(\alpha,\nu)\left(et_{\max}^\nu\right)^{-\frac{\lambda}{t_{\max}^\nu}}\Gamma(t_{\max}+1). \qquad (2.28)
\end{aligned}$$

Similarly,

$$\begin{aligned}
p(y;\alpha,\nu) &= K(\alpha,\nu)\int_0^\infty \left(e^{-\frac{\lambda}{t^\nu}}t^{-\zeta_+}\right)\left(t^{t_{\max}}e^{-t}\right)dt \\
&\le K(\alpha,\nu)e^{-t_{\max}}t_{\max}^{t_{\max}}\int_0^\infty e^{-\frac{\lambda}{t^\nu}}t^{-\zeta_+}dt \\
&= K(\alpha,\nu)e^{-t_{\max}}t_{\max}^{t_{\max}}\int_\infty^0 e^{-z}\lambda^{-\frac{\zeta_+}{\nu}}z^{\frac{\zeta_+}{\nu}}\lambda^{\frac{1}{\nu}}\left(-\frac{1}{\nu}\right)z^{-\frac{1}{\nu}-1}dz \text{ (by letting } \tfrac{\lambda}{t^\nu}=z) \\
&= K(\alpha,\nu)e^{-t_{\max}}t_{\max}^{t_{\max}}\frac{1}{\nu}\lambda^{\frac{1-\zeta_+}{\nu}}\int_0^\infty e^{-z}z^{\frac{\zeta_+-1}{\nu}-1}dz \\
&= K(\alpha,\nu)\left(e^{-1}t_{\max}\right)^{t_{\max}}\frac{1}{\nu}\lambda^{\frac{1-\zeta_+}{\nu}}\Gamma\left(\frac{\zeta_+-1}{\nu}\right) \\
&= \frac{K(\alpha,\nu)}{\nu}\lambda^{\frac{1-\zeta_+}{\nu}}\left(e^{-1}t_{\max}\right)^{t_{\max}}\Gamma\left(\frac{\zeta_+-1}{\nu}\right). \qquad (2.29)
\end{aligned}$$

Note this estimation is valid only when $\zeta_+ > 1$. Also note that both (2.28) and (2.29) are upper bounds on $p(y;\alpha,\nu)$, thus we can give an upper bound on the pdf by

$$p(y;\alpha,\nu) \le K(\alpha,\nu)\min\left\{\left(et_{\max}^\nu\right)^{-\frac{\lambda}{t_{\max}^\nu}}\Gamma(t_{\max}+1), \frac{1}{\nu}\lambda^{\frac{1-\zeta_+}{\nu}}\left(e^{-1}t_{\max}\right)^{t_{\max}}\Gamma\left(\frac{\zeta_+-1}{\nu}\right)\right\}. \qquad (2.30)$$

To show to what extent these estimates work, some examples are presented below. Both Figure 2.2 and Figure 2.3 present the plots of functions

$$K(\alpha,\nu)e^{-\frac{\lambda}{t^\nu}}t^{\alpha-\frac{\nu}{2}-1}e^{-t}, \qquad (2.31)$$

denoted by "TRUE", which corresponds to the true pdf $p(y;\alpha,\nu)$;

$$K(\alpha,\nu)\,(e t_{\max}^{\nu})^{-\frac{\lambda}{t_{\max}^{\nu}}}\, t^{t_{\max}} e^{-t}, \tag{2.32}$$

denoted by (2.32), which corresponds to the integrand function associated with the estimate (2.28); and

$$K(\alpha,\nu)\left(e^{-1}t_{\max}\right)^{t_{\max}} e^{-\frac{\lambda}{t^{\nu}}} t^{-\zeta_{+}}, \tag{2.33}$$

denoted by (2.33), which corresponds to the integrand function associated with the estimate (2.29).

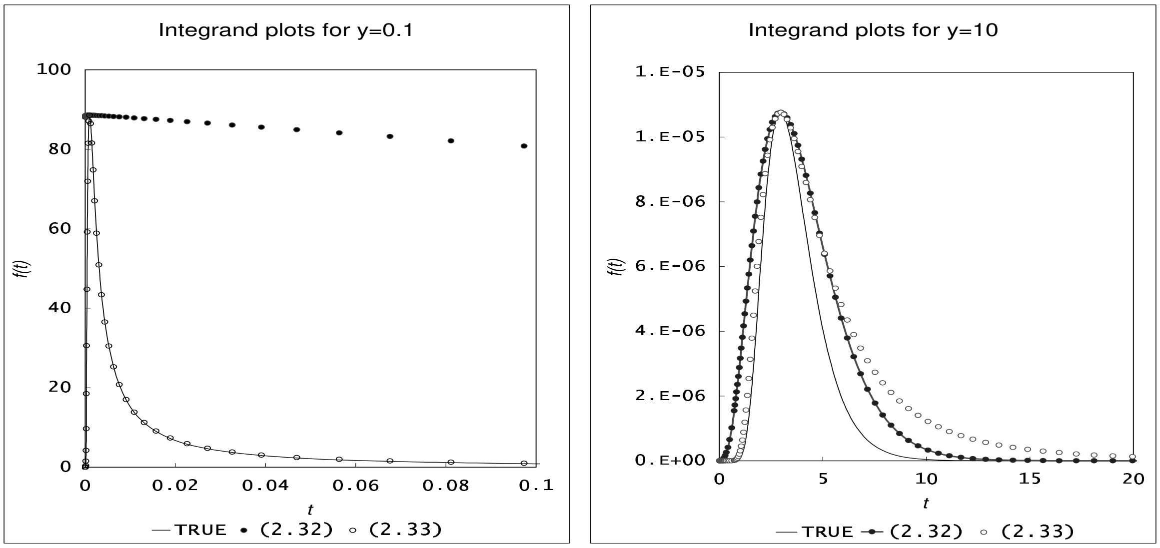

Figure 2.2: Integrand plots for $\alpha = 0.25$ and $\nu = 1$

Figure 2.2 presents the behavior of the integrand functions (2.31), (2.32), and (2.33) for $\alpha = 0.25$ and $\nu = 1$. For this pair of shape parameters $\alpha - \frac{\nu}{2} < 0$, so $p(y;\alpha,\nu) \to +\infty$ as $y \to 0$. The sharp peaks of $f(t)$ are clearly shown by the curve "TRUE" in the left plot. In this case, $t_{\max} \approx 0.001$, while $\zeta_{+} \approx 1.251$. It can be seen that (2.29) gives a better estimate than (2.28) does. In the right plot, the curves associated with (2.32) and (2.33) are not significantly different and the estimate is not as accurate as the more accurate one shown in the left plot. However, both estimates give the correct scale of the pdf.

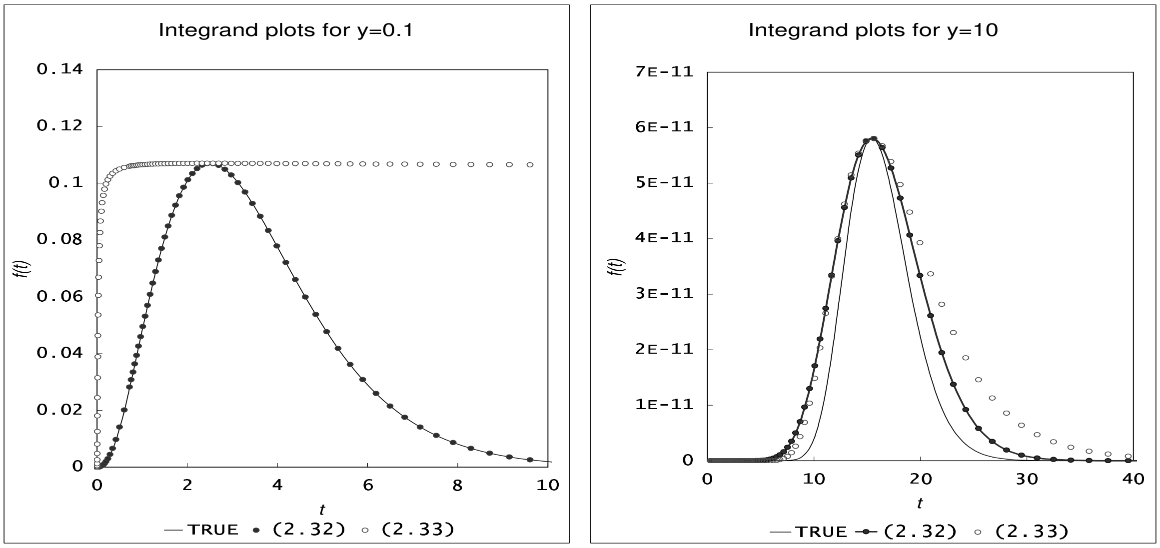

Figure 2.3: Integrand plots for $\alpha = 4$ and $\nu = 1$

To give more intuitive understanding, another set of two plots are presented in Figure 2.3 for $\alpha = 4$ and $\nu = 1$. Hence $\alpha - \nu > 0$. From the left plot, we can see that (2.28) gives a very accurate estimate to the true function, while (2.29) does not. In fact, in this case $\zeta_+ \approx 0.008$ which implied by the comment following (2.29) that estimate (2.29) does not apply. The right plot also shows that (2.28) gives a better estimate than (2.29) does, although both estimates are not as accurate as the one in the left plot. But we can see that both estimates give the correct scale of the pdf.

Now we consider the upper bounds on the pdf for the case $\nu < 0$. From THEOREM 3 it is known that $t_{\max} = 0$ if $\alpha - \frac{\nu}{2} - 1 \leq 0$. Thus in this case the pdf can be estimated either as

$$\begin{aligned} p(y;\alpha,\nu) &= K(\alpha,\nu)\int_0^\infty e^{-\lambda t^{|\nu|}} t^{\alpha-\frac{\nu}{2}-1} e^{-t} dt \\ &\leq K(\alpha,\nu)\int_0^\infty t^{\alpha-\frac{\nu}{2}-1} e^{-t} dt \\ &= K(\alpha,\nu)\Gamma(\alpha-\nu/2) \qquad (2.34) \end{aligned}$$

or as

$$p(y;\alpha,\nu) \leq K(\alpha,\nu)\int_0^\infty e^{-\lambda t^{|\nu|}} t^{\alpha-\frac{\nu}{2}-1} dt$$

$$
\begin{aligned}
&= K(\alpha,\nu)\int_0^\infty e^{-z}\left(\frac{z}{\lambda}\right)^{\frac{\alpha-\frac{\nu}{2}-1}{|\nu|}}\lambda^{-\frac{1}{|\nu|}}\frac{1}{|\nu|}z^{\frac{1}{|\nu|}-1}dz \text{ (by letting } \lambda t^{|\nu|}=z)\\
&= K(\alpha,\nu)\frac{1}{|\nu|}\lambda^{-\frac{\alpha-\nu/2}{|\nu|}}\int_0^\infty e^{-z}z^{\frac{\alpha-\frac{\nu}{2}}{|\nu|}-1}dz\\
&= K(\alpha,\nu)\frac{1}{|\nu|}\lambda^{-\frac{\alpha-\nu/2}{|\nu|}}\Gamma\left(\frac{\alpha-\nu/2}{|\nu|}\right). \qquad (2.35)
\end{aligned}
$$

So from (2.34) and (2.35) we have

$$
p(y;\alpha,\nu)\le K(\alpha,\nu)\min\left\{\Gamma(\alpha-\nu/2),\,\frac{1}{|\nu|}\lambda^{-\frac{\alpha-\nu/2}{|\nu|}}\Gamma\left(\frac{\alpha-\nu/2}{|\nu|}\right)\right\}. \qquad (2.36)
$$

To have some understanding on how these estimates perform, two examples for $y = 0.1$ and $y = 10$ with $\alpha = 0.6$ and $\nu = -0.4$ are presented below. Figure 2.4 presents the plots of the integrands

$$
K(\alpha,\nu)e^{-\lambda t^{|\nu|}}t^{\alpha-\frac{\nu}{2}-1}e^{-t}, \qquad (2.37)
$$

denoted by "TRUE", which corresponds to the true pdf $p(y,\alpha,\nu)$;

$$
K(\alpha,\nu)t^{\alpha-\frac{\nu}{2}-1}e^{-t}, \qquad (2.38)
$$

denoted by (2.38), which corresponds to the integrand function associated with the estimate (2.34); and

$$
K(\alpha,\nu)e^{-\lambda t^{|\nu|}}t^{\alpha-\frac{\nu}{2}-1}, \qquad (2.39)
$$

denoted by (2.39), which corresponds to the integrand function associated with the estimate (2.35). Since $\alpha-\frac{\nu}{2}-1=-0.2<0$, $t_{\max}=0$. In the left plot, we can see that (2.38) gives a better approximation to (2.37) than (2.39) does. Note that when $\nu<0$, the pdf $p(y;\alpha,\nu)$ is always finite. We know that (2.34) gives an estimate independent of y, while (2.35) gives an estimate that goes to infinity when $y\to 0$. So, as expected, (2.38) gives a better approximation to (2.37) than (2.39) does. In fact, (2.34) gives $p(0.1;0.6,-0.4)\le 0.54760682$, while (2.35) gives $p(0.1;0.6,-0.4)\le 4949.333138$. In the right plot, (2.39) gives a better approximation to (2.37) than (2.38) does. In this case, (2.34) still gives $p(10;0.6,-0.4)\le 0.54760682$, while (2.35) gives $p(10;0.6,-0.4)\le 4.94933E-05$.

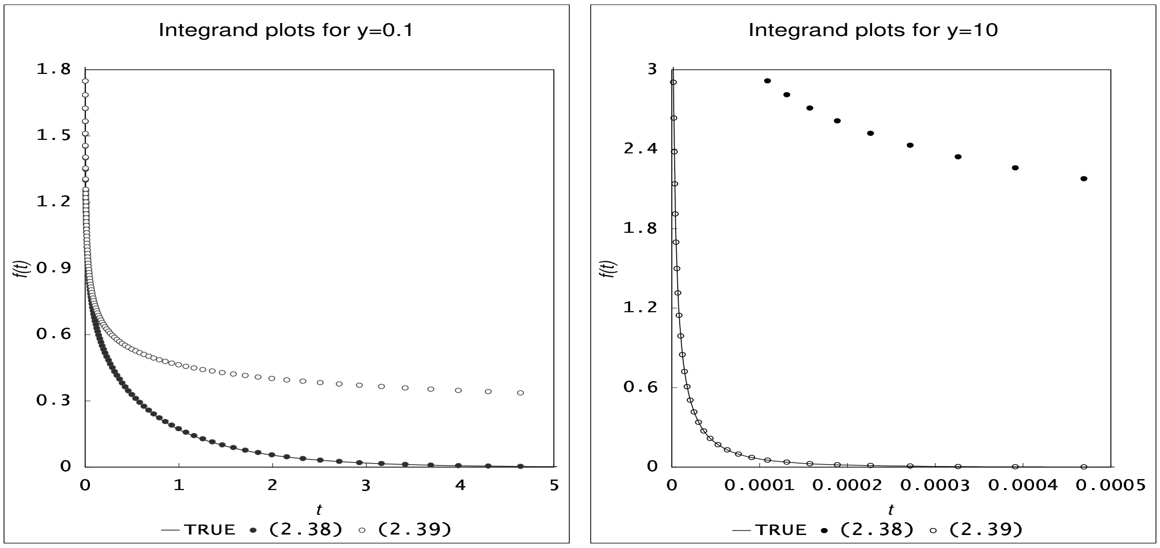

Figure 2.4: Integrand plots for $\alpha = 0.6$ and $\nu = -0.4$

When $\alpha - \frac{\nu}{2} - 1 > 0$, it is known from THEOREM 3 that $t_{\max} > 0$. As in the case $\nu > 0$ considered earlier, the integrand function can be written as the multiplication of two functions:

$$f(t) = e^{-\lambda t^{|\nu|}} t^{\alpha - \frac{\nu}{2} - 1} e^{-t} = \left(e^{-\lambda t^{|\nu|}} t^{\zeta_-}\right) \cdot \left(t^{\alpha - \frac{\nu}{2} - 1 - \zeta_-} e^{-t}\right).$$

By choosing ζ_- appropriately, we can ensure that $e^{-\lambda t^{|\nu|}} t^{\zeta_-}$ and $t^{\alpha - \frac{\nu}{2} - 1 - \zeta_-} e^{-t}$ attain their maximum values at $t_{\max}$. Similar to the derivation for $\nu > 0$ we get $\zeta_- = \lambda |\nu| t_{\max}^{|\nu|} > 0$. From (2.26) we can see that ζ_- satisfies

$$t_{\max} = \left(\alpha - \frac{\nu}{2} - 1\right) - \zeta_-. \tag{2.40}$$

We can estimate the pdf either by

$$\begin{aligned} p(y; \alpha, \nu) &= K(\alpha, \nu) \int_0^\infty e^{-\lambda t^{|\nu|}} t^{\alpha - \frac{\nu}{2} - 1} e^{-t} dt \\ &= K(\alpha, \nu) \int_0^\infty \left(e^{-\lambda t^{|\nu|}} t^{\zeta_-}\right) \left(t^{\alpha - \frac{\nu}{2} - 1 - \zeta_-} e^{-t}\right) dt \\ &\leq K(\alpha, \nu) \left(e^{-\lambda t_{\max}^{|\nu|}} t_{\max}^{\zeta_-}\right) \int_0^\infty t^{t_{\max}} e^{-t} dt \\ &= K(\alpha, \nu) \left(e t_{\max}^{\nu}\right)^{-\frac{\lambda}{t_{\max}^{\nu}}} \Gamma(t_{\max} + 1), \end{aligned} \tag{2.41}$$

or by

$$
\begin{aligned}
p(y;\alpha,\nu) &\leq K(\alpha,\nu)\left(e^{-t_{\max}}t_{\max}^{t_{\max}}\right)\int_0^\infty e^{-\lambda t^{|\nu|}}t^{\zeta_-}dt \\
&= K(\alpha,\nu)\left(e^{-1}t_{\max}\right)^{t_{\max}}\int_0^\infty e^{-z}\left(\frac{z}{\lambda}\right)^{\frac{\zeta_-}{|\nu|}}\lambda^{-\frac{1}{|\nu|}}\frac{1}{|\nu|}z^{\frac{1}{|\nu|}-1}dz \text{ (by letting } \lambda t^{|\nu|}=z) \\
&= K(\alpha,\nu)\left(e^{-1}t_{\max}\right)^{t_{\max}}\frac{1}{|\nu|}\lambda^{-\frac{\zeta_-+1}{|\nu|}}\int_0^\infty e^{-z}z^{\frac{\zeta_-+1}{|\nu|}-1}dz \\
&= K(\alpha,\nu)\frac{1}{|\nu|}\lambda^{-\frac{\zeta_-+1}{|\nu|}}\left(e^{-1}t_{\max}\right)^{t_{\max}}\Gamma\left(\frac{\zeta_-+1}{|\nu|}\right). \qquad (2.42)
\end{aligned}
$$

Note that both (2.41) and (2.42) are upper bounds on $p(y;\alpha,\nu)$, so we have

$$
p(y;\alpha,\nu)\leq K(\alpha,\nu)\min\left\{(et_{\max}^{\nu})^{-\frac{\lambda}{t_{\max}^{\nu}}}\Gamma(t_{\max}+1),\frac{1}{|\nu|}\lambda^{-\frac{\zeta_-+1}{|\nu|}}\left(e^{-1}t_{\max}\right)^{t_{\max}}\Gamma\left(\frac{\zeta_-+1}{|\nu|}\right)\right\}. \qquad (2.43)
$$

To gain an intuitive understanding on how these two estimates work, some examples are presented below. Figure 2.5 presents the plots of the functions

$$
K(\alpha,\nu)e^{-\lambda t^{|\nu|}}t^{\alpha-\frac{\nu}{2}-1}e^{-t}, \qquad (2.44)
$$

denoted by "TRUE", which corresponds to the true pdf $p(y;\alpha,\nu)$;

$$
K(\alpha,\nu)\left(et_{\max}^{\nu}\right)^{-\frac{\lambda}{t_{\max}^{\nu}}}t^{t_{\max}}e^{-t}, \qquad (2.45)
$$

denoted by (2.45), which corresponds to the integrand function associated with the estimate (2.41); and

$$
K(\alpha,\nu)\left(e^{-1}t_{\max}\right)^{t_{\max}}e^{-\lambda t^{|\nu|}}t^{\zeta_-}, \qquad (2.46)
$$

denoted by (2.46), which corresponds to the integrand function associated with the estimate (2.42). In these plots, $\alpha = 4$ and $\nu = -1$. For this pair of shape parameters we have $\alpha - \frac{\nu}{2} > 0$, thus $t_{\max} > 0$. In the left plot, we can see that (2.45) gives a better approximation to (2.44) than (2.46) does. While in the right plot, (2.46) gives a better approximation to (2.44) than (2.45) does.

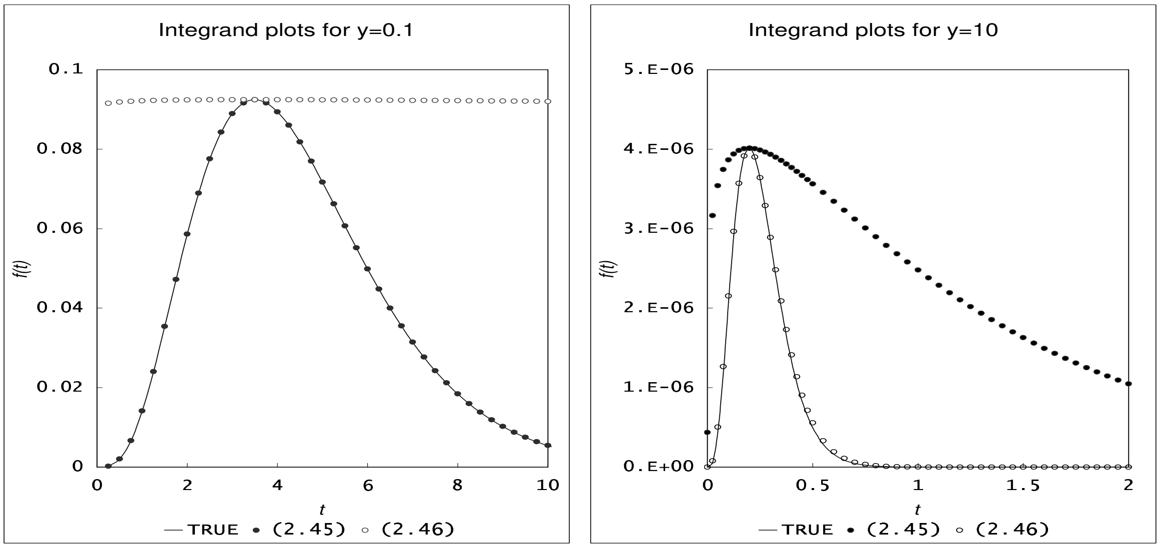

Figure 2.5: Integrand plots for $\alpha = 4$ and $\nu = -1$

2.4 More about the Integrand

The maximum of the integrand function $f(t)$ and the upper bounds on the pdf $p(y;\alpha,\nu)$ have been discussed in Section 2.2 and Section 2.3, respectively. In this section we see when the integrand function has a sharp peak and how its maximizer moves.

First, we consider the case $\nu = 0$. From (2.1), we obtain that for any y the pdf has a closed-form expression

$$p(y;\alpha,0) = \frac{1}{\sqrt{2\pi}} e^{-\frac{y^2}{2}}.$$

Hence this is a simple case because for any y the pdf can be easily computed.

Second, we consider the case $\nu > 0$. When $y = 0$, we get from (1.6) that

$$p(0;\alpha,\nu) = K(\alpha,\nu)\Gamma(\alpha - \nu/2). \tag{2.47}$$

Noting the definition of the Gamma function given in integral form, we know from (2.47) that $p(0;\alpha,\nu)$ is finite for any shape parameters α and ν satisfying $\alpha - \nu/2 > 0$ and it can be easily computed, while it is infinite when $\alpha - \nu/2 \le 0$. When $y \neq 0$, from THEOREM 2 and (2.30), we know that $p(y;\alpha,\nu)$ is finite for any shape parameters $\alpha > 0$ and $\nu > 0$.

To see when the integrand function has a sharp peak we need to know the position of the integrand's maximizer and how it moves. By (2.18), the equation that $t_{\max}$ satisfies, it can be shown that $t_{\max}$ is strictly increasing in $|y|$. Furthermore, we have $t_{\max} \to 0$ as $y \to 0$ when $\alpha - \nu/2 - 1 \leq 0$. Thus the integrand function $f(t)$ may have a sharp peak around $t = 0$ when y is very small and $\alpha - \nu/2 - 1 \leq 0$. Under any other circumstances, the integrand function's maximizer will not approach zero although it might be small.

In Figure 2.6, we illustrate how the integrand function's maximizer moves with y. In the left plot the shape parameters are set to $\alpha = 1, \nu = 2$. Hence $\alpha - \nu/2 - 1 < 0$. When $y = 0.01$, the corresponding integrand function $f(t)$ has a very sharp high peak around $t = 0$. When $y = 0.1$, the corresponding integrand $f(t)$ also has a sharp peak near $t = 0$. When $y = 1$, the integrand's maximizer is around $t = 1$. In addition, we can see that in this case the integrand function does not have a sharp peak. In the right plot, the shape parameters are set to $\alpha = 5, \nu = 2$. Hence $\alpha - \nu/2 - 1 > 0$. We can see that the three curves do not have sharp peaks.

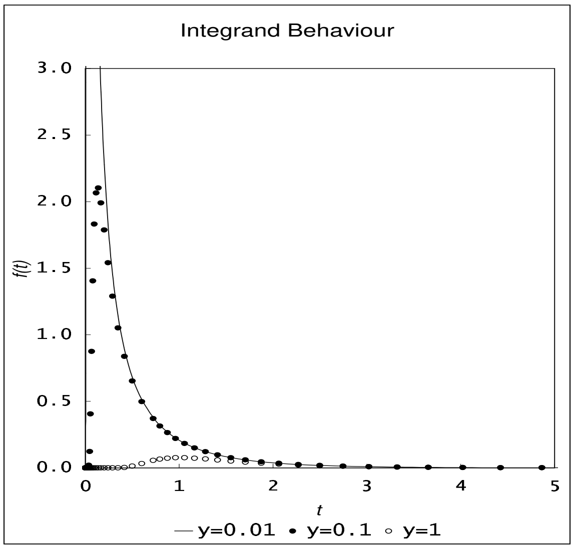

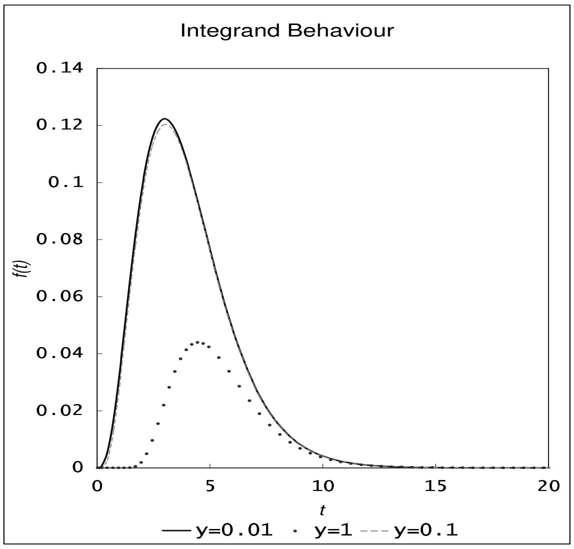

Figure 2.6: Integrand function evolution for positive ν

Finally, we consider the case $\nu < 0$. When $y = 0$, $p(0; \alpha, \nu)$ satisfies (2.47) too. From (2.47) we can see that $p(0; \alpha, \nu)$ is finite if $\alpha + \nu > 0$ and it can be easily computed.

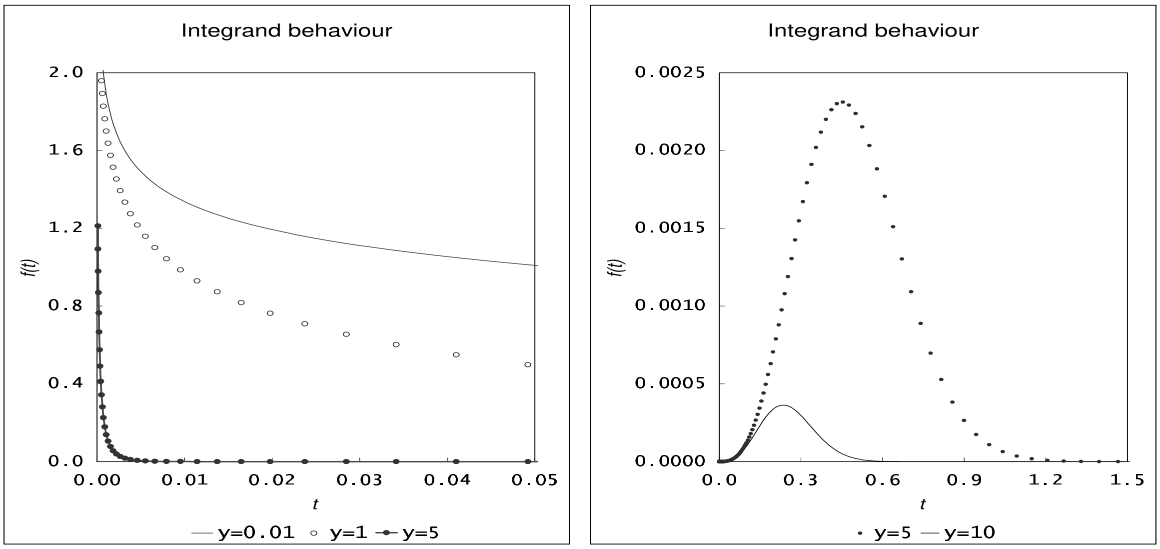

Figure 2.7: Integrand function evolution for negative ν

When $y \neq 0$, by THEOREM 3, $f(t)$ attains its maximum at $t = 0$ when $\alpha - \nu/2 - 1 \leq 0$ (the maximum may be infinite if $\alpha - \nu/2 - 1 < 0$). From the curves shown in the left plot of Figure 2.7 with $\alpha = 0.6, \nu = -0.5$, we see that when $y = 5$, the integrand function not only goes to infinity at $t = 0$ but also behaves like the Dirac delta function. Evaluating such an improper integral is not easy because the larger the $|y|$, the more the integrand function behaves like the Dirac delta function around $t = 0$. When $\alpha - \nu/2 - 1 > 0$, it can be shown from (2.26) that $t_{\max}$ is strictly decreasing in $|y|$. Furthermore, $t_{\max} \to 0$ when $|y| \to \infty$. The curves in the right plot of Figure 2.7 with $\alpha = 3, \nu = -2$, illustrate this. From the curve for $y = 10$ we see that the interval $[0, 1]$ gives the main contribution to the pdf $p(10; \alpha, \nu)$.

Chapter 3

Computation of the Probability Density Function

3.1 Introduction

Properties of the probability density function

$$p(y;\alpha,\nu) = \frac{1}{\Gamma(\alpha)}\sqrt{\frac{\Gamma(\alpha+\nu)}{2\pi\Gamma(\alpha)}}\int_0^\infty e^{-\frac{y^2}{2}\frac{\Gamma(\alpha+\nu)}{\Gamma(\alpha)}\frac{1}{t^\nu}} t^{\alpha-\frac{\nu}{2}-1}e^{-t}dt \tag{3.1}$$

were discussed in the previous chapter. In this chapter, we will address the problem of how to compute this pdf.

For convenience, we introduce the function

$$f(t;y,\alpha,\nu) = e^{-\frac{y^2}{2}\frac{\Gamma(\alpha+\nu)}{\Gamma(\alpha)}\frac{1}{t^\nu}} t^{\alpha-\frac{\nu}{2}-1}e^{-t} \tag{3.2}$$

to denote the integrand in the improper integral (3.1). Recalling the definition

$$K(\alpha,\nu) = \frac{1}{\Gamma(\alpha)}\sqrt{\frac{\Gamma(\alpha+\nu)}{2\pi\Gamma(\alpha)}}$$

in (2.7), we can rewrite (3.1) in the compact form

$$p(y;\alpha,\nu) = K(\alpha,\nu)\int_0^\infty f(t;y,\alpha,\nu)dt. \tag{3.3}$$

Let $\tilde{p}(y;\alpha,\nu)$ denote the tightest upper bound on $p(y;\alpha,\nu)$ obtained in the previous chapter. Then from (2.30), (2.36), and (2.43) we have

$$\tilde{p}(y;\alpha,\nu) = \min\{p_1(y;\alpha,\nu), p_2(y;\alpha,\nu)\}, \tag{3.4}$$

where the two estimates $p_1(y;\alpha,\nu)$ and $p_2(y;\alpha,\nu)$ are given by

$$\begin{aligned} p_1(y;\alpha,\nu) &= K(\alpha,\nu)\,(et^{\nu}_{\max})^{-\frac{\lambda}{t^{\nu}_{\max}}}\,\Gamma(t_{\max}+1), && (3.5)\\ p_2(y;\alpha,\nu) &= K(\alpha,\nu)\frac{1}{\nu}\lambda^{\frac{1-\zeta_+}{\nu}}\left(e^{-1}t_{\max}\right)^{t_{\max}}\Gamma\left(\frac{\zeta_+-1}{\nu}\right) && (3.6)\end{aligned}$$

when $\nu > 0$; or

$$\begin{aligned} p_1(y;\alpha,\nu) &= K(\alpha,\nu)\Gamma(\alpha-\nu/2), && (3.7)\\ p_2(y;\alpha,\nu) &= K(\alpha,\nu)\frac{1}{|\nu|}\lambda^{-\frac{\alpha-\nu/2}{|\nu|}}\Gamma\left(\frac{\alpha-\nu/2}{|\nu|}\right) && (3.8)\end{aligned}$$

when $\nu < 0$ and $t_{\max} = 0$; or

$$\begin{aligned} p_1(y;\alpha,\nu) &= K(\alpha,\nu)\,(et^{\nu}_{\max})^{-\frac{\lambda}{t^{\nu}_{\max}}}\,\Gamma(t_{\max}+1), && (3.9)\\ p_2(y;\alpha,\nu) &= K(\alpha,\nu)\frac{1}{|\nu|}\lambda^{-\frac{\zeta_-+1}{|\nu|}}\left(e^{-1}t_{\max}\right)^{t_{\max}}\Gamma\left(\frac{\zeta_-+1}{|\nu|}\right) && (3.10)\end{aligned}$$

when $\nu < 0$ and $t_{\max} > 0$. Here $\lambda = \frac{y^2}{2}\frac{\Gamma(\alpha+\nu)}{\Gamma(\alpha)}$, $t_{\max} \geq 0$ is the unique maximizer of $f(t;y,\alpha,\nu)$ in $[0,\infty)$, $\zeta_+ = \lambda\nu/t^{\nu}_{\max}$ and $\zeta_- = \lambda|\nu|t^{|\nu|}_{\max}$. We say, for specified y, α and ν, that $p_1(y;\alpha,\nu)$ gives a better estimate than $p_2(y;\alpha,\nu)$ if $\tilde{p}(y;\alpha,\nu) = p_1(y;\alpha,\nu) \leq p_2(y;\alpha,\nu)$. Otherwise we say that $p_2(y;\alpha,\nu)$ gives a better estimate than $p_1(y;\alpha,\nu)$.

There are three special cases for which the pdf has a closed-form expression. First, when $\nu = 0$, $p(y;\alpha,\nu)$ reduces to the pdf for the normal distribution with mean 0 and standard deviation 1 given by

$$p(y;\alpha,0) = \frac{1}{\sqrt{2\pi}}e^{-\frac{y^2}{2}}. \tag{3.11}$$

Second, when $y = 0$, $p(y;\alpha,\nu)$ has the closed-form representation

$$p(0;\alpha,\nu) = K(\alpha,\nu)\Gamma(\alpha-\nu/2). \tag{3.12}$$

In this case, $p(0; \alpha, \nu)$ goes to infinity if $\alpha < \nu/2$. Finally, when $\nu = -1$, $p(y; \alpha, \nu)$ is related to the t-distribution of degree 2α by the formula

$$p(y; \alpha, -1) = \frac{\Gamma(\alpha + 0.5)}{\Gamma(\alpha)\sqrt{2\pi(\alpha - 1)}} \left(1 + \frac{y^2}{2} \frac{1}{\alpha - 1}\right)^{-(\alpha+0.5)} = \sqrt{\frac{\alpha}{\alpha - 1}} p_{t_{2\alpha}} \left(y \sqrt{\frac{\alpha}{\alpha - 1}}\right), \tag{3.13}$$

where

$$p_{t_\delta}(t) = \frac{\Gamma\left(\frac{1}{2}(\delta + 1)\right)}{\sqrt{\pi\delta}\,\Gamma\left(\frac{1}{2}\delta\right)} \left(1 + \frac{t^2}{\delta}\right)^{-(\delta+1)/2}$$

is the $t-$distribution of degree δ [7, Chapter 28]. (Recall that we require $\alpha + \nu > 0$. So, if $\nu = -1$, $\alpha > 1$. Hence the terms under the square roots are positive.)

Except for these three cases, there is no known closed-form expression for $p(y; \alpha, \nu)$. Hence, we must resort to numerical approximations. To evaluate $p(y; \alpha, \nu)$ to within the relative accuracy of $\varepsilon = 10^{-5}$, we will use different methods depending on whether $\nu > 0$ or $\nu < 0$ and whether or not the integrand function $f(t; y, \alpha, \nu)$ has a sharp peak. A top-level algorithm for computing the $p(y; \alpha, \nu)$ is outlined in Algorithm 1. In Section 3.2, we propose an algorithm for $\nu > 0$. An algorithm for $\nu < 0$, but $\nu \neq -1$, is presented in Section 3.3. An improved method for the case $\nu < 0$ is discussed in Section 3.4.

3.2 A Method for $\nu > 0$

In this section we consider a numerical method for computing the pdf $p(y; \alpha, \nu)$ for the case $\nu > 0$. One of two different algorithms will be applied, depending on whether or not the integrand function $f(t; y, \alpha, \nu)$ has a sharp peak. We will explain at the end of this section how to decide whether or not the integrand has a sharp peak.

3.2.1 When the integrand does not have a sharp peak

When the integrand function $f(t; y, \alpha, \nu)$ does not have a sharp peak, we propose truncating the semi-infinite interval $[0, \infty)$ to a bounded subinterval $[L_1, U_1] \subset [0, \infty)$. Instead of

Algorithm 1 Approximate $p(y;\alpha,\nu)$ for any $y \in (-\infty,+\infty)$, $\alpha > 0$, and $\nu \in (-\alpha,+\infty)$

if $((\alpha \leq 0)$ or $(\alpha+\nu \leq 0))$ **then**

  Return "Invalid parameter(s)";

end if

if $(y = 0)$ **then**

  if $(\alpha - \frac{\nu}{2} \leq 0)$ **then**

    $p(0;\alpha,\nu) = +\infty$

  else

    $p(0;\alpha,\nu) = \frac{\Gamma(\alpha-\nu/2)}{\Gamma(\alpha)}\sqrt{\frac{\Gamma(\alpha+\nu)}{2\pi\Gamma(\alpha)}}$

  end if

else

  if $(\nu = 0)$ **then**

    $p(y;\alpha,0) = \frac{1}{\sqrt{2\pi}}e^{-\frac{y^2}{2}}$;

  else if $(\nu > 0)$ **then**

    Calculate $p(y;\alpha,\nu)$ using an algorithm for $\nu > 0$;

  else

    if $(\nu = -1)$ **then**

      $p(y;\alpha,-1) = \frac{\Gamma(\alpha+0.5)}{\Gamma(\alpha)\sqrt{2\pi(\alpha-1)}}\left(1+\frac{y^2}{2}\frac{1}{\alpha-1}\right)^{-(\alpha+0.5)}$;

    else

      Calculate $p(y;\alpha,\nu)$ using an algorithm for $\nu < 0$;

    end if

  end if

end if

Return $p(y;\alpha,\nu)$.

numerically evaluating the improper integral $\int_0^\infty f(t;y,\alpha,\nu)dt$, we will use a quadrature method to approximate the integral of $f(t;y,\alpha,\nu)$ over $[L_1,U_1]$. The lower bound L_1 and the upper bound U_1 are chosen such that

$$K(\alpha,\nu)\int_0^{L_1} f(t;y,\alpha,\nu)dt \le \frac{1}{3}\varepsilon p(y;\alpha,\nu), \quad \text{and} \tag{3.14}$$

$$K(\alpha,\nu)\int_{U_1}^{\infty} f(t;y,\alpha,\nu)dt \le \frac{1}{3}\varepsilon p(y;\alpha,\nu), \tag{3.15}$$

where $\varepsilon = 10^{-5}$ is the relative accuracy requirement for the approximation of $p(y;\alpha,\nu)$ as mentioned in §3.1. These two tails can be ignored since they each make a relative contribution of less than $\frac{1}{3}\varepsilon$ to $p(y;\alpha,\nu)$. From the discussions in Section 2.2 and Section 2.4, we know that $f(t;y,\alpha,\nu)$ is nonnegative and has single maximizer $t_{\max} \in (0,\infty)$. Furthermore, $f(t;y,\alpha,\nu) \to 0$ when $t \to 0$ or $t \to +\infty$. Thus L_1 and U_1 satisfying (3.14) and (3.15), respectively, exist. We will explain in Section 3.2.3 how L_1 and U_1 may be determined.

To speed up the integration process, the interval $[L_1,U_1]$ is further divided into three subintervals $[L_1,L_2]$, $[L_2,U_2]$ and $[U_2,U_1]$. The points L_2 and U_2 are chosen such that

$$K(\alpha,\nu)\int_0^{L_2} f(t;y,\alpha,\nu)dt \approx 1\% p(y;\alpha,\nu), \quad \text{and} \tag{3.16}$$

$$K(\alpha,\nu)\int_{U_2}^{\infty} f(t;y,\alpha,\nu)dt \approx 1\% p(y;\alpha,\nu), \tag{3.17}$$

respectively. Note that $\frac{1}{3}\varepsilon < 1\%$, thus we have $L_1 < L_2 < U_2 < U_1$. We will discuss in Section 3.2.3 how L_2 and U_2 may be determined. Numerical results presented in Table 3.1 support the proposal of this strategy. In this table, "Single interval" denotes the number of function evaluations performed by the adaptive Gauss-Kronrod quadrature method when it is applied to the entire interval $[L_1,U_1]$. The entry "Three intervals" denotes the number of function evaluations performed by the method when the quadrature method is applied to each of the intervals $[L_1,L_2]$, $[L_2,U_2]$ and $[U_2,U_1]$.

The reason we choose L_2 and U_2 as 1% points instead of any other interior points is that it is expected that the regions covered by $[L_1,L_2] \cup [U_2,U_1]$ and $[L_2,U_2]$ have

$(y;\alpha,\nu)$	Single interval	Three intervals
$(1.2;4,-1.2)$	147	21/21/21
$(1.2;4,1.2)$	147	21/21/21
$(1.2;0.4,1.2)$	651	21/189/21

Table 3.1: Comparison of the numbers of function evaluations

almost the same length and that the integrals over $[L_1, L_2]$ and $[U_2, U_1]$ are almost equal in value. By studying the integrand for the Gamma function, which has some similarity to $f(t;y,\alpha,\nu)$ and is used in evaluating the pdf $p(y;\alpha,\nu)$, we have found that using the 1% points reduces the overall computation time. We do not know whether or not this is an optimal choice. We will study this in the future.

The integral over $[L_2, U_2]$ is evaluated with a relative accuracy tolerance of $\frac{1}{9}\varepsilon$. The integrals over $[L_1, L_2]$ and $[U_2, U_1]$ are evaluated with relative accuracy tolerance of $\frac{1}{9}\varepsilon \times 100$. Let $Q(f(t;y,\alpha,\nu);[a,b];\tau)$ denote a quadrature method applied to the integrand function $f(t;y,\alpha,\nu)$ over $[a,b]$ with a relative accuracy tolerance of τ. Our method for computing $p(y;\alpha,\nu)$ when $f(t;y,\alpha,\nu)$ does not have a sharp peak uses the steps described above and is summarized in Algorithm 2.

Algorithm 2 Approximate $p(y;\alpha,\nu)$ when $\nu > 0$ and $f(t;y,\alpha,\nu)$ has no high peak

Suppose that L_1, L_2, U_2, U_1 have been determined and satisfy

$$0 < L_1 < L_2 < U_2 < U_1 < \infty;$$

Let $p_1 = Q(f(t;y,\alpha,\nu);[L_1,L_2];\frac{100}{9}\varepsilon)$;

Let $p_2 = Q(f(t;y,\alpha,\nu);[L_2,U_2];\frac{1}{9}\varepsilon)$;

Let $p_3 = Q(f(t;y,\alpha,\nu);[U_2,U_1];\frac{100}{9}\varepsilon)$;

$p(y;\alpha,\nu) := K(\alpha,\nu)(p_1+p_2+p_3)$.

In this algorithm, it is assumed that $K(\alpha,\nu)$ can be computed accurately. Suppose that the quadrature method Q can evaluate the integrals to within the required relative error tolerance τ and that all points L_i and U_i, $i = 1, 2$, satisfy the inequalities (3.14)-(3.15) and that we have equality in (3.16)-(3.17). Then we can see that as an approximation to $p(y; \alpha, \nu)$, $K(\alpha, \nu)(p_1 + p_2 + p_3)$ satisfies the required relative accuracy requirement. To be specific, we have

$$K(\alpha,\nu)p_1 \in \left(\frac{1}{100} - \frac{1}{3}\varepsilon\right) p(y;\alpha,\nu) \left[1 - \frac{100}{9}\varepsilon, 1 + \frac{100}{9}\varepsilon\right], \tag{3.18}$$

since

$$p_1 \in \left[1 - \frac{100}{9}\varepsilon, 1 + \frac{100}{9}\varepsilon\right] \int_{L_1}^{L_2} f(t; y, \alpha, \nu) dt$$

and

$$\begin{aligned}
& K(\alpha,\nu) \int_{L_1}^{L_2} f(t; y, \alpha, \nu) dt \\
= \; & K(\alpha,\nu) \left[\int_0^{L_2} f(t; y, \alpha, \nu) dt - \int_0^{L_1} f(t; y, \alpha, \nu) dt\right] \\
= \; & \left(\frac{1}{100} - \frac{1}{3}\varepsilon\right) p(y;\alpha,\nu).
\end{aligned}$$

Similarly, we have

$$K(\alpha,\nu)p_2 \in \frac{98}{100} p(y;\alpha,\nu) \left[1 - \frac{\varepsilon}{9}, 1 + \frac{\varepsilon}{9}\right], \tag{3.19}$$

$$K(\alpha,\nu)p_3 \in \left(\frac{1}{100} - \frac{1}{3}\varepsilon\right) p(y;\alpha,\nu) \left[1 - \frac{100}{9}\varepsilon, 1 + \frac{100}{9}\varepsilon\right]. \tag{3.20}$$

From (3.18)-(3.20) we have

$$\begin{aligned}
K(\alpha,\nu)(p_1+p_2+p_3) &\le \left[2\left(\frac{1}{100} - \frac{1}{3}\varepsilon\right)\left(1 + \frac{100}{9}\varepsilon\right) + \frac{98}{100}\left(1 + \frac{\varepsilon}{9}\right)\right] p(y;\alpha,\nu) \\
&= \left[1 + \left(-\frac{4}{9} + \frac{98}{100}\frac{1}{9} - \frac{200}{27}\varepsilon\right)\varepsilon\right] p(y;\alpha,\nu) \\
&< (1+\varepsilon) p(y;\alpha,\nu)
\end{aligned}$$

and

$$\begin{aligned}
K(\alpha,\nu)(p_1+p_2+p_3) &\ge \left[2\left(\frac{1}{100} - \frac{1}{3}\varepsilon\right)\left(1 - \frac{100}{9}\varepsilon\right) + \frac{98}{100}\left(1 - \frac{\varepsilon}{9}\right)\right] p(y;\alpha,\nu) \\
&= \left[1 - \left(\frac{8}{9} + \frac{98}{100}\frac{1}{9} - \frac{200}{27}\varepsilon\right)\varepsilon\right] p(y;\alpha,\nu) \\
&= \left[1 - \varepsilon + \left(\frac{2}{100}\frac{1}{9} + \frac{200}{27}\varepsilon\right)\varepsilon\right] p(y;\alpha,\nu) \\
&> (1-\varepsilon) p(y;\alpha,\nu).
\end{aligned}$$

Thus we have that

$$K(\alpha,\nu)(p_1+p_2+p_3) \in p(y;\alpha,\nu)\,[1-\varepsilon, 1+\varepsilon]\,,$$

which implies that the computed value satisfies our accuracy requirement.

3.2.2 When the integrand has a sharp peak

When the integrand function $f(t;y,\alpha,\nu)$ has a sharp peak, a quadrature method often either fails to give a correct result or spends too much time evaluating the integrand function near the sharp peak. To deal with the sharp peak problem, we compute the integral over an interval in a neighbourhood of the sharp peak using an approximation technique. For the integral over the remaining parts of the interval, we use a quadrature method.

Similar to the case discussed in Section 3.2.1, the infinite interval $[0,\infty)$ is truncated to a finite interval $[L_1, U_1] \subset [0,\infty)$ and $[L_1, U_1]$ is further divided into three subintervals $[L_1, L_2]$, $[L_2, U_2]$ and $[U_2, U_1]$, where L_i and U_i, $i = 1, 2$, are determined as described in Section 3.2.1 and satisfy (3.14)-(3.17).

First, we describe the approximation technique. It is known that when $0 \le t \le T_L$, with T_L not too large, the function e^{-t} is well approximated by a suitably chosen polynomial

$$\mathcal{P}_N(t) = \sum_{i=0}^{N} c_i t^i. \tag{3.21}$$

Many expressions of this form can be found in [1] and [14]. In our method, we use a formula with $T_L = 1$ and $N = 7$ [1, 4.2.45]. The coefficients are

$$\begin{array}{llll} c_0 = 1, & c_1 = -0.9999999995, & c_2 = 0.4999999206, & c_3 = -0.1666653019, \\ c_4 = 0.0416573475, & c_5 = -0.0083013598, & c_6 = 0.0013298820, & c_7 = -0.0001410000. \end{array}$$

Furthermore, this formula satisfies $|\mathcal{P}_N(t) - e^{-t}| \le 10^{-6}$ and $|\mathcal{P}_N(t) - e^{-t}|/e^{-t} \le 10^{-6}$ for any $t \in [0, T_L]$.

We know that a sharp peak occurs only when $t_{\max}$ is small. Thus it is expected that the point at which the sharp peak occurs lies in $[0, T_L]$. In this case, if the function e^{-t} in $f(t; y, \alpha, \nu)$ is replaced by $\mathcal{P}_N(t)$, then the integration over $[0, T_L]$ can be approximated by

$$\begin{aligned}
p_L(T_L) &\triangleq K(\alpha,\nu)\int_0^{T_L} e^{-\frac{\lambda}{t^\nu}} t^{\alpha-\frac{\nu}{2}-1} e^{-t}dt \\
&\approx K(\alpha,\nu)\int_0^{T_L} e^{-\frac{\lambda}{t^\nu}} t^{\alpha-\frac{\nu}{2}-1} \sum_{i=0}^{N} c_i t^i dt \\
&= K(\alpha,\nu)\sum_{i=0}^{N} c_i \int_0^{T_L} e^{-\frac{\lambda}{t^\nu}} t^{\alpha-\frac{\nu}{2}-1+i} dt \\
&= \frac{K(\alpha,\nu)}{\nu}\sum_{i=0}^{N} c_i \lambda^{\frac{\alpha}{\nu}-\frac{1}{2}+\frac{i}{\nu}} \int_{\frac{\lambda}{T_L^\nu}}^{\infty} e^{-z} z^{-\frac{\alpha-\nu/2+i}{\nu}-1} dz \qquad \text{(by letting } \tfrac{\lambda}{t^\nu} = z\text{)} \\
&= \frac{K(\alpha,\nu)}{\nu}\sum_{i=0}^{N} c_i \lambda^{\frac{\alpha}{\nu}-\frac{1}{2}+\frac{i}{\nu}} \Gamma\left(\frac{\lambda}{T_L^\nu}, -\frac{\alpha-\nu/2+i}{\nu}\right),
\end{aligned} \tag{3.22}$$

where $\Gamma(\tau, \varsigma) = \int_\tau^\infty t^{\varsigma-1}e^{-t}dt$, with $\tau = 0$ and $\varsigma > 0$, or $\tau > 0$ and $\varsigma \in R$, is the complementary incomplete Gamma (CIG) function [1, Chapter 6]. (The symbol Γ is overloaded. The one-parameter notation $\Gamma(\cdot)$ denotes the standard Gamma function, whereas the two-parameter notation $\Gamma(\cdot,\cdot)$ denotes the complementary incomplete Gamma function. The meaning of the symbol Γ will be clear from the context.) Hence we can approximate the integral $p_L(T_L)$ by computing $N + 1$ CIG functions. In practice, we prefer to use this technique to evaluate the part of $p(y; \alpha, \nu)$ from L_1 to T_L when $L_2 \le T_L$.

Suppose that the Gamma function and the CIG function can be computed accurately. Recall that $|\mathcal{P}_N(t) - e^{-t}| \le 10^{-6}e^{-t}$. Hence the relative error of approximating $p_L(T_L)$ by (3.22) is bounded by

$$\begin{aligned}
&\frac{\left|K(\alpha,\nu)\left(\int_0^{T_L} e^{-\frac{\lambda}{t^\nu}} t^{\alpha-\frac{\nu}{2}-1} e^{-t}dt - \int_0^{T_L} e^{-\frac{\lambda}{t^\nu}} t^{\alpha-\frac{\nu}{2}-1} \sum_{i=0}^N c_i t^i dt\right)\right|}{K(\alpha,\nu)\int_0^{T_L} e^{-\frac{\lambda}{t^\nu}} t^{\alpha-\frac{\nu}{2}-1} e^{-t}dt} \\
= &\frac{\left|\int_0^{T_L} e^{-\frac{\lambda}{t^\nu}} t^{\alpha-\frac{\nu}{2}-1} \left(e^{-t} - \sum_{i=0}^N c_i t^i\right) dt\right|}{\int_0^{T_L} e^{-\frac{\lambda}{t^\nu}} t^{\alpha-\frac{\nu}{2}-1} e^{-t}dt} \\
\le &\frac{\int_0^{T_L} e^{-\frac{\lambda}{t^\nu}} t^{\alpha-\frac{\nu}{2}-1} e^{-t} 10^{-6} dt}{\int_0^{T_L} e^{-\frac{\lambda}{t^\nu}} t^{\alpha-\frac{\nu}{2}-1} e^{-t}dt} \\
= &10^{-6}.
\end{aligned}$$

Therefore, this approximation is acceptable.

In addition, note that the exponential function $e^{-\frac{\lambda}{t^\nu}}$ appears in $f(t;y,\alpha,\nu)$. When $\lambda \leq T_L^{\nu+1}$, we can see that $0 < \frac{\lambda}{t^\nu} \leq T_L$ for any $t \in [T_L, \infty)$. In this case, $e^{-\frac{\lambda}{t^\nu}}$ can be well approximated by

$$\sum_{i=0}^{N} c_i \left(\frac{\lambda}{t^\nu}\right)^i = \sum_{i=0}^{N} c_i \lambda^i t^{-i\nu}. \tag{3.23}$$

Thus the integration over $[T_L, \infty)$ can be approximated by

$$\begin{aligned} p_R(T_L) &\triangleq K(\alpha,\nu)\int_{T_L}^{\infty} e^{-\frac{\lambda}{t^\nu}} t^{\alpha-\frac{\nu}{2}-1} e^{-t} dt \\ &= K(\alpha,\nu)\int_{T_L}^{\infty} \sum_{i=0}^{N} c_i \lambda^i t^{-i\nu} t^{\alpha-\frac{\nu}{2}-1} e^{-t} dt \\ &= K(\alpha,\nu)\sum_{i=0}^{N} c_i \lambda^i \int_{T_L}^{\infty} t^{\alpha-\frac{\nu}{2}-i\nu-1} e^{-t} dt \\ &= K(\alpha,\nu)\sum_{i=0}^{N} c_i \lambda^i \Gamma\left(T_L, \alpha - \frac{\nu}{2} - i\nu\right). \end{aligned} \tag{3.24}$$

As in the previous case, we can show that this approximation is within the relative error of 10^{-6}. Therefore, $p(y;\alpha,\nu)$ can be approximated by $p(y;\alpha,\nu) := p_L(T_L) + p_R(T_L)$.

Unfortunately, $\lambda \leq T_L^{\nu+1}$ does not always hold. So the infinite interval $[0,\infty)$ may not be completely covered by $[0, T_L]$ and $[T_L, \infty)$. However, for any λ there always exists a threshold $T_U > 0$ such that $\lambda / T_U^\nu = T_L$ (note that $\lambda \neq 0$). Then for any $t \geq T_U$ we have $\lambda / t^\nu \leq T_L$. Hence (3.23) can be used to approximate $e^{-\frac{\lambda}{t^\nu}}$ for $t \in [T_U, \infty)$, and the integration over $[T_U, +\infty)$ can be approximated by

$$p_R(T_U) = K(\alpha,\nu)\sum_{i=0}^{N} c_i \lambda^i \Gamma\left(T_U, \alpha - \frac{\nu}{2} - i\nu\right), \tag{3.25}$$

which is similar to (3.24) and is within the relative error of 10^{-6} too.

To avoid very small values of λ / T_L^ν that may cause numerical difficulty in computing the CIG functions, we approximate $p(y;\alpha,\nu)$ by

$$p(y;\alpha,\nu) := p_L((T_L + T_U)/2) + p_R((T_L + T_U)/2), \tag{3.26}$$

instead of by $p(y;\alpha,\nu) := p_L(T_L) + p_R(T_L)$ when $\lambda \leq T_L^{\nu+1}$.

When $\lambda > T_L^{\nu+1}$, which implies that $T_U > T_L$, the infinite interval $[0, \infty)$ can not be completely covered by $[0, T_L]$ and $[T_U, \infty)$. So we must resort to a quadrature method to approximate the integral over the remaining interval $[T_L, T_U]$. In our algorithm, (3.22) is applied when $L_2 \leq T_L$, and (3.25) is applied when $U_2 \leq T_U$. Thus when $\lambda > T_L^{\nu+1}$, by considering the relative positions of L_2, T_L, U_2 and T_U, we only need to consider the eight cases shown in Figure 3.1.

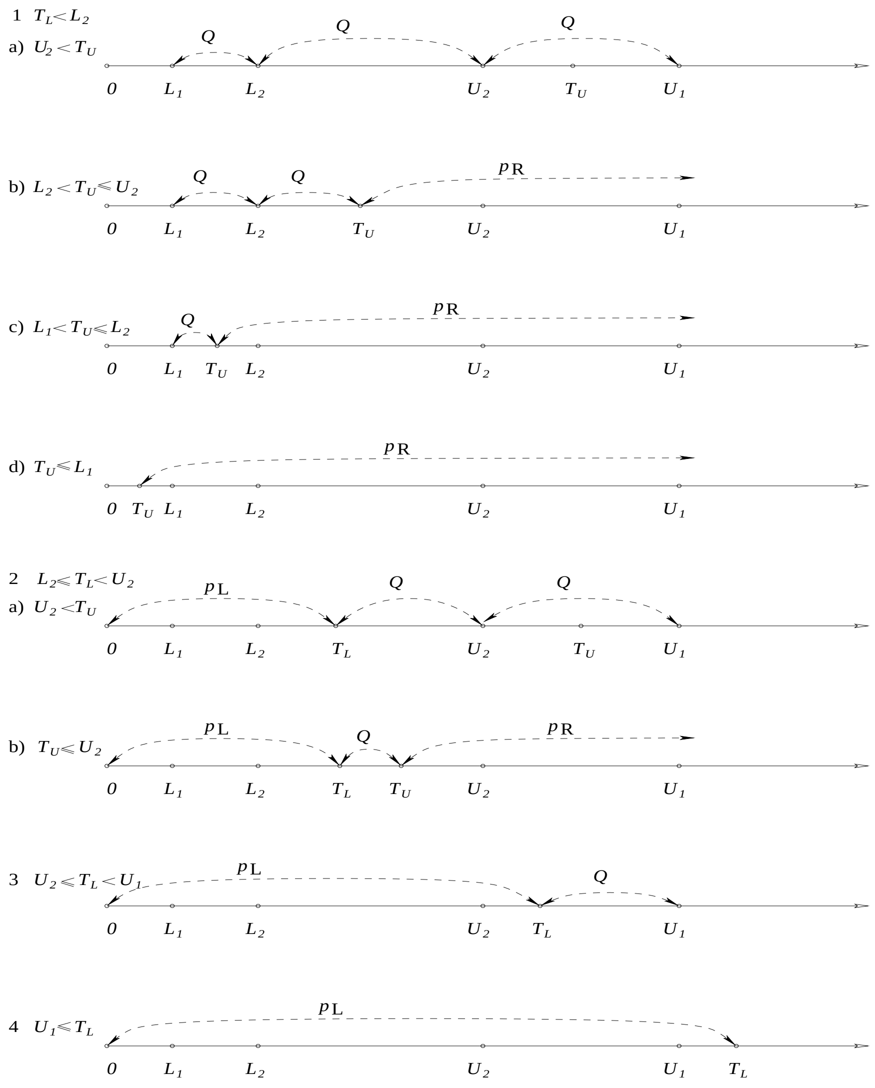

Figure 3.1: All cases for the integrand has a sharp peak

Our procedure for computing the pdf $p(y;\alpha,\nu)$ when the integrand $f(t;y,\alpha,\nu)$ has a sharp peak is summarized in Algorithm 3. In this algorithm, f stands for $f(t;y,\alpha,\nu)$ and it is assumed that L_i and U_i, $i=1,2$, satisfying (3.14)-(3.17) have been computed and that T_U has been determined. Note that both approximations (3.22) and (3.25) are accurate to within a relative error of 10^{-6}. An analysis similar to the one given at the end of Section 3.2.1 shows that the Algorithm 3 approximates $p(y;\alpha,\nu)$ to within a relative accuracy of 10^{-5}.

3.2.3 How to find L_1, U_1 and L_2, U_2

In this section we explain how to effectively find L_1, U_1, and L_2, U_2 that satisfy (3.14)-(3.17). Let $\mathcal{L}_q$ and $L(q)$ be defined by

$$\mathcal{L}_q \triangleq K(\alpha,\nu)\int_0^{L(q)} f(t;y,\alpha,\nu)dt = qp(y;\alpha,\nu)$$

for $0 \le q \le \frac{1}{2}$. Similarly, let $\mathcal{U}_q$ and $U(q)$ be defined by

$$\mathcal{U}_q \triangleq K(\alpha,\nu)\int_{U(q)}^{\infty} f(t;y,\alpha,\nu)dt = qp(y;\alpha,\nu)$$

for $0 \le q \le \frac{1}{2}$. Thus we have $L_1 = L\left(\frac{1}{3}\varepsilon\right), U_1 = U\left(\frac{1}{3}\varepsilon\right)$ and $L_2 = L(1\%), U_2 = U(1\%)$.

If (3.5) gives a better estimate of $p(y;\alpha,\nu)$ than (3.6) does, we can assume that the corresponding integrand $\left(e^{-\frac{\lambda}{t_{\max}^{\nu}}} t_{\max}^{-\zeta_+}\right) t^{t_{\max}} e^{-t}$ that gives estimate (3.5) approximates $f(t;y,\alpha,\nu)$ well. Then we can estimate $\mathcal{L}_q$ by

$$\begin{aligned}
\mathcal{L}_q &= K(\alpha,\nu)\int_0^{L(q)} e^{-\frac{\lambda}{t^{\nu}}} t^{\alpha-\frac{\nu}{2}-1} e^{-t} dt \\
&\le K(\alpha,\nu)\left(e^{-\frac{\lambda}{t_{\max}^{\nu}}} t_{\max}^{-\zeta_+}\right)\int_0^{L(q)} t^{t_{\max}} e^{-t} dt \\
&= K(\alpha,\nu)\left(e t_{\max}^{\nu}\right)^{-\frac{\lambda}{t_{\max}^{\nu}}} \gamma(L(q), t_{\max}+1),
\end{aligned} \tag{3.27}$$

where $\gamma(\tau,\varsigma) = \int_0^{\tau} t^{\varsigma-1}e^{-t}dt$, $\tau \ge 0$ and $\varsigma > 0$, is the incomplete Gamma (IG) function [1, Chapter 6]. Note that $\tilde{p}(y;\alpha,\nu) = K(\alpha,\nu)\left(e t_{\max}^{\nu}\right)^{-\frac{\lambda}{t_{\max}^{\nu}}}\Gamma(t_{\max}+1)$. Thus we can approximate $L(q)$ by solving

$$K(\alpha,\nu)\left(e t_{\max}^{\nu}\right)^{-\frac{\lambda}{t_{\max}^{\nu}}} \gamma(L(q), t_{\max}+1) = qK(\alpha,\nu)\left(e t_{\max}^{\nu}\right)^{-\frac{\lambda}{t_{\max}^{\nu}}}\Gamma(t_{\max}+1),$$

Algorithm 3 Approximate $p(y;\alpha,\nu)$ when $\nu > 0$ and the integrand has a high peak

if $(T_L \geq T_U)$ **then**

  $p(y;\alpha,\nu) := p_L((T_L+T_U)/2) + p_R((T_L+T_U)/2);$

else

  if $(T_L < L_2)$ **then**

    if $(T_U > U_2)$ **then**

      $p(y;\alpha,\nu) := K(\alpha,\nu)[Q(f;[L_1,L_2];\frac{100}{9}\varepsilon)+Q(f;[L_2,U_2];\frac{\varepsilon}{9})+Q(f;[U_2,U_1];\frac{100}{9}\varepsilon)];$

    else if $((L_2 < T_U)$ and $(T_U \leq U_2))$ **then**

      $p(y;\alpha,\nu) := K(\alpha,\nu)[Q(f;[L_1,L_2];\frac{100}{9}\varepsilon) + Q(f;[L_2,T_U];\frac{\varepsilon}{9})] + p_R(T_U);$

    else if $((L_1 < T_U)$ and $(T_U \leq L_2))$ **then**

      $p(y;\alpha,\nu) := K(\alpha,\nu)Q(f;[L_1,T_U];\frac{100}{9}\varepsilon) + p_R(T_U);$

    else

      $p(y;\alpha,\nu) := p_R(T_U);$

    end if

  else if $((L_2 \leq T_L)$ and $(T_L < U_2))$ **then**

    if $(T_U > U_2)$ **then**

      $p(y;\alpha,\nu) := p_L(T_L) + K(\alpha,\nu)[Q(f;[T_L,U_2];\frac{\varepsilon}{9}) + Q(f;[U_2,U_1];\frac{100}{9}\varepsilon)];$

    else

      $p(y;\alpha,\nu) := p_L(T_L) + K(\alpha,\nu)Q(f;[T_L,T_U];\frac{\varepsilon}{9}) + p_R(T_U);$

    end if

  else

    if $((U_2 \leq T_L)$ and $(T_L < U_1))$ **then**

      $p(y;\alpha,\nu) := p_L(T_L) + K(\alpha,\nu)Q(f;[T_L,U_1];\frac{100}{9}\varepsilon);$

    else

      $p(y;\alpha,\nu) := p_L(T_L);$

    end if

  end if

end if

or equivalently

$$\gamma(L(q), t_{\max} + 1) = q\Gamma(t_{\max} + 1). \tag{3.28}$$

Similarly, we approximate $U(q)$ by solving

$$\Gamma(U(q), t_{\max} + 1) = q\Gamma(t_{\max} + 1). \tag{3.29}$$

Note that in (3.28) and (3.29), $L(q)$ and $U(q)$ are completely determined by $t_{\max}$ and q, in which q equals to $\frac{1}{3}\varepsilon$ or 1%. Using the inverse Gamma cumulative distribution function GAMMAINV in Excel, we pre-calculate $L(q)$ and $U(q)$ with $q = \frac{1}{3}\varepsilon$ and $q = 1\%$ for some values of $t_{\max}$. When values of $L(q)$ and $U(q)$ are needed for other values of $t_{\max}$, we can approximate them by evaluating an interpolant through these particular points. This approach is relatively efficient because finding the unique root of equation (3.28) or (3.29) is a time consuming job [2]. All equations of these two types that appear in the remainder of this thesis are solved by this approach. We illustrate how well the interpolation works in Figure 3.2. The two curves represent the relative error in approximations to L_1 and U_1 versus $t_{\max}$, respectively. We define $RelErrL = (L_1 - \hat{L}_1)/\max\{L_1, 1\}$ and $RelErrU = (U_1 - \hat{U}_1)/\max\{U_1, 1\}$, where L_1 and U_1 are values generated by GAMMAINV, $\hat{L}_1$ and $\hat{U}_1$ are the approximation values of L_1 and U_1 produced by interpolation. We see from the two curves that $\hat{L}_1$ generally underestimates and that $\hat{U}_1$ generally overestimates.

On the other hand, if (3.6) gives a better estimate of $p(y; \alpha, \nu)$ than (3.5) does, we can assume that the corresponding integrand $e^{-t_{\max}} t_{\max}^{t_{\max}} e^{-\frac{\lambda}{t^\nu}} t^{-\zeta_+}$ approximates $f(t; y, \alpha, \nu)$ well. Thus we can estimate $\mathcal{L}_q$ by

$$\begin{aligned}
\mathcal{L}_q &= K(\alpha,\nu)\int_0^{L(q)} e^{-\frac{\lambda}{t^\nu}} t^{\alpha-\frac{\nu}{2}-1} e^{-t}\,dt \\
&\leq K(\alpha,\nu) e^{-t_{\max}} t_{\max}^{t_{\max}} \int_0^{L(q)} e^{-\frac{\lambda}{t^\nu}} t^{-\zeta_+}\,dt \\
&= \frac{K(\alpha,\nu)}{\nu}\lambda^{\frac{1-\zeta_+}{\nu}} \left(e^{-1} t_{\max}\right)^{t_{\max}} \Gamma\left(\frac{\lambda}{L(q)^\nu}, \frac{\zeta_+ - 1}{\nu}\right).
\end{aligned} \tag{3.30}$$

Then we approximate $L(q)$ by solving

$$\frac{K(\alpha,\nu)}{\nu}\lambda^{\frac{1-\zeta_+}{\nu}} \left(e^{-1} t_{\max}\right)^{t_{\max}} \Gamma\left(\frac{\lambda}{L(q)^\nu}, \frac{\zeta_+ - 1}{\nu}\right) = q\frac{K(\alpha,\nu)}{\nu}\lambda^{\frac{1-\zeta_+}{\nu}} \left(e^{-1} t_{\max}\right)^{t_{\max}} \Gamma\left(\frac{\zeta_+ - 1}{\nu}\right),$$

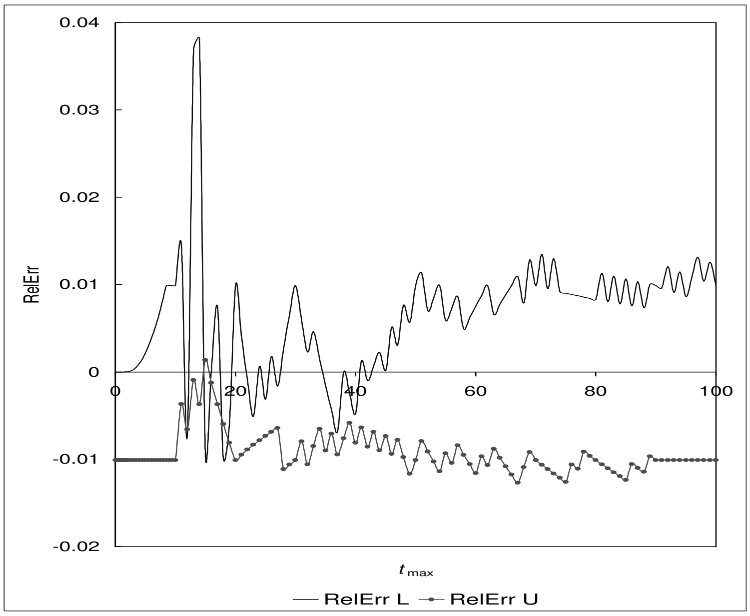

Figure 3.2: Relative errors in approximations to L_1 and U_1

or equivalently

$$\Gamma\left(\frac{\lambda}{L(q)^\nu}, \frac{\zeta_+ - 1}{\nu}\right) = q\Gamma\left(\frac{\zeta_+ - 1}{\nu}\right). \tag{3.31}$$

Similarly, we approximate $U(q)$ by solving

$$\gamma\left(\frac{\lambda}{U(q)^\nu}, \frac{\zeta_+ - 1}{\nu}\right) = q\Gamma\left(\frac{\zeta_+ - 1}{\nu}\right). \tag{3.32}$$

Let $z = \lambda/L(q)^\nu, w = \lambda/U(q)^\nu$, and $\tau = (\zeta_+ - 1)/\nu$. Then we can rewrite (3.31) and (3.32) as

$$\Gamma(z, \tau) = q\Gamma(\tau) \quad \text{and} \quad \gamma(w, \tau) = q\Gamma(\tau).$$

Note that τ can be determined through ζ_+ and ν. Thus z and w can be approximated through the interpolation process described above. Then we have $L(q) = (\lambda/z)^{1/\nu}$ and $U(q) = (\lambda/w)^{1/\nu}$.

3.2.4 Criterion for a sharp peak

We have not yet explained how to decide whether or not the integrand $f(t; y, \alpha, \nu)$ has a sharp peak. Note that we estimated the pdf $p(y; \alpha, \nu)$ in §2.3 by means of a Γ function.

In practice, we say the integrand has a sharp peak if $t_{\max} < 3.5$. We choose 3.5 because, when $\varsigma = 3.5 + 1 = 4.5$, equation (3.28) has the solution $L(1\%) \approx 1$, and $T_L = 1$ in the method we implemented. Moreover, we know that the integrand associated with $\Gamma(\varsigma)$ does not have a sharp peak when $\varsigma \geq 4.5$.

3.3 A Method for $\nu < 0$

In this section we consider a method for computing the pdf $p(y;\alpha,\nu)$ when $\nu < 0$. As in the case $\nu > 0$, the infinite interval $[0,\infty)$ is truncated to a bounded subinterval $[L_1, U_1] \subset [0,\infty)$ and this interval is further divided into three subintervals $[L_1, L_2]$, $[L_2, U_2]$ and $[U_2, U_1]$, where $L_i, U_i, i = 1, 2$, satisfy (3.14)-(3.17). We will describe how these values may be determined in Section 3.3.2.

3.3.1 Algorithm description

Instead of developing two algorithms that depend on whether or not the integrand $f(t;y,\alpha,\nu)$ has a sharp peak as we did in Section 3.2, we combine both cases together for $\nu < 0$. To deal with a possible sharp peak, we use the polynomial $\mathcal{P}_N(t)$ (3.21) to approximate e^{-t} over $[0, T_L]$. Thus we have the approximation

$$
\begin{aligned}
n_1(T_L) &\triangleq K(\alpha,\nu)\int_0^{T_L} e^{-\lambda t^{|\nu|}} t^{\alpha-\frac{\nu}{2}-1} e^{-t}\,dt \\
&\approx K(\alpha,\nu)\int_0^{T_L} \sum_{i=0}^{N} c_i e^{-\lambda t^{|\nu|}} t^{\alpha-\frac{\nu}{2}-1} t^i\,dt \\
&= \frac{K(\alpha,\nu)}{|\nu|}\sum_{i=0}^{N} c_i \lambda^{-\frac{\alpha-\frac{\nu}{2}+i}{|\nu|}} \int_0^{\lambda T_L^{|\nu|}} e^{-z} z^{\frac{\alpha-\frac{\nu}{2}+i}{|\nu|}-1}\,dz \quad \text{(by letting } \lambda t^{|\nu|} = z\text{)} \\
&= \frac{K(\alpha,\nu)}{|\nu|}\sum_{i=0}^{N} c_i \lambda^{-\frac{\alpha-\frac{\nu}{2}+i}{|\nu|}} \gamma\left(\lambda T_L^{|\nu|}, \frac{\alpha-\frac{\nu}{2}+i}{|\nu|}\right). \qquad (3.33)
\end{aligned}
$$

On the other hand, we could choose to approximate the other exponential in the integrand. Note there always exists a value $\tilde{T}_L \in (0,\infty)$ such that $\lambda \tilde{T}_L^{|\nu|} = T_L$, since it is assumed that $\lambda > 0$. Note that $\lambda t^{|\nu|} \leq T_L$ for any $t \in [0, \tilde{T}_L]$. Therefore $e^{-\lambda t^{|\nu|}}$ is well approximated by

$$\sum_{i=0}^{N} c_i \left(\lambda t^{|\nu|}\right)^i$$

for all $t \in [0, \tilde{T}_L]$. Thus the integral over $[0, \tilde{T}_L]$ can be approximated by

$$\begin{aligned} n_2(\tilde{T}_L) &\triangleq K(\alpha,\nu)\int_0^{\tilde{T}_L} e^{-\lambda t^{|\nu|}} t^{\alpha-\frac{\nu}{2}-1} e^{-t} dt \\ &\approx K(\alpha,\nu)\int_0^{\tilde{T}_L} \sum_{i=0}^{N} c_i \left(\lambda t^{|\nu|}\right)^i t^{\alpha-\frac{\nu}{2}-1} e^{-t} dt \\ &= K(\alpha,\nu)\sum_{i=0}^{N} c_i \lambda^i \gamma\left(\tilde{T}_L, \alpha - \frac{\nu}{2} + i|\nu|\right). \end{aligned} \tag{3.34}$$

To decide which of (3.33) or (3.34) to employ, we use the following simple criterion. If $\tilde{T}_L = (T_L/\lambda)^{1/|\nu|} > T_L$, then we use (3.34). Otherwise, we use (3.33). Let $T_L^* = \max\left\{\tilde{T}_L, T_L\right\}$. This technique is used when $T_L^* \geq L_2$. To evaluate the integral over the interval $[T_L^*, U_1]$, a quadrature method is applied. Based on these considerations an algorithm for calculating $p(y;\alpha,\nu)$ when $\nu < 0$ is listed below in Algorithm 4. It is assumed that $L_i, U_i, i = 1, 2$ are precomputed. In the algorithm,

$$n(T_L^*) = \begin{cases} n_1(T_L^*) & \text{if} \quad T_L^* = T_L; \\ n_2(T_L^*) & \text{if} \quad T_L^* = \tilde{T}_L. \end{cases}$$

Using an analysis similar to that in Section 3.2.1, we can show that this algorithm can evaluate the pdf $p(y;\alpha,\nu)$ to within a relative accuracy of $\varepsilon = 10^{-5}$.

3.3.2 How to find L_1, U_1, and L_2, U_2

In this section, we briefly explain how to find $L_i, U_i, i = 1, 2$, when $\nu < 0$.

First, we consider the case $t_{\max} = 0$. If (3.7) is a better estimate of $p(y;\alpha,\nu)$ than (3.8), we let

$$\begin{aligned} \mathcal{L}_q &= K(\alpha,\nu)\int_0^{L(q)} e^{-\lambda t^{|\nu|}} t^{\alpha-\frac{\nu}{2}-1} e^{-t} dt \\ &\leq K(\alpha,\nu)\int_0^{L(q)} t^{\alpha-\frac{\nu}{2}-1} e^{-t} dt \\ &= K(\alpha,\nu)\gamma(L(q), \alpha - \nu/2). \end{aligned} \tag{3.35}$$

Algorithm 4 Approximate $p(y;\alpha,\nu)$ when $\nu < 0$

Compute T_L^*;

if $(T_L^* \geq U_1)$ **then**

$p(y;\alpha,\nu) := n(T_L^*)$;

else if $((U_2 \leq T_L^*)$ and $(T_L^* < U_1))$ **then**

$p_1 = n(T_L^*)$;

$p(y;\alpha,\nu) := p_1 + K(\alpha,\nu)Q(f;[T_L^*,U_1];\frac{100}{9}\varepsilon)$;

else if $((L_2 \leq T_L^*)$ and $(T_L^* < U_2))$ **then**

$p_1 = n(T_L^*)$;

$p(y;\alpha,\nu) = p_1 + K(\alpha,\nu)[Q(f;[T_L^*,U_2];\frac{\varepsilon}{9}) + Q(f;[U_2,U_1];\frac{100}{9}\varepsilon)]$;

else

$p(y;\alpha,\nu) = K(\alpha,\nu)[Q(f;[L_1,L_2];\frac{100}{9}\varepsilon) + Q(f;[L_2,U_2];\frac{\varepsilon}{9}) + Q(f;[U_2,U_1];\frac{100}{9}\varepsilon)$;

end if

Thus $L(q)$ can be approximated by solving

$$K(\alpha,\nu)\gamma(L(q),\alpha-\nu/2) = qK(\alpha,\nu)\Gamma(\alpha-\nu/2),$$

or equivalently

$$\gamma(L(q),\alpha-\nu/2) = q\Gamma(\alpha-\nu/2). \tag{3.36}$$

Similarly, we can approximate $U(q)$ by solving

$$\Gamma(U(q),\alpha-\nu/2) = q\Gamma(\alpha-\nu/2). \tag{3.37}$$

On the other hand, if (3.8) is a better estimate of $p(y;\alpha,\nu)$ than (3.7), we let

$$\begin{aligned}
\mathcal{L}_q &= K(\alpha,\nu)\int_0^{L(q)} e^{-\lambda t^{|\nu|}} t^{\alpha-\frac{\nu}{2}-1} e^{-t}\,dt \\
&\leq K(\alpha,\nu)\int_0^{L(q)} e^{-\lambda t^{|\nu|}} t^{\alpha-\frac{\nu}{2}-1}\,dt \\
&= \frac{K(\alpha,\nu)}{|\nu|}\lambda^{-\frac{\alpha-\nu/2}{|\nu|}}\gamma\left(\lambda L(q)^{|\nu|}, \frac{\alpha-\nu/2}{|\nu|}\right).
\end{aligned} \tag{3.38}$$

Thus we can approximate $L(q)$ by solving

$$\frac{K(\alpha,\nu)}{|\nu|}\lambda^{-\frac{\alpha-\nu/2}{|\nu|}}\gamma\left(\lambda L(q)^{|\nu|},\frac{\alpha-\nu/2}{|\nu|}\right)=q\frac{K(\alpha,\nu)}{|\nu|}\lambda^{-\frac{\alpha-\nu/2}{|\nu|}}\Gamma\left(\frac{\alpha-\nu/2}{|\nu|}\right),$$

or equivalently

$$\gamma\left(\lambda L(q)^{|\nu|},\frac{\alpha-\nu/2}{|\nu|}\right)=q\Gamma\left(\frac{\alpha-\nu/2}{|\nu|}\right). \tag{3.39}$$

Similarly $U(q)$ can be approximated by solving

$$\Gamma\left(\lambda U(q)^{|\nu|},\frac{\alpha-\nu/2}{|\nu|}\right)=q\Gamma\left(\frac{\alpha-\nu/2}{|\nu|}\right). \tag{3.40}$$

Now consider $t_{\max} > 0$. We follow an argument similar to the one presented in Section 3.2.3 for the case $\nu > 0$. When $\nu < 0$ and $t_{\max} > 0$, $L(q)$ and $U(q)$ can be approximated by solving

$$\gamma(L(q),t_{\max}+1)=q\Gamma(t_{\max}+1)\quad\text{and}\quad\Gamma(U(q),t_{\max}+1)=q\Gamma(t_{\max}+1), \tag{3.41}$$

if (3.9) is a better estimate of $p(y;\alpha,\nu)$ than (3.10), or by solving

$$\gamma\left(\lambda L(q)^{|\nu|},\frac{\zeta_-+1}{|\nu|}\right)=q\gamma\left(\frac{\zeta_-+1}{|\nu|}\right)\qquad\text{and}\qquad\Gamma\left(\lambda U(q)^{|\nu|},\frac{\zeta_-+1}{|\nu|}\right)=q\gamma\left(\frac{\zeta_-+1}{|\nu|}\right), \tag{3.42}$$

if (3.10) is a better estimate of $p(y;\alpha,\nu)$ than (3.9).

3.4 An Improved Method for the Case $\nu < 0$

Up to now, we have a hybrid method for calculating the pdf $p(y;\alpha,\nu)$ with the RF Y and the shape parameters α and ν in the reasonable ranges $y \in [-10,10]$, $0.5 \le \alpha \le 90$, $-10 \le \nu \le -0.5$, and $0.5 \le \nu \le 10$. Preliminary numerical results suggest that these methods are accurate and efficient. However the number of the integrand function evaluations can be as large as 200 to 300 and sometimes even larger due to the high relative accuracy requirement and the rapidly changing integrand.

However, these methods are much more costly than more traditional methods, such as continued fractions, polynomial approximation or rational approximation [1, 14] for computing special functions based on integrals, such as the error function and the incomplete Gamma function. These more traditional methods do not explicitly use quadrature. It is not known whether these more traditional methods are applicable to $p(y;\alpha,\nu)$, because the standard special functions have one or two parameters only, while $p(y;\alpha,\nu)$ has three. Note that there are robust computer programs for evaluating special functions. Therefore, it is desirable, if possible, to approximate the improper integral associated with $p(y;\alpha,\nu)$ by a sum of special functions. We expect this will lead to an improvement over the method proposed in the previous section in some cases. Here we consider an improved method for $\nu < 0$.

Note that for any $t \geq 0$

$$e^{-t} = \sum_{k=0}^{n} \frac{(-1)^k}{k!} t^k + \epsilon_n(t), \quad \text{where } |\epsilon_n(t)| \leq \frac{t^{n+1}}{(n+1)!}, \; n = 0, 1, 2, \ldots.$$

Thus we can write

$$\begin{aligned}
p(y;\alpha,\nu) &= K(\alpha,\nu) \int_0^\infty e^{-\lambda t^{|\nu|}} t^{\alpha-\frac{\nu}{2}-1} e^{-t} dt \\
&= K(\alpha,\nu) \int_0^\infty e^{-\lambda t^{|\nu|}} t^{\alpha-\frac{\nu}{2}-1} \left[\sum_{k=0}^{n} \frac{(-1)^k}{k!} t^k + \epsilon_n(t) \right] dt \\
&= K(\alpha,\nu) \left[\sum_{k=0}^{n} \frac{(-1)^k}{k!} \int_0^\infty e^{-\lambda t^{|\nu|}} t^{\alpha-\frac{\nu}{2}+k-1} dt + \int_0^\infty e^{-\lambda t^{|\nu|}} t^{\alpha-\frac{\nu}{2}-1} \epsilon_n(t) dt \right] \\
&= K(\alpha,\nu) \left[\sum_{k=0}^{n} \frac{(-1)^k}{|\nu| k!} \lambda^{-\frac{\alpha-\nu/2+k}{|\nu|}} \Gamma\left(\frac{\alpha-\nu/2+k}{|\nu|} \right) \right. \\
&\quad \left. + \int_0^\infty e^{-\lambda t^{|\nu|}} t^{\alpha-\frac{\nu}{2}-1} \epsilon_n(t) dt \right],
\end{aligned} \tag{3.43}$$

Let

$$a_k = \frac{1}{|\nu| k!} \lambda^{-\frac{\alpha-\nu/2+k}{|\nu|}} \Gamma\left(\frac{\alpha-\nu/2+k}{|\nu|} \right). \tag{3.44}$$

Then using one of Stirling's formulas [1, the first term of formula 6.1.37]

$$\Gamma(z) \sim e^{-z} z^{z-\frac{1}{2}} (2\pi)^{\frac{1}{2}}, \qquad \text{as} \;\; z \to +\infty,$$

and noting that $k! = \Gamma(k+1)$ for any natural number k, we see that

$$a_k \to 0 \quad \text{as} \quad k \to +\infty, \quad \text{if} \quad |\nu| > 1, \quad \text{and} \quad \lambda \neq 0.$$

To be specific, we have

$$k! = \Gamma(k+1) \sim e^{-(k+1)}(k+1)^{k+1-\frac{1}{2}}(2\pi)^{\frac{1}{2}},$$
$$\Gamma\left(\frac{\alpha-\frac{\nu}{2}+k}{|\nu|}\right) \sim e^{-\frac{\alpha-\frac{\nu}{2}+k}{|\nu|}}\left(\frac{\alpha-\frac{\nu}{2}+k}{|\nu|}\right)^{\frac{\alpha-\frac{\nu}{2}+k}{|\nu|}-\frac{1}{2}}(2\pi)^{\frac{1}{2}}.$$

Hence

$$a_k \sim \frac{1}{|\nu|}\lambda^{-\frac{\alpha-\nu/2+k}{|\nu|}}\frac{e^{-\frac{\alpha-\frac{\nu}{2}+k}{|\nu|}}\left(\frac{\alpha-\frac{\nu}{2}+k}{|\nu|}\right)^{\frac{\alpha-\frac{\nu}{2}+k}{|\nu|}-\frac{1}{2}}}{e^{-(k+1)}(k+1)^{k+1-\frac{1}{2}}}.$$

Let $m = k+1$, then $m \to +\infty$ as $k \to +\infty$, and we have

$$a_{m-1} \sim \frac{1}{|\nu|}\lambda^{-\frac{\alpha-\nu/2-1+m}{|\nu|}}\frac{e^{-\frac{\alpha-\frac{\nu}{2}-1+m}{|\nu|}}\left(\frac{\alpha-\frac{\nu}{2}-1+m}{|\nu|}\right)^{\frac{\alpha-\frac{\nu}{2}-1+m}{|\nu|}-\frac{1}{2}}}{e^{-m}m^{m-\frac{1}{2}}}.$$

Note that $\frac{\alpha-\frac{\nu}{2}-1+m}{|\nu|} < m$ and $\frac{\alpha-\frac{\nu}{2}-1+m}{|\nu|} - \frac{1}{2} > 0$ when m is large enough and $\nu < -1$. Thus, we have

$$\frac{\left(\frac{\alpha-\frac{\nu}{2}-1+m}{|\nu|}\right)^{\frac{\alpha-\frac{\nu}{2}-1+m}{|\nu|}-\frac{1}{2}}}{m^{m-\frac{1}{2}}} < \frac{m^{\frac{\alpha-\frac{\nu}{2}-1+m}{|\nu|}-\frac{1}{2}}}{m^{m-\frac{1}{2}}} = m^{-\left(m-\frac{\alpha-\frac{\nu}{2}-1+m}{|\nu|}\right)}.$$

Thus

$$\begin{aligned}
&\frac{1}{|\nu|}\lambda^{-\frac{\alpha-\nu/2-1+m}{|\nu|}}\frac{e^{-\frac{\alpha-\frac{\nu}{2}-1+m}{|\nu|}}\left(\frac{\alpha-\frac{\nu}{2}-1+m}{|\nu|}\right)^{\frac{\alpha-\frac{\nu}{2}-1+m}{|\nu|}-\frac{1}{2}}}{e^{-m}m^{m-\frac{1}{2}}} \\
&\qquad \leq \frac{1}{|\nu|}\lambda^{-\frac{\alpha-\nu/2-1+m}{|\nu|}}e^{m-\frac{\alpha-\nu/2-1+m}{|\nu|}}m^{-\left(m-\frac{\alpha-\frac{\nu}{2}-1+m}{|\nu|}\right)} \\
&\qquad \leq \frac{1}{|\nu|}\left(\frac{e}{\min(\lambda,1)}\right)^m m^{-m\left(1-\frac{1}{|\nu|}\right)+\frac{\alpha-\frac{\nu}{2}}{|\nu|}}.
\end{aligned}$$

Noting that $c_1^m m^{-c_2 m + c_3} \to 0$ when $m \to +\infty$ for any constants $c_1 > 0$, $c_2 > 0$, and $c_3 \in R$, we have

$$\frac{1}{|\nu|}\left(\frac{e}{\min(\lambda,1)}\right)^m m^{-m\left(1-\frac{1}{|\nu|}\right)+\frac{\alpha-\frac{\nu}{2}}{|\nu|}} \to 0,$$

which implies that $a_{m-1} \to 0$. Hence we have

$$a_k \to 0 \quad \text{as} \quad k \to +\infty, \quad \text{if} \quad \nu < -1 \quad \text{and} \quad \lambda \neq 0.$$

From the Cauchy criterion for alternating series, it is known that when $n \to +\infty$ the sum in (3.43) converges for any $\nu < -1$ and any $\lambda \neq 0$. Furthermore, the absolute error between $p(y; \alpha, \nu)$ and the finite sum

$$K(\alpha, \nu) \left[\sum_{k=0}^{n} \frac{(-1)^k}{|\nu| k!} \lambda^{-\frac{\alpha - \nu/2 + k}{|\nu|}} \Gamma\left(\frac{\alpha - \nu/2 + k}{|\nu|} \right) \right] \tag{3.45}$$

is bounded by

$$\epsilon_n'(\lambda) = K(\alpha, \nu) \frac{1}{|\nu|(n+1)!} \lambda^{-\frac{\alpha - \nu/2 + n + 1}{|\nu|}} \Gamma\left(\frac{\alpha - \nu/2 + n + 1}{|\nu|} \right), \tag{3.46}$$

and $\epsilon_n'(\lambda) \to 0$ as $n \to +\infty$ for any $\nu < -1$ and $\lambda \neq 0$. From (3.43) we get

$$p(y; \alpha, \nu) \leq K(\alpha, \nu) \left[\sum_{k=0}^{n} \frac{(-1)^k}{|\nu| k!} \lambda^{-\frac{\alpha - \nu/2 + k}{|\nu|}} \Gamma\left(\frac{\alpha - \nu/2 + k}{|\nu|} \right) \right] + \epsilon_n'(\lambda). \tag{3.47}$$

Moreover, we have an upper bound

$$\frac{\epsilon_n'(\lambda)}{\left| K(\alpha, \nu) \left[\sum_{k=0}^{n} \frac{(-1)^k}{|\nu| k!} \lambda^{-\frac{\alpha - \nu/2 + k}{|\nu|}} \Gamma\left(\frac{\alpha - \nu/2 + k}{|\nu|} \right) \right] - \epsilon_n'(\lambda) \right|} \tag{3.48}$$

on the relative error. Thus for fixed y, α and ν, we can take the sum (3.45) as an approximation to $p(y; \alpha, \nu)$ if n is large enough so that

$$\frac{a_{n+1}}{\left| \sum_{k=0}^{n} (-1)^k a_k - a_{n+1} \right|} \leq \varepsilon = 10^{-5}. \tag{3.49}$$

To make the sum (3.45) converge rapidly, to avoid numerical overflow/underflow, and to satisfy the accuracy requirement (3.49), we impose the following conditions:

1. $n \leq 100$, to ensure that the sum (3.45) does not have too many terms;

2. for all $k \leq n$, $a_k \leq$ the largest floating point number, to avoid overflow;

3. $\frac{a_{n+1}}{\left| \sum_{k=0}^{n} (-1)^k a_k - a_{n+1} \right|} \leq 10^{-5}$, for some $n \leq 100$, to satisfy the accuracy requirement.

Some threshold values of y for which we know the three conditions above hold are listed in Table 3.2. Note that in Table 3.2 threshold values of y for $\nu = -1$ and several

$\nu\backslash\alpha$	2	3	4	5	10	15	20
-1	1.58	2.27	2.83	3.32	5.38	7.14	8.79
-1.5	0.42	$\boxed{0.84}$	1.21	1.56	3.2	5.04	7.18
-2		0.3	0.52	0.75	2.27	4.28	6.69
-2.5		0.1	0.24	0.41	1.73	3.75	6.42
-3			0.11	0.23	1.33	3.34	6.25
-4				0.055	0.78	2.67	6.07
-5					0.44	2.12	5.89
-6					0.23	1.63	5.66
-7					0.11	1.2	5.31
-8					0.038	0.84	4.85
-9					0.011	0.55	4.27
-10						0.34	3.61

Table 3.2: Threshold values of y for the applicability of (3.45)

values of α are also listed, although the case $\nu = -1$ was excluded in the analysis above. These values for $\nu = -1$ were verified numerically. Thus they can be used in practice.

These threshold values are used as follows. For example, 0.84 in the box in the third column is the threshold value of y for $\alpha = 3$ and $\nu = -1.5$. If $\alpha = 3$, $\nu = -1.5$, and $|y| \geq 0.84$, then $p(y;\alpha,\nu)$ can be approximated accurately by (3.45) with some $n \leq 100$. For parameters α and ν that are not listed in the table, for example $\alpha = 3.3$ and $\nu = -1.75$, (3.45) is applicable when $|y| \geq 1.21$, which is the threshold for $\alpha^* = 4$, the first α value in the table greater than 3.3, and $\nu^* = -1.5$, the first ν value in the table greater than -1.7. If for some α and ν, there are no values $\alpha^* \geq \alpha$ and $\nu^* \geq \nu$ in the table, then (3.45) may not be applicable.

When (3.45) is not applicable, we consider instead the expansion

$$e^{-\lambda t^{|\nu|}} = \sum_{k=0}^{n} \frac{(-1)^k}{k!} \left(\lambda t^{|\nu|}\right)^k + \tilde{\epsilon}_n(t), \quad \text{where} \quad |\tilde{\epsilon}_n(t)| \leq \frac{\left(\lambda t^{|\nu|}\right)^{n+1}}{(n+1)!}$$

for $t \geq 0$. Thus,

$$\begin{aligned} p(y;\alpha,\nu) &= K(\alpha,\nu)\int_0^\infty e^{-\lambda t^{|\nu|}} t^{\alpha-\frac{\nu}{2}-1} e^{-t}dt \\ &= K(\alpha,\nu)\left[\int_0^\infty \sum_{k=0}^{n} \frac{(-1)^k}{k!}\left(\lambda t^{|\nu|}\right)^k t^{\alpha-\frac{\nu}{2}-1}e^{-t}dt + \int_0^\infty \tilde{\epsilon}_n(t) t^{\alpha-\frac{\nu}{2}-1}e^{-t}dt\right] \\ &= K(\alpha,\nu)\left[\sum_{k=0}^{n} \frac{(-1)^k}{k!}\lambda^k \Gamma\left(\alpha-\frac{\nu}{2}+k|\nu|\right) + \int_0^\infty \tilde{\epsilon}_n(t) t^{\alpha-\frac{\nu}{2}-1}e^{-t}dt\right]. \end{aligned} \quad (3.50)$$

If $p(y;\alpha,\nu)$ is approximated by

$$K(\alpha,\nu)\left[\sum_{k=0}^{n} \frac{(-1)^k}{k!}\lambda^k \Gamma\left(\alpha-\frac{\nu}{2}+k|\nu|\right)\right] \quad (3.51)$$

then the absolute error is bounded by

$$\tilde{\epsilon}'_n(\lambda) = K(\alpha,\nu)\frac{\lambda^{n+1}}{(n+1)!}\Gamma\left(\alpha-\frac{\nu}{2}+(n+1)|\nu|\right). \quad (3.52)$$

Furthermore, the relative error is bounded by

$$\frac{\tilde{\epsilon}'_n(\lambda)}{\left|K(\alpha,\nu)\sum_{k=0}^{n}\frac{(-1)^k}{k!}\lambda^k\Gamma\left(\alpha-\frac{\nu}{2}+k|\nu|\right)-\tilde{\epsilon}'_n(\lambda)\right|} = \frac{b_{n+1}}{\left|\sum_{k=0}^{n}(-1)^k b_k - b_{n+1}\right|}, \quad (3.53)$$

where $b_k = \frac{\lambda^k}{k!}\Gamma\left(\alpha-\frac{\nu}{2}+k|\nu|\right)$.

Note that

$$\tilde{\epsilon}'_n(\lambda) \to 0 \quad \text{as} \quad n \to +\infty, \quad \text{if} \quad -1 < \nu \leq 0.$$

Then (3.51) converges for any y if $-1 < \nu \leq 0$. We impose the previously used conditions 1 and 2 and

3′. $b_{n+1} \leq 10^{-5}\left|\sum_{k=0}^{n}(-1)^k b_k - b_{n+1}\right|$ for some $n \leq 100$.

Then (3.51) is applicable when $|y|$ is small enough.

But (3.51) will not converge for any $\nu < -1$ except $y = 0$. However, if $\tilde{\epsilon}'_n(\lambda)$ is small enough that the relative error bound (3.53) is less than 10^{-5}, which is the case when $|y|$ is small enough, then the first few terms in (3.51) will give a good estimate of $p(y;\alpha,\nu)$. To determine how small the y should be so that (3.51) is applicable when $\nu < -1$, conditions similar to these previously imposed are adopted here except that conditions 1 and 3 are replaced here by

1′. there exists a number $n \le 100$ such that $b_{n+1} \le 10^{-5}\left|\sum_{k=0}^{n}(-1)^k b_k - b_{n+1}\right|$.

$\nu\backslash\alpha$	1	2	3	4	5	10	15	20
-0.5	2.85	3.7	3.97	4.15	4.3	5.07	5.68	5.75
-1		1.27	1.77	2.13	2.41	3.35	3.92	4.33
-1.5		0.31	0.6	0.82	1.01	1.7	2.22	2.63
-2			$\boxed{0.21}$	0.34	0.46	0.93	1.29	1.59
-2.5			0.063	0.14	0.22	0.54	0.81	1.038
-3				0.054	0.09	0.32	0.52	0.69
-4					0.015	0.11	0.21	0.32
-5						0.034	0.088	0.15
-6						0.01	0.023	0.069
-7						0.0024	0.013	0.03
-8						0.00048	0.0044	0.012
-9						0.000067	0.0014	0.0051
-10							0.0004	0.0019

Table 3.3: Threshold values of y for the applicability of (3.51)

Precalculated threshold values satisfying these conditions are presented in Table 3.3. These values are used as follow. For example, 0.21 in the box in the fourth column is the threshold value of y for $\alpha = 3$ and $\nu = -2$. If $\alpha = 3$, $\nu = -1.5$, and $|y| \le 0.21$, then $p(y;\alpha,\nu)$ can be approximated accurately by (3.51) with some $n \le 100$. For parameters α and ν that are not listed in the table, for example $\alpha = 6.3$ and $\nu = -1.75$, (3.51) is applicable only when $|y| \le 0.46$, which is the threshold for $\alpha^* = 5$, the first α in the table less than 6.3, and $\nu^* = -2$, the first ν value in the table less than -1.7. If for some α and ν, there are no values $\alpha^* \leq \alpha$ and $\nu^* \leq \nu$ in the table, then (3.51) may not be applicable.

Chapter 4

Numerical Results

Numerical methods for computing the pdf $p(y; \alpha, \nu)$, depending on whether $\nu > 0$ or $\nu < 0$, are proposed in Section 3.2 and Section 3.3, respectively. An improvement to the method for $\nu < 0$ is discussed in Section 3.4. In this chapter, we address algorithm implementation issues and report some numerical testing results.

4.1 Algorithm Implementation

In this section, we consider some issues concerning the implementation of the methods described in Chapter 3.

The first decision to be made is what method to use to evaluate an integral over a finite interval. There are many methods designed for this purpose [8]. Both adaptive and non-adaptive programs based on these methods have been developed and incorporated into major numerical libraries such as NAG and IMSL. We prefer the adaptive integrators over non-adaptive ones because the former automatically generate a result in an attempt to satisfy a user specified accuracy requirement. After considering many adaptive integrators, we chose the C version of DQAGS, a routine in QUADPACK [16], a subroutine package for automatic integration. We used the 21-point Gauss-Kronrod quadrature rule in DQAGS. The C version of DQAGS, a translation of its FORTRAN 77 counterpart, is available at http://nis-www.lanl.gov/~mgh/QuadPack.shtml. For more details about QUADPACK, please see [16]. To run DQAGS on the Sun workstations in the Department of Computer Science, the following machine dependent parameters compatible with the IEEE standard for floating point arithmetic are provided.

The smallest positive number	2.2250738585072014E-308
The largest positive number	1.7976931348623157E+308
The largest relative spacing	2.2204460492503E-16

Table 4.1: Machine dependent parameters for QUADPACK

Next, we turn to the computation of some special functions. Instead of directly calculating the Gamma function $\Gamma(z)$, we call the Numerical Recipes program GAMMLN to calculate $\ln(\Gamma(z))$ for any $z > 0$ [17, Section 6.1], because $\Gamma(z)$, which is often a very large number that may overflow, is usually divided by another large number with the result being a number of moderate size. We compute the logarithm of such ratios by subtracting two logarithms. The task of evaluating the incomplete Gamma function, $\gamma(z, \alpha)$, and the complementary incomplete Gamma function, $\Gamma(z, \alpha)$, is handled by calling the function NAG_INCOMPLETE_GAMMA in the NAG library. For more details about the NAG library and this function, please visit the NAG web site http://www.nag.co.uk/.

A C program was produced to implement the methods proposed in Chapter 3. Numerical testing was carried out and the results are reported in the next two sections.

4.2 Numerical Results for Special Cases

In this section, we compare results generated by our program and those produced by other approaches for two particular choices of parameter values.

First, we consider $\nu = 1$. In this case, the pdf $p(y; \alpha, \nu)$ reduces to

$$p(y;\alpha,1) \quad = \quad \sqrt{\frac{\alpha}{2\pi}}\frac{1}{\Gamma(\alpha)}\int_0^{\infty} e^{-\frac{y^2\alpha}{2t}} t^{\alpha-\frac{1}{2}-1} e^{-t} dt$$

$$= \sqrt{\frac{2\alpha}{\pi}}\frac{1}{\Gamma(\alpha)}\left(\frac{\alpha y^2}{2}\right)^{\frac{\alpha}{2}-\frac{1}{4}} K_{\alpha-\frac{1}{2}}\left(\sqrt{2\alpha y^2}\right), \quad (4.1)$$

where $K_\xi(z) = K_{-\xi}(z) = \frac{z^\xi}{2}\int_0^\infty e^{-\frac{1}{2}\left(t+\frac{z^2}{t}\right)} t^{-\xi-1}dt$ is the modified K-Bessel function of the third kind [5, 8.432.7]. The authors of [17, Section 6.7] claim that the double precision program BESSIK can evaluate $K_\xi(z)$, for $z > 0$ and any ξ, with a relative error less than 10^{-14}. So we use the BESSIKfunction to produce benchmark results.

We compare the numerical results generated by our program and BESSIK for $\alpha =$ 0.25, 0.5, 1, 5, 10, 20, 40, and 60. With these parameters, a variety of integrand behaviors are included. Note that when $\nu > 0$, the integrand function may have a sharp high peak when $|y|$ is close to 0. To illustrate the robustness of our algorithms, we choose more test points near $y = 0$ than for large $|y|$. In practice, y usually lies in $[-5, +5]$. It occurs with small probability outside of this range and rarely outside of $[-10, +10]$. Note that the pdf $p(y; \alpha, \nu)$ is a symmetric function, so all test points are chosen from $[0, 10]$. The 100 test points, denoted by $y_i = 10^{-7} \times i^4$, $i = 1, 2, \ldots, 100$, are shown in Figure 4.1.

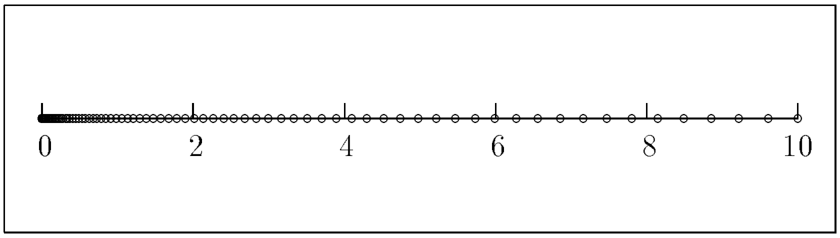

Figure 4.1: Test points for $\nu = 1$

Numerical results are presented in Table 4.2. The relative error $RelErr(\alpha, y)$ with respect to the risk factor value y and the shape parameter α with $\nu = 1$ is given by

$$RelErr(\alpha, y) = (general(\alpha, y) - bessik(\alpha, y))/bessik(\alpha, y),$$

where $general(\alpha, y)$ and $bessik(\alpha, y)$ are the values of $p(y; \alpha, 1)$ produced by our program and from (4.1) using BESSIK, respectively. In this table, $\max|RelErr(\alpha)| = \max_{i=1,100}\{|RelErr(\alpha, y_i)|\}$.

α	$\max \lvert RelErr(\alpha)\rvert$	α	$\max \lvert RelErr(\alpha)\rvert$
0.25	1.21758E-06	10	7.11232E-06
0.5	7.26122E-07	20	7.27935E-06
1	9.48884E-07	40	8.16943E-06
5	2.01468E-06	60	7.07805E-06

Table 4.2: Maximum relative errors for $\nu = 1$

From this table we can see that our program satisfies the relative accuracy requirement $\varepsilon = 10^{-5}$ for the special choice of $\nu = 1$. Detailed relative errors versus risk factor values $y_i, i = 1, 2, \cdots, 100$, for $\alpha = 0.25$, $\alpha = 10$ and $\alpha = 60$ are plotted in Figure 4.2. In this figure, the relative errors are multiplied by 10^5. From this figure we can see that all relative errors are small.

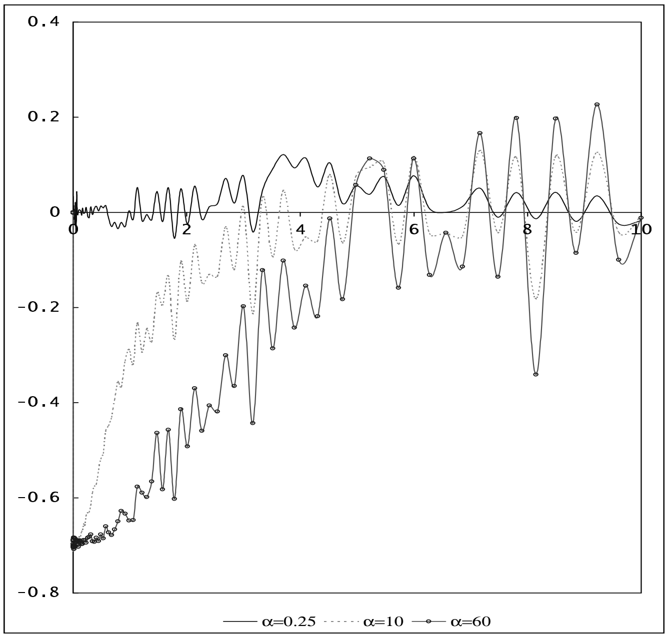

Figure 4.2: Relative error$\times 10^5$ as a function of risk factor y for $\nu = 1$

Next, we consider the case $\nu = -1$. From (3.13), we see that $p(y; \alpha, \nu)$ can be expressed in closed-form as

$$p(y;\alpha,-1) = \frac{\Gamma(\alpha+0.5)}{\Gamma(\alpha)\sqrt{2\pi(\alpha-1)}}\left(1+\frac{y^2}{2}\frac{1}{\alpha-1}\right)^{-(\alpha+0.5)}. \tag{4.2}$$

Hence, in this case, an accurate approximation to the exact value of $p(y;\alpha,-1)$ is readily available.

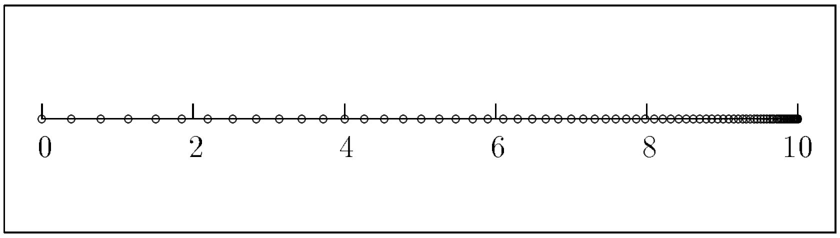

Figure 4.3: Test points for $\nu = -1$

We compare the results produced by our program with $\nu = -1$ and those computed using (4.2) for $\alpha = 1.5$, 2, 5, 10, 20, 30, 45, and 60. It is known that, when $\nu < 0$ and $\alpha - \frac{\nu}{2} - 1 > 0$, the maximizer of the integrand function $f(t;y,\alpha,\nu)$ approaches 0 for $|y|$ large. Therefore, in this case, to see the robustness of our program, we chose more points near $y = 10$ than near $y = 0$. The test points $y_i = 10 - 10^{-7}\times(100-i)^4$, $i = 1,2,\ldots,100$, are plotted in Figure 4.3. For $\nu = -1$, all results are obtained by applying the methods described in Section 3.3 and Section 3.4 together. The numerical results are presented in Table 4.3. The relative error $RelErr(\alpha, y)$ with respect to the risk factor value y and the shape parameter α with $\nu = -1$ is given by

$$RelErr(\alpha,y) = (general(\alpha,y) - accurate(\alpha,y))/accurate(\alpha,y),$$

where $general(\alpha,y)$ and $accurate(\alpha,y)$ are the values of $p(y;\alpha,1)$ produced by our program and by (4.2), respectively. In this table, $\max|RelErr(\alpha)| = \max_{i=1,100}\{|RelErr(\alpha,y_i)|\}$. We see that $\max|RelErr(20)| = 1.23187E-05$. This value is slightly bigger than the required relative accuracy of 10^{-5}. We also note that this problem occurs only at $y = 8.86835$ among these 100 test points. In this case, we have $p(8.86835;20,-1) =$

$4.206751E-11$. The relative errors times 10^5 for all the y-values considered for $\alpha = 1.5$, $\alpha = 20$ and $\alpha = 60$ are plotted in Figure 4.4. From this figure we can see that the relative errors at all test points except at $y = 8.86835$ with $\alpha = 20$ are satisfactorily controlled.

α	$\max\lvert RelErr(\alpha)\rvert$	α	$\max\lvert RelErr(\alpha)\rvert$
1.5	2.80827E-06	20	1.23187E-05*
2	3.75903E-06	30	2.5207E-06
5	3.82686E-06	45	3.76302E-06
10	4.07244E-06	60	2.94026E-06

Table 4.3: Maximum relative errors for $\nu = -1$

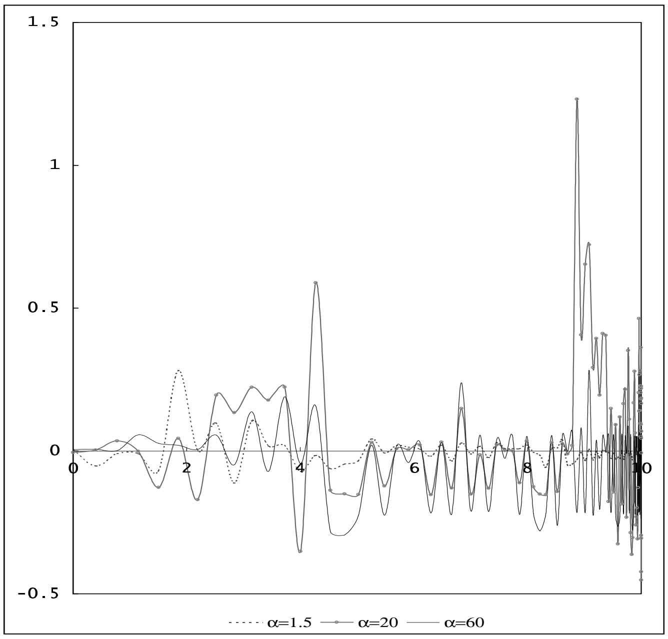

Figure 4.4: Relative error$\times 10^5$ as a function of risk factor y for $\nu = -1$

4.3 An Application

In this section, we present an application of the generalized Gamma variance (GGV) model for plotting the log-likelihood surface for the S&P 500 Stock Index as a function of the shape parameters α and ν. Let the standardized historical daily log-returns be $y_i, i = 1, 2 \ldots, 2500$. Then the log-likelihood function $L(\alpha, \nu)$ is defined by

$$L(\alpha, \nu) = \sum_{i=1}^{2500} \ln(p(y_i; \alpha, \nu)). \tag{4.3}$$

One purpose in plotting this log-likelihood surface is to find a pair of shape parameters α and ν such that $L(\alpha, \nu)$ attains its maximum value.

The log-likelihood surface generated by calling our program to compute the $p(y; \alpha, \nu)$ is presented in Figure 4.5. To generate this surface, we chose shape parameters

$$\alpha = 0.5, 1, 2, 3, 3.5(1)12.5, 13.5(1.5)49.5, 51(2)91,$$

$$\nu = -8.4(0.3) - 1.2, -0.9(0.2) - 0.3, 0, 0.3(0.2)0.9, 1.2(0.3)9,$$

where $x(d)y$ denotes values from x to y in steps of d. When $\alpha + \nu \leq 0$, we simply let $L(\alpha, \nu) = -10000$.

From this figure we see that the normal distribution corresponds to the deep valley. Both the left wing, which corresponds to the pure polynomial tails with $\nu < 0$, and the right wing, which corresponds to the compound tails with $\nu > 0$, have significantly larger log-likelihood values than the normal distribution. Therefore, it is expected that the GGV model matches the observed data better than the normal model.

The maximum log-likelihood value over all grid points considered for which $\alpha + \nu > 0$ is $L(16.5, -3.6) = -3347.931979$. In Figure 4.6, we show the observed S&P 500 daily log-return density together with a fit by a normal distribution with mean 0 and standard deviation 1, and a fit by the GGV distribution with $\alpha = 16.5$ and $\nu = -3.6$. In the left graph, the density is plotted on a linear scale, while, in the right graph, it is plotted on a log scale. From these two figures, we see that the GGV model fits the observed log-returns better than the normal model.

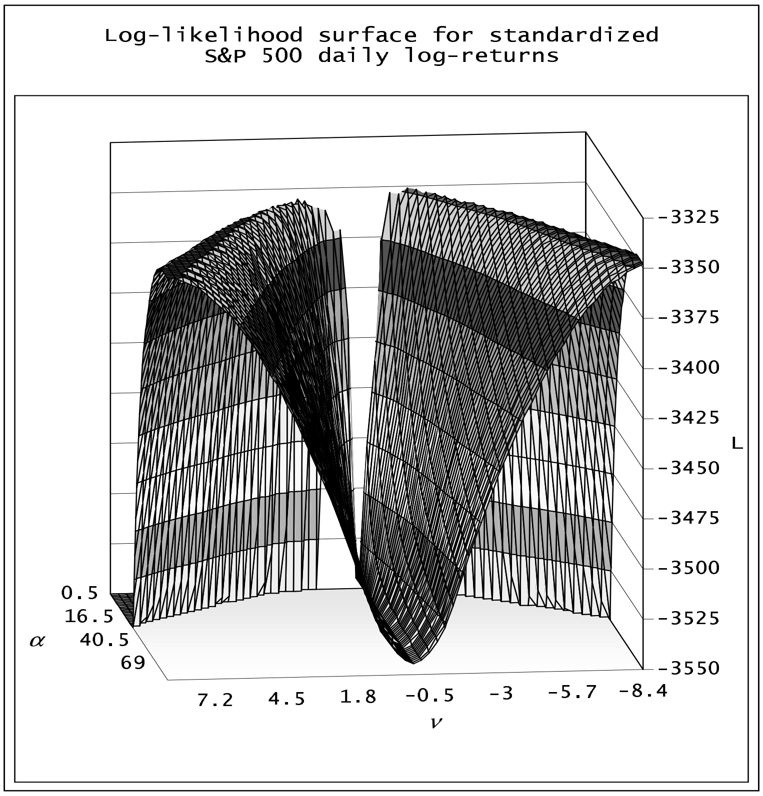

Figure 4.5: GGV model log-likelihood surface for S&P 500

To measure the performance of our program, we measured the time to compute every log-likelihood function value $L(\alpha, \nu)$ considered above. The computer time versus the shape parameters α and ν are plotted in Figure 4.7. For $\nu > 0$, the average time spent by the program per $L(\alpha, \nu)$ evaluation is 0.548 second, while for $\nu < 0$, the average time spent by the program is 0.217 second. If the improvement discussed in Section 3.4 is not used, then the average time is 0.298 second. Hence the improvement reduces the computer time required by (0.298-0.217)/0.298=27%. For $\nu = 0$, the time to obtain a $L(\alpha, 0)$ is 0.01 second.

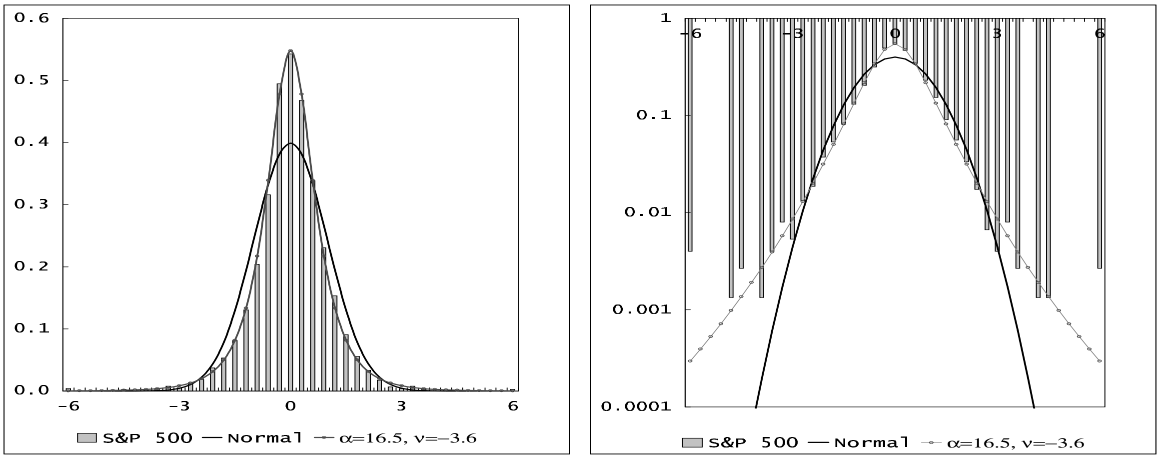

Figure 4.6: Observed and calibrated densities for S&P 500 daily log-returns

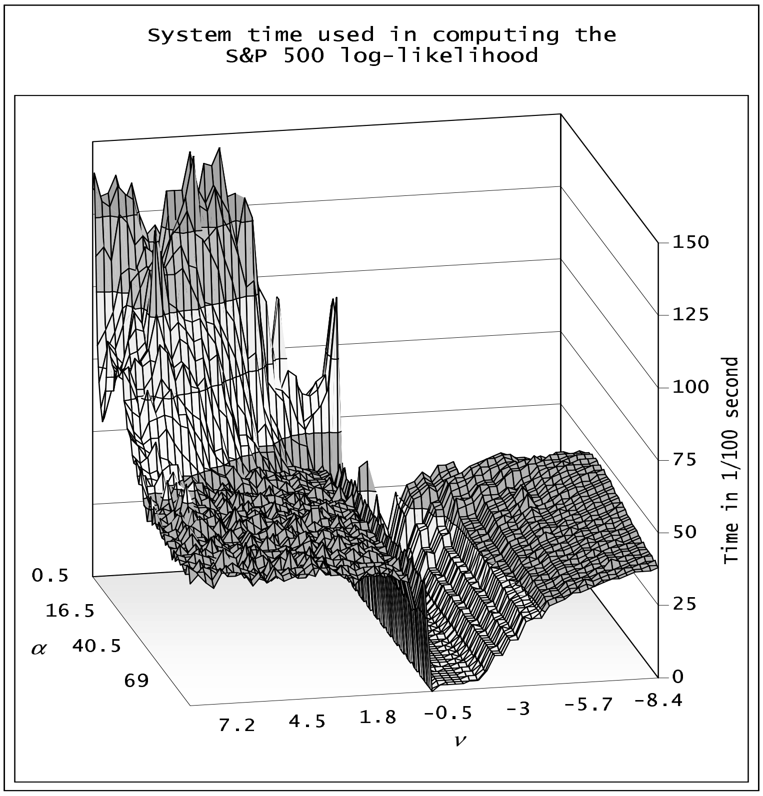

Figure 4.7: System time used for calculating the surface in Figure 4.5

Chapter 5

Computation of the Cumulative Distribution Function

In this chapter, we consider the problem of computing the standardized cumulative distribution function (cdf)

$$F(\xi;\alpha,\nu,\sigma_X) = \frac{1}{\Gamma(\alpha)}\sqrt{\frac{\Gamma(\alpha+\nu)}{2\pi\Gamma(\alpha)}}\int_{-\infty}^{\xi/\sigma_X}\int_0^{\infty} e^{-\frac{y^2}{2}\frac{\Gamma(\alpha+\nu)}{\Gamma(\alpha)}\frac{1}{t^\nu}} t^{\alpha-\frac{\nu}{2}-1}e^{-t}dtdy \tag{5.1}$$

where $\xi \in (-\infty, +\infty)$ is an upper bound on the risk factor X and σ_X^2 is the variance of X. By changing the order of variables, (5.1) is reformulated as

$$\begin{aligned} F(\xi;\alpha,\nu,\sigma_X) &= \frac{1}{\Gamma(\alpha)}\int_0^{\infty} t^{\alpha-\frac{\nu}{2}-1}e^{-t}\int_{-\infty}^{\xi/\sigma_X}\sqrt{\frac{\Gamma(\alpha+\nu)}{2\pi\Gamma(\alpha)}}e^{-\frac{y^2}{2}\frac{\Gamma(\alpha+\nu)}{\Gamma(\alpha)}\frac{1}{t^\nu}}dydt \\ &= \frac{1}{\Gamma(\alpha)}\int_0^{\infty} t^{\alpha-1}e^{-t}P\left(\xi/\sigma_X\sqrt{\frac{\Gamma(\alpha+\nu)}{\Gamma(\alpha)t^\nu}}\right)dt, \end{aligned} \tag{5.2}$$

where $P(z) = \frac{1}{\sqrt{2\pi}}\int_{-\infty}^{z} e^{-\frac{s^2}{2}}ds$ is the cdf of the normal density with mean 0 and standard deviation 1. Without loss of generality, we assume that $\xi \geq 0$, since for any $\xi' < 0$ we have

$$F(\xi';\alpha,\nu,\sigma_X) = 1 - F(|\xi'|;\alpha,\nu,\sigma_X). \tag{5.3}$$

In Section 5.1, a method for calculating the cdf within the specified absolute accuracy $\varepsilon_a = 10^{-5}$ is proposed. Numerical results are reported in Section 5.2. The developed cdf program is used in performing the Pearson χ^2 test to check whether the calibrated GGV model with the pair of shape parameters $(\alpha, \nu) = (16.5, -3.6)$ obtained in §4.3 fits the S&P 500 daily log-returns well.

5.1 Numerical Method for Computing the cdf

To calculate the cdf within the given absolute accuracy ε_a, we truncate the semi-infinite interval $[0, \infty)$ to a bounded subinterval $[L, U] \subset [0, \infty)$ such that the two integrals over the two intervals $[0, L]$ and $[U, \infty)$ are small enough to be ignored. To be more specific, we choose the lower and upper limits L and U so that

$$\frac{1}{\Gamma(\alpha)} \int_0^L t^{\alpha-1} e^{-t} P\left(\xi/\sigma_X \sqrt{\frac{\Gamma(\alpha+\nu)}{\Gamma(\alpha)t^\nu}}\right) dt \le \frac{1}{3}\varepsilon_a, \quad \text{and} \tag{5.4}$$

$$\frac{1}{\Gamma(\alpha)} \int_U^\infty t^{\alpha-1} e^{-t} P\left(\xi/\sigma_X \sqrt{\frac{\Gamma(\alpha+\nu)}{\Gamma(\alpha)t^\nu}}\right) dt \le \frac{1}{3}\varepsilon_a, \tag{5.5}$$

with near equality in (5.4) and (5.5). If we can evaluate

$$\frac{1}{\Gamma(\alpha)} \int_L^U t^{\alpha-1} e^{-t} P\left(\xi/\sigma_X \sqrt{\frac{\Gamma(\alpha+\nu)}{\Gamma(\alpha)t^\nu}}\right) dt \tag{5.6}$$

to within an absolute accuracy of $\frac{1}{3}\varepsilon_a$, then this computed value approximates $F(\xi; \alpha, \nu, \sigma_X)$ to within an absolute accuracy of ε_a.

Note that, for any $z \ge 0$, $0.5 \le P(z) \le 1$. Thus we have

$$\frac{1}{\Gamma(\alpha)} \int_0^L t^{\alpha-1} e^{-t} P\left(\xi/\sigma_X \sqrt{\frac{\Gamma(\alpha+\nu)}{\Gamma(\alpha)t^\nu}}\right) dt \le \frac{1}{\Gamma(\alpha)} \int_0^L t^{\alpha-1} e^{-t} dt = \frac{1}{\Gamma(\alpha)}\gamma(L, \alpha). \tag{5.7}$$

If L is determined by requiring

$$\frac{1}{\Gamma(\alpha)}\gamma(L, \alpha) = \frac{1}{3}\varepsilon_a, \tag{5.8}$$

then, from (5.7) and (5.8) we see that (5.4) is satisfied. Similarly, we can determine the upper limit U needed to satisfy (5.5) by solving

$$\frac{1}{\Gamma(\alpha)}\Gamma(U, \alpha) = \frac{1}{3}\varepsilon_a. \tag{5.9}$$

Equations (5.8) and (5.9) are solved by the same method applied to equations (3.28) and (3.29). Having calculated L and U, we can then apply a quadrature method to (5.6) to obtain an approximation to the cdf $F(\xi; \alpha, \nu, \sigma_X)$. Note that $0.5 \leq F(\xi; \alpha, \nu, \sigma_X) \leq 1$ for any $\xi \geq 0$, thus a relative accuracy of $\frac{1}{3}\varepsilon_a$ implies an absolute error of at most $\frac{1}{3}\varepsilon_a$. Thus we can apply a quadrature method Q to compute (5.6) to within a relative error of $\frac{1}{3}\varepsilon_a$.

To compute the cdf $P(z)$ of the normal density function with mean 0 and variance 1 we use the approximation

$$1 - \frac{1}{\sqrt{2\pi}} e^{-\frac{z^2}{2}} (b_1 t + b_2 t^2 + b_3 t^3 + b_4 t^4 + b_5 t^5), \quad t = \frac{1}{1 + pz}, \tag{5.10}$$

where $p = 0.2316419$, and $b_1 = 0.319381530, b_2 = -0.356563782, b_3 = 1.781477937, b_4 = -1.821255978$ and $b_5 = 1.330274429$. This function approximates $P(z)$ to within an absolute error of $\epsilon(z)$ with $|\epsilon(z)| < 7.5 \times 10^{-8}$ [1, 26.2.17]. Note that $P(z) \geq 0.5$ for $z \geq 0$ and the absolute error of this approximation is less than 7.5×10^{-8}, so the relative error of this approximation is less than 1.5×10^{-7}.

5.2 Numerical Results

A Microsoft Visual C++ program based on the method described in Section 5.1 was developed and compiled into a dynamic link library (DLL) file $GGV\_SymmetricCumul(\xi, \alpha, \nu, \sigma)$ so that is could be called from any Excel, VBA or other Windows application program. In this program, the quadrature method used in Chapter 4 is used to approximate (5.6) with a relative accuracy of $\frac{1}{3}\varepsilon_a$ to obtain an approximation to the cdf $F(\xi; \alpha, \nu, \sigma_X)$.

We compare results generated by *GGV_SymmetricCumul* and those produced by other methods for two particular sets of parameter values.

First, we consider $\nu = 1$. From (4.1),

$$p(y; \alpha, 1) = \sqrt{\frac{2\alpha}{\pi}} \frac{1}{\Gamma(\alpha)} \left(\frac{\alpha y^2}{2} \right)^{\frac{\alpha}{2} - \frac{1}{4}} K_{\alpha - \frac{1}{2}} \left(\sqrt{2\alpha y^2} \right).$$

Thus, for $\alpha = 1$, we have

$$p(y;1,1) = \sqrt{\frac{2}{\pi}}\left(\frac{y^2}{2}\right)^{\frac{1}{4}} K_{1/2}\left(\sqrt{2}|y|\right).$$

Since $K_{1/2}(z) = \sqrt{\frac{\pi}{2z}}e^{-z}$,

$$p(y;1,1) = \frac{1}{\sqrt{2}}e^{-\sqrt{2}|y|}.$$

Since $\xi \geq 0$, it follows from the definition of the cdf that

$$F(\xi;1,1,\sigma_X) = \int_{-\infty}^{\xi/\sigma_X} p(y;1,1)dy = 1 - 0.5e^{-\sqrt{2}\xi/\sigma_X}. \tag{5.11}$$

Similarly, when $\alpha = 2$, we have

$$p(y;2,1) = \left(y + \frac{1}{2}\right)e^{-2|y|}.$$

Hence,

$$F(\xi;2,1,\sigma_X) = 1 - 0.5e^{-2\xi/\sigma_X}(\xi/\sigma_X + 1). \tag{5.12}$$

Next, we consider $\nu = -1$. From (4.2), we have

$$p(y;\alpha,-1) = \frac{\Gamma(\alpha+0.5)}{\Gamma(\alpha)\sqrt{2\pi(\alpha-1)}}\left(1 + \frac{y^2}{2}\frac{1}{\alpha-1}\right)^{-(\alpha+0.5)}.$$

Therefore, when $\alpha = 1.5$, we have

$$p(y;1.5,-1) = \frac{2}{\pi}\left(1+y^2\right)^{-2}.$$

Note that $\int \frac{dz}{(z^2+1)^2} = \frac{z}{2(z^2+1)^2} + \frac{1}{2}\arctan(z)$ [18, 1.2.10.15]. Therefore, for $\xi \geq 0$,

$$\begin{aligned} F(\xi;1.5,-1,\sigma_X) &= 0.5 + \frac{2}{\pi}\int_0^{\xi/\sigma_X} \frac{1}{(1+y^2)^2}dy \\ &= 0.5 + \frac{1}{\pi}\left[\frac{\xi/\sigma_X}{(1+(\xi/\sigma_X)^2)^2} + \arctan(\xi/\sigma_X)\right] \end{aligned} \tag{5.13}$$

Similarly, for $\alpha = 2.5$,

$$F(\xi;2.5,-1,\sigma_X) = 0.5 + \frac{8}{3\pi}\left[\frac{z}{4(z^2+1)^2} + \frac{3z}{8(z^2+1)} + \frac{3}{8}\arctan(z)\right]\Bigg|_{z=\frac{1}{\sqrt{3}}\xi/\sigma_X}. \tag{5.14}$$

For our numerical results, we used $GGV\_SymmetricCumul(\xi, \alpha, \nu, \sigma)$ to compute $F(\xi_i; \alpha, \nu, \sigma_X)$ for $\xi_i = 10^{-7} \times 1.5^i, i = 0, 1, \ldots 46$, $\sigma_X = 1$ and the values of α and ν discussed above and we compared the computed results to the exact values given by (5.11), (5.12), (5.13) and (5.14). Thus ξ changes from 10^{-7} to $10^{-7} \times 1.5^{46} \approx 12.6$. The numerical results are summarized as follows.

$$\max|AbsErr(1,1)| = 6.56627E-06, \qquad \max|AbsErr(2,1)| = 6.49392E-06;$$
$$\max|AbsErr(1.5,-1) = 5.38894E-06, \quad \max|AbsErr(2.5,-1)| = 5.87408E-06.$$

where $\max|AbsErr(\alpha, \nu)| = \max_{i=0,46}|AbsErr(\xi_i; \alpha, \nu, 1)|$, and $AbsErr(\xi; \alpha, \nu, \sigma_X)$ is the difference between the values generated by the function $GGV\_SymmetricCumul$ and the corresponding analytic form. From these results we can see that all absolute errors are small.

In Chapter 4, the observed S&P 500 daily log-returns were matched by the GGV model. It is seen from the two plots shown in Figure 4.6 that this fit works well. From a statistical point of view, the question of whether or not the data is consistent with the GGV model with parameters $\alpha = 16.5, \nu = -3.6$ can be verified by performing Pearson's χ^2 goodness-of-fit test as follows.

First, the 2500 log-returns are grouped into 25 bins as shown in Table 5.1. In this table, b_k denotes the k-th bin, n_{I_O} denotes the number of log-return values that fall into b_k, P_k is the probability under the GGV distribution that the risk factor would be expected to be in b_k, $n\mathrm{P}_k$ is the expected number of log-return values in b_k, $n = 2500$ is the total number of observations.

Next, according to Theorem 9.4.1 of [9], we can evaluate c_1, the obvious analog of Pearson's c, by

$$c_1 = \sum_{k=1}^{25} \frac{(n_{I_O} - n\mathrm{P}_k)^2}{n\mathrm{P}_k} = 12.073872.$$

Finally, note that $c_1 \leq \chi^2_{0.95, 25-1-2} = 12.338$, thus by Theorem 9.4.1, we accept the null hypothesis that the risk factor X follows the GGV distribution with $\alpha = 16.5$ and

$\nu = -3.6$ with a 95% confidence level. This implies that the GGV model with this pair of shape parameters matches the observed daily log-returns well.

To see whether or not the normal distribution fits the observed data, we also computed the value $c_1' = 836.14326$, the obvious analog of Pearson's c, for the normal distribution with the same data bins and procedure as previously used for the GGV distribution. According to Theorem 9.4.1 of [9] and noting that $\chi^2_{1.25E-162,25-1-2} = 836.14326$, we can conclude that the normal distribution does not fit the observed data at all since the confidence level $1.25E{-}162$ is almost 0.

k	b_k	n_{I_O}	P_k	$n\mathrm{P}_k$	$(n_{I_O} - n\mathrm{P}_k)^2/n\mathrm{P}_k$
1	$(-\infty, -4]$	6	0.002310	5.775853	0.008699
2	$(-4, -3.35]$	5	0.002399	5.997592	0.165932
3	$(-3.35, -2.85]$	9	0.003829	9.572345	0.034221
4	$(-2.85, -2.55]$	10	0.003934	9.835494	0.002752
5	$(-2.55, -2.25]$	14	0.006073	15.182073	0.092036
6	$(-2.25, -1.95]$	28	0.009545	23.863497	0.717022
7	$(-1.95, -1.65]$	40	0.015266	38.164031	0.088324
8	$(-1.65, -1.35]$	61	0.024769	61.921350	0.013709
9	$(-1.35, -1.05]$	98	0.040483	101.208048	0.101687
10	$(-1.05, -0.75]$	153	0.065617	164.042451	0.743318
11	$(-0.75, -0.45]$	237	0.102020	255.049078	1.277280
12	$(-0.45, -0.15]$	371	0.142551	356.376667	0.600045
13	$(-0.15, 0.15]$	407	0.162409	406.023046	0.002351
14	$(0.15, 0.45]$	351	0.142551	356.376667	0.081118
15	$(0.45, 0.75]$	254	0.102020	255.049078	0.004315
16	$(0.75, 1.05]$	173	0.065617	164.042451	0.489128
17	$(1.05, 1.35]$	115	0.040483	101.208048	1.879474
18	$(1.35, 1.65]$	68	0.024769	61.921350	0.596725
19	$(1.65, 1.95]$	42	0.015266	38.164031	0.385564
20	$(1.95, 2.25]$	25	0.009545	23.863497	0.054126
21	$(2.25, 2.55]$	13	0.006073	15.182073	0.313623
22	$(2.55, 2.85]$	5	0.003934	9.835494	2.377308
23	$(2.85, 3.35]$	6	0.003829	9.572345	1.333179
24	$(3.35, 4]$	5	0.002399	5.997592	0.165932
25	$(4, \infty)$	4	0.002310	5.775853	0.546006
Total		2500	1	2500	12.073872

Table 5.1: Pearson χ^2 goodness-of-fit test

Chapter 6

Conclusions and Future Work

We studied the properties of the probability density function $p(y;\alpha,\nu)$ of the generalized Gamma variance (GGV) model in Chapter 2. A hybrid method for computing $p(y;\alpha,\nu)$ to within the relative accuracy of $\varepsilon = 10^{-5}$ was proposed in Chapter 3. In this hybrid method, both a quadrature and an approximation technique are used. The approximation technique is employed to deal with difficulties related to sharp peaks in the integrand function associated with $p(y;\alpha,\nu)$. When the integrand has a sharp peak, the integral over a neighborhood of the high peak is evaluated by using well developed special function procedures, while the other parts of the integral are computed by quadrature. To improve the performance of this hybrid method, an alternative method for $\nu < 0$ was discussed in Chapter 3. A C program based on this hybrid method and the improved method was produced. Numerical results reported in Chapter 4 suggest that the methods proposed in Chapter 3 can compute the pdf $p(y;\alpha,\nu)$ to within the required relative accuracy $\varepsilon = 10^{-5}$.

A method for computing the cdf $F(\xi;\alpha,\nu;\sigma_X)$ to within the required absolute accuracy of $\varepsilon_a = 10^{-5}$ was proposed in Section 5.1. A program $GGV\_SymmetricCumul(\xi,\alpha,\nu,\sigma)$ based on this method was produced and compiled into a DLL file. Numerical results reported in Section 5.2 suggest that this method is suitable for computing the cumulative distribution function of the GGV model to within the required absolute accuracy.

We believe the hybrid method for computing the pdf $p(y; \alpha, \nu)$ can be improved in three aspects.

First, we can consider using another polynomial, for example one based on Chebyshev polynomials [14, Chapter III], to replace $\mathcal{P}_N(t)$, $N = 7$, so that e^{-t} can be well approximated over an interval $[0, T^*] \supset [0, T_L]$, where T^* can be as large as 9, whereas $T_L = 1$.

Second, we note that standard methods for computing most special functions based on integrals do not use quadrature explicitly [1, 14]. Therefore, we believe that $p(y; \alpha, \nu)$ can be evaluated more effectively by some scheme that does not use quadrature explicitly. In this case, we would rely solely on the approximation technique described in Chapter 3 and special function evaluations to compute the associated integrals to within the required accuracy. An advantage of this approach is that we believe the pdf could be evaluated to an accuracy higher than $\varepsilon = 10^{-5}$.

Third, the asymptotic properties of the pdf $p(y; \alpha, \nu)$ are not used in computing the pdf, although they were discussed in Section 2.1. We believe these asymptotics may be helpful in computing $p(y; \alpha, \nu)$ when $|y|$ is very small or very large. To use them effectively, more asymptotic terms are needed.

Bibliography

[1] M. Abramowitz and I. Stegun, editors. *Handbook of Mathematical Functions with Formulas, Graphs, and Mathematical Tables.* National Bureau of Standards, Applied Mathematics Series 55. U.S. Government Printing Office, Washington, D.C., 1965.

[2] A. R. Didonato and A. H. Morris. Computation of the incomplete Gamma function ratios and their inverse. *ACM Transactions on Mathematical Software,* 12:377-393, 1986.

[3] E. Eberlein and U. Keller. Hyperbolic distributions in finance. *Bernoulli,* 1:281-299, 1995.

[4] E. Eberlein. Application of generalized hyperbolic Lévy motions to finance. In O. E. Barndorff-Nielsen, T. Mikosch, and S. Resnick, editors, *Lévy Processes: Theory and Applications*, pages 319-337. Birkhäuser, 2001.

[5] I. S. Gradshteyn and I. M. Ryzhik. *Table of Integrals, Series, and Products.* Academic Press, Inc., 4th edition, 1965.

[6] J. C. Hull. *Introduction to Futures and Options Markets.* Prentice Hall, Upper Saddle River, New Jersey 07458, 3rd edition, 1997.

[7] N. L. Johnson, S. Kotz, and N. Balakrishnan. *Continuous Univariate Distributions*, volume 2. John Wiley&Sons, Inc., 2nd edition, 1995.

[8] A. R. Krommer and C. W. Überhuber. *Computational Integration.* SIAM Philadelphia, 1998.

[9] R. J. Larsen and M. L. Marx. *An Introduction to Mathematical Statistics and Its Applications.* Prentice-Hall, Englewood Cliffs, New Jersey, 2nd edition, 1986.

[10] A. Levin and A. Tchernitser. Stochastic volatility and jump Lévy processes in Value-at-Risk modeling. Presentations at the Risk Conference "Math Week 2000", London, December 2000.

[11] A. Levin and A. Tchernitser. Analytical specifications for Monte Carlo simulation engine in comprehensive VaR system (Generalized stochastic variance model). *Market Risk Submission*, Bank of Montreal, April 2001.

[12] A. Levin and A. Tchernitser. Multifactor stochastic variance VaR model: Application to market risk management. Working paper, 2001.

[13] T. J. Linsmeier and N. D. Pearson. *Risk measurement: An introduction to value at risk.* Available at `http://agecon.lib.umn.edu/uiuc/aceo9604.pdf`, 1996.

[14] Y. L. Luke. *Mathematical Functions and Their Approximations.* Academic Press, Inc., 1975.

[15] D. Madan and E. Seneta. The Variance Gamma (VG) model for share market returns. *Journal of Business,* 63:511-524, 1990.

[16] R. Piessens, E. de Doncker-Kapenga, C. W. Überhuber, and D. K. Kahaner. *QUADPACK: A Subroutine Package for Automatic Integration.* Springer-Verlag, 1983.

[17] W. H. Press, S. A. Teukolsky, W. T. Vetterling and B. P. Flannery. *Numerical Recipes in C: The Art of Scientific Computing.* Cambridge University Press, 2nd edition, 1992.

[18] A. P. Prudnikov, Yu. A. Brychkov and O. I. Marichev. *Integrals and Series*, volume 1. Gordon and Breach Science Publishers, 1983.

[19] S. Rachev and S. Mittnik. *Stable Paretian Models in Finance*. John Wiley & Sons, Chichester, New York, 2000.

[20] R. Wong. *Asymptotic Approximations of Integrals*. Academic Press, Inc., 1989.

[21] K. Yosida. *Functional Analysis*. Springer–Verlag, Berlin Heidelberg, New York, 6th edition, 1980.